TABLE 2.2-1

REACTOR TRIP SYSTEM INSTRUMENTATION TRIP SETPOINTS

Functional Unit	Total Allowance (TA)	Z	S	Trip Setpoint	Allowable Value
1. Manual Reactor Trip	Not Applicable	NA	NA	NA	NA
2. Power Range, Neutron Flux High Setpoint	7.5	4.56	0	≤109% of RTP	≤111.2% of RTP
Low Setpoint	8.3	4.56	0	≤25% of RTP	≤27.2% of RTP
3. Power Range, Neutron Flux High Positive Rate	1.6	0.5	0	≤5% of RTP with a time constant ≥2 seconds	≤6.3% of RTP with a time constant ≥2 seconds
4. Power Range, Neutron Flux High Negative Rate	1.6	0.5	0	≤5% of RTP with a time constant ≥2 seconds	≤6.3% of RTP with a time constant ≥2 seconds
5. Intermediate Range, Neutron Flux	17.0	8.4	0	≤25% of RTP	≤31% of RTP
6. Source Range, Neutron Flux	17.0	10.0	0	$\leq 10^5$ cps	$\leq 1.4 \times 10^5$ cps
7. Overtemperature ΔT	7.1	2.94	1.8	See note 1	See note 2
8. Overpower ΔT	4.5	1.4	1.2	See note 3	See note 4
9. Pressurizer Pressure-Low	3.1	0.71	1.5	≥1870 psig	≥1859 psig
10. Pressurizer Pressure-High	3.1	0.71	1.5	≤2380 psig	≤2391 psig
11. Pressurizer Water Level-High	5.0	2.18	1.5	≤92% of instrument span	≤93.8% of instrument span
12. Loss of Flow	2.5	1.0	1.5	≥90% of loop design flow*	≥89.2% of loop design flow*

[redacted] 96200

Loop design flow = [redacted] gpm

RTP = RATED THERMAL POWER

Tech Spec Revision

POWER DISTRIBUTION LIMIT

BASES

HEAT FLUX HOT CHANNEL FACTOR and RCS FLOWRATE and NUCLEAR ENTHALPY RISE HOT CHANNEL FACTOR (Continued)

c. The control rod insertion limits of Specifications 3.1.3.5 and 3.1.3.6 are maintained.

d. The axial power distribution, expressed in terms of AXIAL FLUX DIFFERENCE, is maintained within the limits.

$F^N_{\Delta H}$ will be maintained within its limits provided conditions a. through d. above are maintained. As noted on Figures 3.2-3 ~~and 3.2-1~~, RCS flow rate and $F^N_{\Delta H}$ may be "traded off" against one another (i.e., a low measured RCS flow rate is acceptable if the measured $F^N_{\Delta H}$ is also low) to ensure that the calculated DNBR will not be below the design DNBR value. The relaxation of $F^N_{\Delta H}$ as a function of THERMAL POWER allows changes in the radial power shape for all permissible rod insertion limits.

R_2 as calculated in 3.2.3 and used in Figure 3.2.3, accounts for $F^N_{\Delta H}$ less than or equal to 1.49. This value is used in the various accident analyses where $F^N_{\Delta H}$ influences parameters other than DNBR, e.g., peak clad temperature and thus is the maximum "as measured" value allowed. ~~R_2, as defined, allows for the inclusion of a penalty for rod bow on DNBR only. Thus knowing this "as measured" values of $F^N_{\Delta H}$ and RCS flow allows for "tradeoffs" in excess of R equal to 1.0 for the purpose of offsetting the rod bow DNBR penalty.~~

Insert A here.

When an F_Q measurement is taken, an allowance for both experimental error and manufacturing tolerance must be made. An allowance of 5% is appropriate for a full core map taken with the incore detector flux mapping system and a 3% allowance is appropriate for manufacturing tolerance.

The radial peaking factor $F_{xy}(Z)$ is measured periodically to provide assurance that the hot channel factor, $F_Q(Z)$, remains within its limit. The F_{xy} limit for Rated Thermal Power (F^{RTP}_{xy}) as provided in the Radial Peaking Factor Limit Report per specification 6.9.1.14 was determined from expected power control maneuvers over the full range of burnup conditions in the core.

When RCS flow rate and $F^N_{\Delta H}$ are measured, no additional allowances are necessary prior to comparison with the limits of Figures 3.2-3, ~~and 3.2-4.~~ Measurement errors of 3.5% for RCS total flow rate and 4% for $F^N_{\Delta H}$ have been allowed for in ~~determination of the design DNBR value.~~ determining the limits of Figure 3.2-3.

HEAT FLUX HOT CHANNEL FACTOR and RCS FLOWRATE and NUCLEAR ENTHALPY RISE HOT CHANNEL FACTOR (Continued)

The 12 hour periodic surveillance of indicated RCS flow is sufficient to detect only flow degradation which could lead to operation outside the acceptable region of operation shown on Figure 3.2-3.

~~Fuel rod bowing reduces the value of DNB ratio. Credit is available to partially offset this reduction. This credit comes from a generic margin which totals 9.1 percent. The penalties applied to $F_{\Delta H}$ to account for Rod Bow (Figure 3.2-4) as a function of burnup are consistent with those described in Mr. John F. Stolz's (NRC) letter to T. M. Anderson (Westinghouse) dated April 5, 1979 and W 8691, Rev. 1 (partial rod bow test data).~~

3/4.2.4 QUADRANT POWER TILT RATIO

The quadrant power tilt ratio limit assures that the radial power distribution satisfies the design values used in the power capability analysis. Radial power distribution measurements are made during startup testing and periodically during power operation.

The limit of 1.02, at which corrective action is required, provides DNB and linear heat generation rate protection with x-y plane power tilts. A limiting tilt of 1.025 can be tolerated before the margin for uncertainty in F_Q is depleted. The limit of 1.02 was selected to provide an allowance for the uncertainty associated with the indicated power tilt.

The two hour time allowance for operation with a tilt condition greater than 1.02 but less than 1.09 is provided to allow identification and correction of a dropped or misaligned control rod. In the event such action does not correct the tilt, the margin for uncertainty on F_Q is reinstated by reducing the maximum allowed power by 3 percent for each percent of tilt in excess of 1.0.

For purposes of monitoring QUADRANT POWER TILT RATIO when one excore detector is inoperable, the movable incore detectors are used to confirm that the normalized symmetric power distribution is consistent with the QUADRANT POWER TILT RATIO. The incore detector monitoring is done with a full incore flux map or two sets of 4 symmetric thimbels. These locations are C-8, E-5, E-11, H-3, H-13, L-5, 2-11, N-8.

3/4.2.5 DNB PARAMETERS

The limits on the DNB related parameters assure that each of the parameters are maintained within the normal steady state envelope of operation assumed in the transient and accident analyses. The limits are consistent with the initial FSAR assumptions and have been analytically demonstrated adequate to maintain a minimum DNBR of 1.30 throughout each analyzed transient.

The 12 hour periodic surveillance of these parameters through instrument readout is sufficient to ensure that the parameters are restored within their limits following load changes and other expected transient operation.

Insert A

Tech. Spec. Insert

Fuel rod bowing reduces the value of DNB ratio. Credit is available to offset this reduction in the generic margin. The generic design margins, totaling 9.1% DNBR, completely offset any rod bow penalties. This margin includes the following:

1) Design limit DNBR of 1.30 vs. 1.28
2) Grid Spacing (K_s) of 0.046 vs. 0.059
3) Thermal Diffusion Coefficient of 0.038 vs. 0.059
4) DNBR Multiplier of 0.86 vs. 0.88
5) Pitch reduction

The applicable value of rod bow penalties are referenced in the FSAR.

3/4.2.3 RCS FLOW RATE AND NUCLEAR ENTHALPY RISE HOT CHANNEL FACTOR

LIMITING CONDITION FOR OPERATION

3.2.3 The combination of indicated Reactor Coolant System (RCS) total flow rate and R ~~$= R_1 / R_2$~~ shall be maintained within the region of allowable operation shown on Figure 3.2-3 for 3 loop operation.

Where:

a. $R = \dfrac{F^N_{\Delta H}}{1.49\,[1.0 + 0.2\,(1.0 - P)]}$,

~~b. $R_2 = \dfrac{R_1}{[1 - RBP(BU)]}$~~

b ~~c~~. $P = \dfrac{\text{THERMAL POWER}}{\text{RATED THERMAL POWER}}$,

c ~~d~~. $F^N_{\Delta H}$ = Measured values of $F^N_{\Delta H}$ obtained by using the movable incore detectors to obtain a power distribution map. The measured values of $F^N_{\Delta H}$ shall be used to calculate R since Figure 3.2-3 includes measurement uncertainties of 3.5% for flow and 4% for incore measurement of $F^N_{\Delta H}$, and

~~e. RBP (BU) = Rod Bow Penalty as a function of region average burnup as shown in Figure 3.2-4, where a region is defined as those assemblies with the same loading date (reloads) or enrichment (first core).~~

APPLICABILITY: MODE 1.

ACTION:

With the combination of RCS total flow rate and R ~~$= R_1 / R_2$~~ outside the region of acceptable operation shown on Figure 3.2-3:

a. Within 2 hours either:

1. Restore the combination of RCS total flow rate and R ~~$= R_1 / R_2$~~ to within the above limits, or

2. Reduce THERMAL POWER to less than 50% of RATED THERMAL POWER and reduce the Power Range Neutron Flux - High trip setpoint to less than or equal to 55% of RATED THERMAL POWER within the next 4 hours.

POWER DISTRIBUTION LIMITS

ACTION: (Continued)

b. Within 24 hours of initially being outside the above limits, verify through incore flux mapping and RCS total flow rate comparison that the combination of R_1, R_2 and RCS total flow rate are restored to within the above limits, or reduce THERMAL POWER to less than 5% of RATED THERMAL POWER within the next 2 hours.

c. Identify and correct the cause of the out-of-limit condition prior to increasing THERMAL POWER above the reduced THERMAL POWER limit required by ACTION items a.2. and/or b. above; subsequent POWER OPERATION may proceed provided that the combination of R_1, R_2 and indicated RCS total flow rate are demonstrated, through incore flux mapping and RCS total flow rate comparison, to be within the region of acceptable operation shown on Figure 3.2-3 prior to exceeding the following THERMAL POWER levels:

1. A nominal 50% of RATED THERMAL POWER,

2. A nominal 75% of RATED THERMAL POWER, and

3. Within 24 hours of attaining greater than or equal to 95% of RATED THERMAL POWER.

SURVEILLANCE REQUIREMENTS

4.2.3.1 The provisions of Specification 4.0.4 are not applicable.

4.2.3.2 The combination of indicated RCS total flow rate and R_1, R_2 shall be determined to be within the region of acceptable operation of Figure 3.2-3:

a. Prior to operation above 75% of RATED THERMAL POWER after each fuel loading, and

b. At least once per 31 Effective Full Power Days.

4.2.3.3 The indicated RCS total flow rate shall be verified to be within the region of acceptable operation of Figure 3.2-3 at least once per 12 hours when the most recently obtained values of R_1 and R_2, obtained per Specification 4.2.3.2, ~~are~~ 15 assumed to exist.

4.2.3.4 The RCS total flow rate indicators shall be subjected to a CHANNEL CALIBRATION at least once per 18 months.

4.2.3.5 The RCS total flow rate shall be determined by measurement at least once per 18 months.

Replace with following page

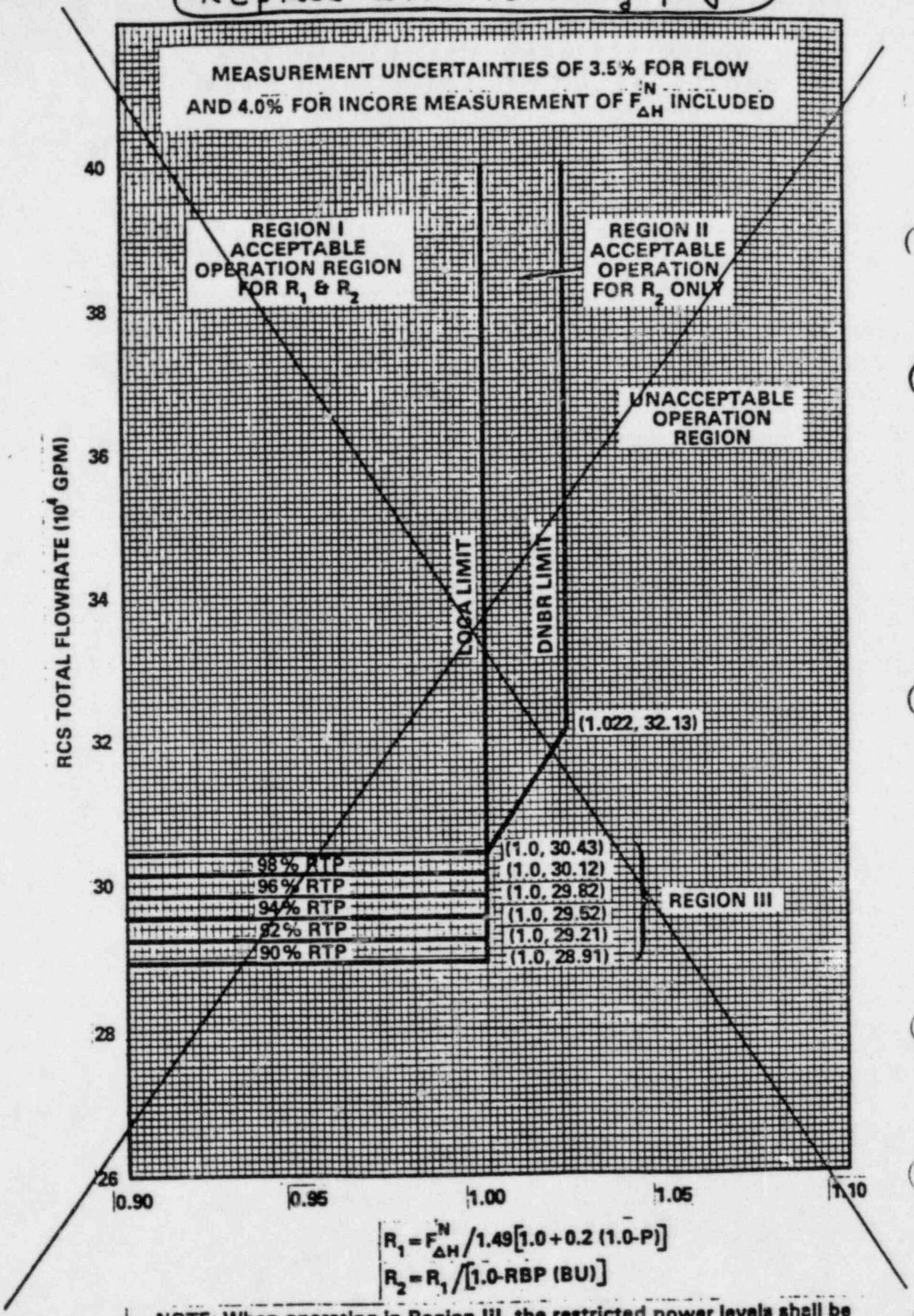

NOTE: When operating in Region III, the restricted power levels shall be considered to be 100% of Rated Thermal Power (RTP) for Figure 2.1-1.

Figure 3.2-3 RCS FLOW RATE VERSUS R

MEASUREMENT UNCERTAINTIES OF 3.5% FOR FLOW AND 4.0% FOR INCORE MEASUREMENT OF $F_{\Delta H}^{N}$ ARE INCLUDED IN THIS FIGURE

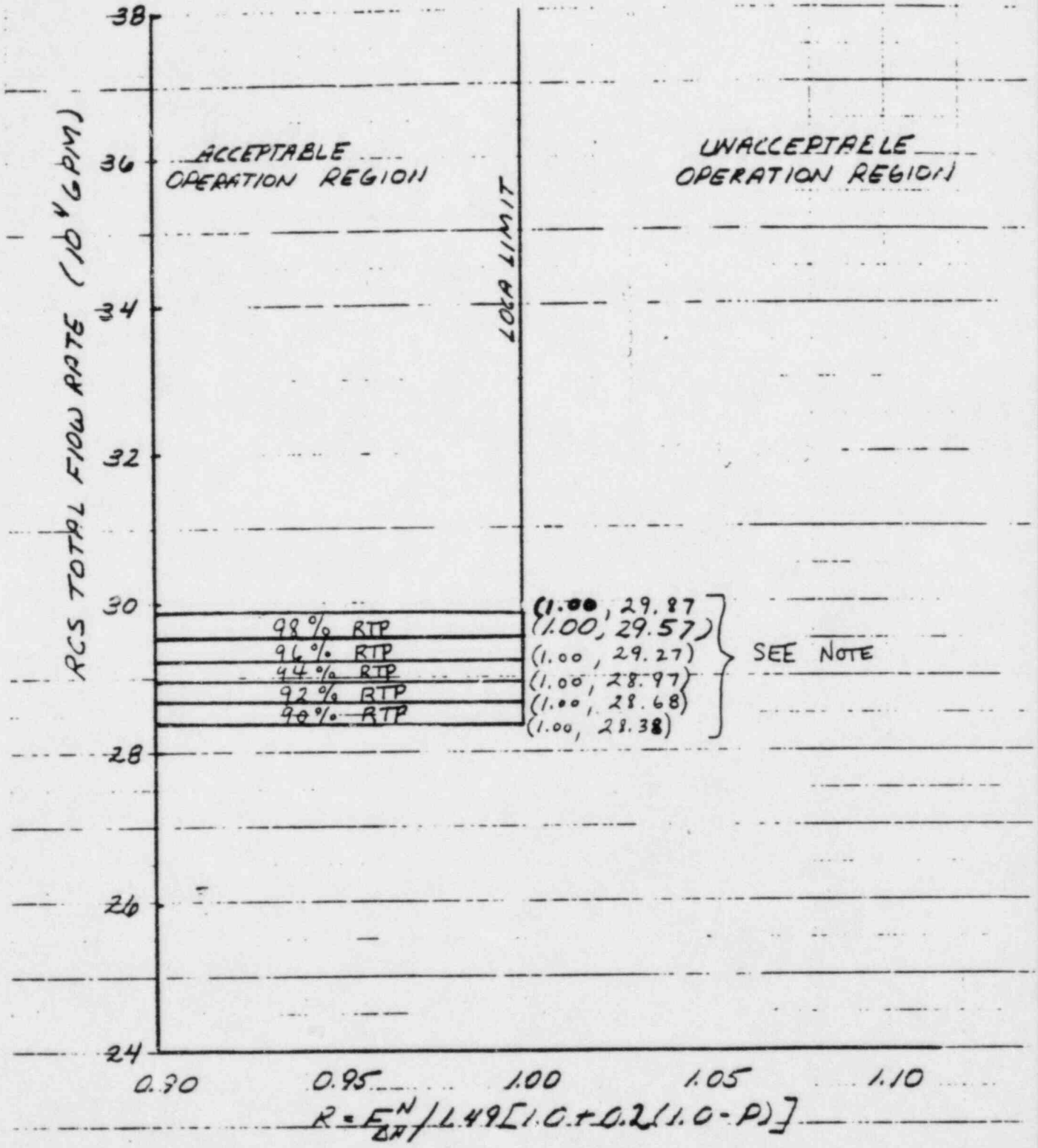

FIGURE 3.2-3 RCS TOTAL FLOW RATE VS R

THREE LOOP OPERATION

NOTE: When operating in this region, the restricted power levels shall be considered to be 100% of Rated Thermal Power (RTP) for Figure 2.

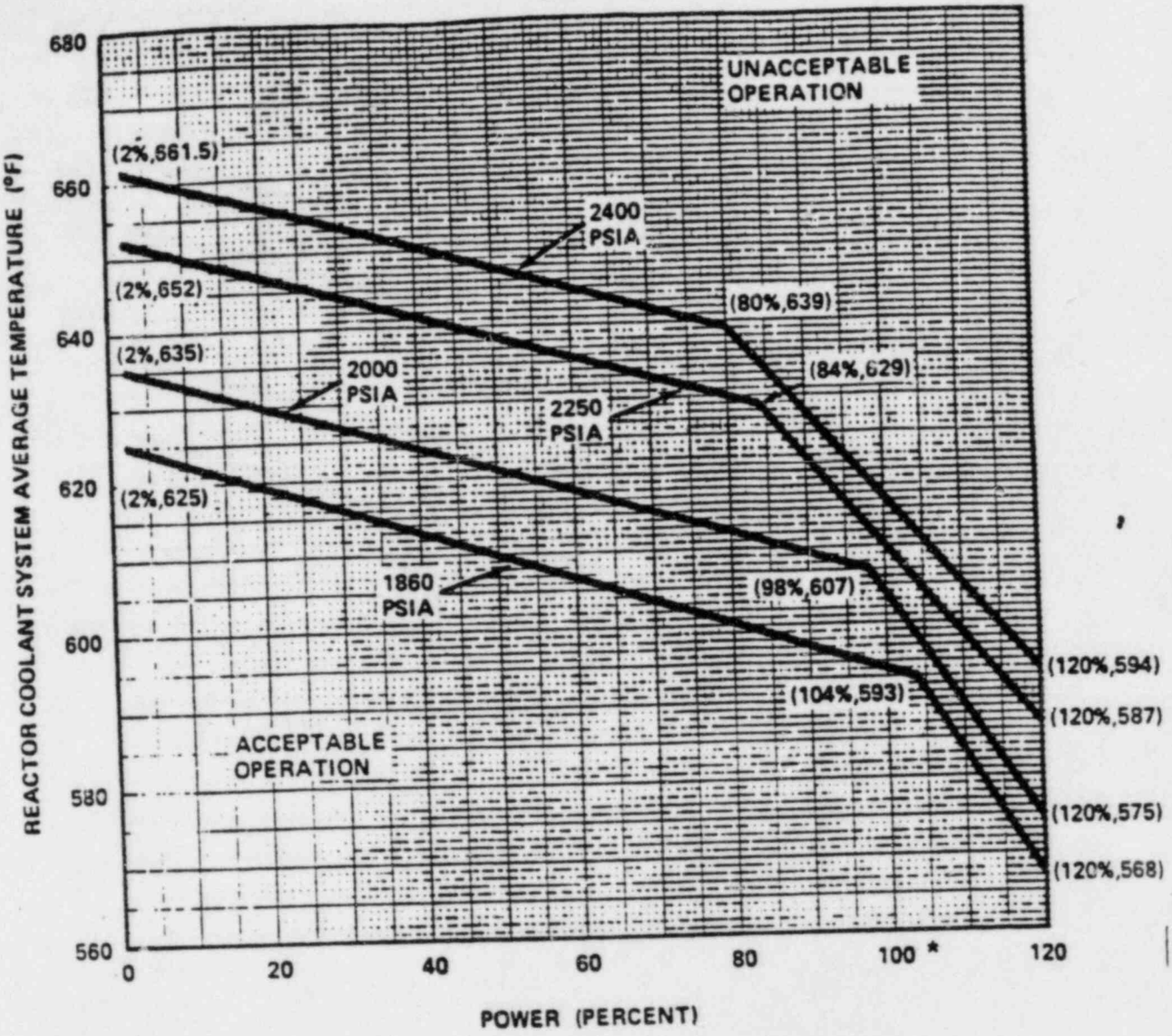

Figure 2.1-1
Reactor Core Safety Limit - Three Loops in Operation

* When operating in ~~Region III~~ the reduced RTP region of Technical Specificial 3.2.3 (Figure 3.2-3), the restricted power level must be considered 100% RTP for this figure.

Delete this page

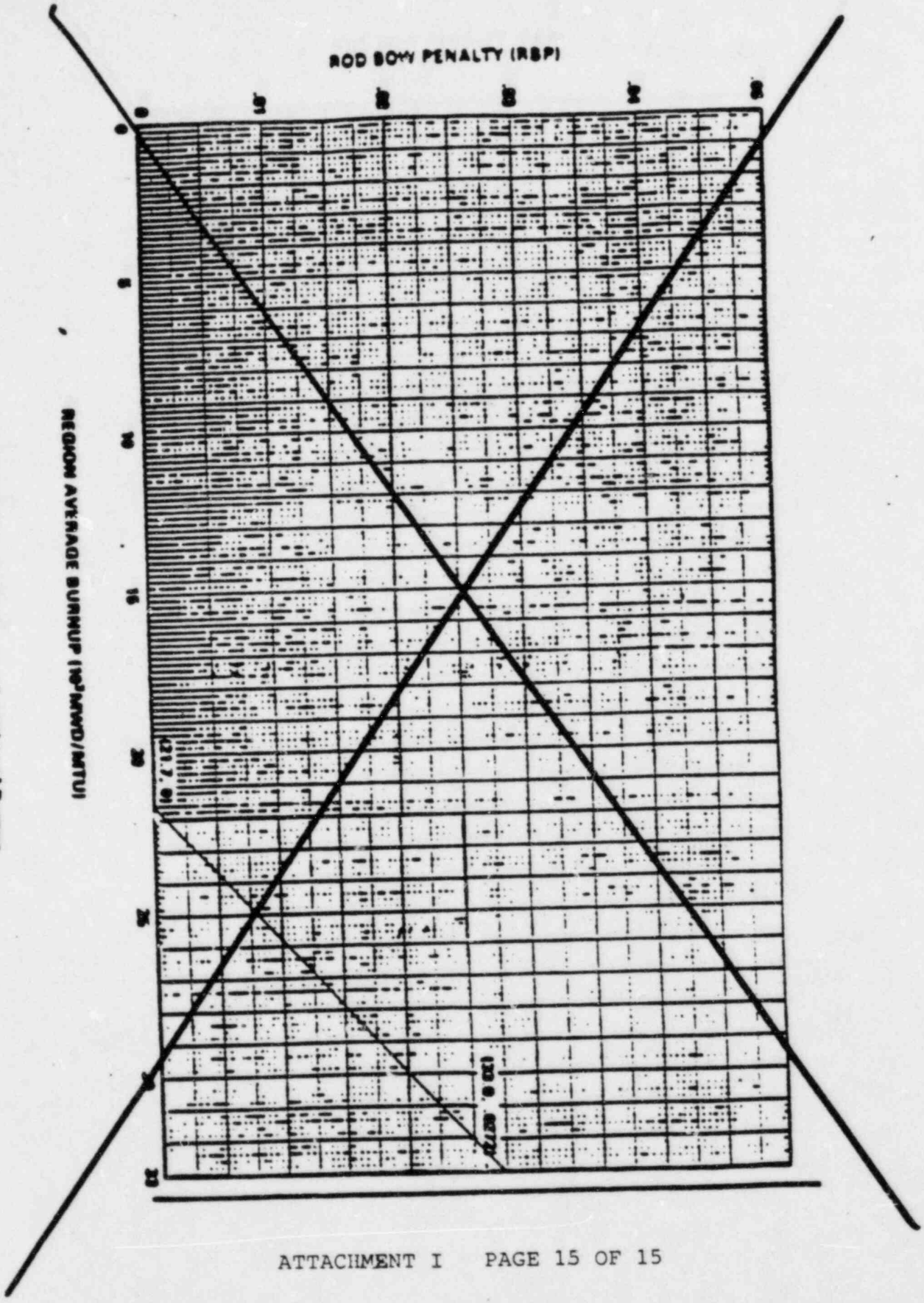

Figure 3.2-4 Rod Bow Penalty as a Function of Burnup

FSAR Revision

2. Inlet Flow Maldistribution:

The consideration of inlet flow maldistribution in core thermal performances is discussed in Section 4.4.3.1.2. A design basis of 5 percent reduction in coolant flow to the hot assembly is used in the THINC-IV analysis.

3. Flow Redistribution:

The flow redistribution accounts for the reduction in flow in the hot channel resulting from the high flow resistance in the channel due to the local or bulk boiling. The effect of the nonuniform power distribution is inherently considered in the THINC analysis for every operating condition which is evaluated.

4. Flow Mixing:

The subchannel mixing model incorporated in the THINC Code and used in reactor design is based on experimental data[51] discussed in Section 4.4.3.4.1. The mixing vanes incorporated in the spacer grid design induce additional flow mixing between the various flow channels in a fuel assembly as well as between adjacent assemblies. This mixing reduces the enthalpy rise in the hot channel resulting from local power peaking or unfavorable mechanical tolerances.

(PLACE INSERT B here)

4.4.2.4 Flux Tilt Considerations

Significant quadrant power tilts are not anticipated during normal operation since this phenomenon is caused by some asymmetric perturbation. A dropped or misaligned rod cluster control assembly could cause changes in hot channel factors; however, these events are analyzed separately in Chapter 15. This discussion will be confined to flux tilts caused by x-y xenon transients, inlet temperature mismatches, enrichment variations within tolerances and so forth.

The design value of the enthalpy rise hot channel factor $F^N_{\Delta H}$, which includes an eight percent uncertainty (as discussed in Section 4.3.2.2.7), is assumed to be sufficiently conservative that flux tilts up to and including the alarm point (see Technical Specifications) will not result in values of $F^N_{\Delta H}$ greater than that assumed in this submittal. The design value of F_Q does not include a specific allowance for quadrant flux tilts.

4.4.2.5 Void Fraction Distribution

The calculated core average and the hot subchannel maximum average void fractions are presented in Table 4.4-3 for operation at full power with design hot channel factors. The void fraction distribution in the core at various radial and axial locations is presented in Reference [52]. The void models used in the THINC-IV computer code are described in Section 4.4.2.8.3.

FSAR INSERT B
(NEW SECTION)

4.4.2.3.4.3 - Effects of Rod Bow on DNBR

The phenomenon of fuel rod bowing, as described in Reference (95), must be accounted for in the DNBR safety analysis of Condition 1 and Condition II events for each plant application. Applicable generic credits for margin resulting from retained conservatism in the evaluation of the DNBR and/or margin obtained from the measured plant operating parameters (such as $F^N_{\Delta H}$ or core flow) -- which are less limiting that those required by the plant safety analysis -- can be used to offset the effect of rod bow.

For the safety analysis of the Virgil C. Summer Unit, sufficient margin was maintained (9.1%)* to accommodate full and low flow DNBR penalties (<3% for the worst case, which is a burnup of 33,000 MWD/MTU) identified in Reference (96).

The maximum rod bow penalties accounted for in the design safety analysis are based on an assembly average burnup of 33,000 MWD/MTU. At burnups greater than 33,000 MWD/MTU, credit is taken for the effect of $F^N_{\Delta H}$ burndown, due to the decrease in fissionable isotopes and the buildup of fission product inventory, and no additional rod bow penalty is required.

---

*Design Limit DNBR of 1.30 vs. 1.28
Grid Spacing (K_s) of 0.046 vs. 0.059
Thermal Diffusion Coefficient of 0.038 vs. 0.059
DB Multiplier of 0.86 vs. 0.88
Pitch Reduction

Add following to FSAR Section 4.4 Reference List:

95. Skaritka, J. (Ed.), "Fuel Rod Bow Evaluation," WCAP-8691 Revision 1, July, 1979.

96. "Partial Response to Request Number 1 for Additional Information on WCAP-8691, Revision 1" letter, E. P. Rahe, Jr. (Westinghouse to J. R. Miller (NRC), NS-EPR-2515, dated October 9, 1981; "Remaining Response to Request Number 1 for Additional Information on WCAP-8691, Revision 1" letter, E. P. Rahe, Jr. (Westinghouse) to J. R. Miller (NRC), NS-EPR-2572, dated March 15, 1982.

15.4.1 MAJOR REACTOR COOLANT SYSTEM PIPE RUPTURES (LOSS OF COOLANT ACCIDENT)

Identification of Causes and Frequency Classification

A loss-of-coolant accident (LOCA) is the result of a pipe rupture of the RCS pressure boundary. For the analyses reported here, a major pipe break (large break) is defined as a rupture with a total cross-sectional area equal to or greater than 1.0 ft^2. This event is considered an ANS Condition IV event, a limiting fault, in that it is not expected to occur during the lifetime of Virgil C. Summer, but is postulated as a conservative design basis. The results for the small break loss of coolant accident are presented in Section 15.3.1. The boundary considered for loss of coolant accidents are related to connecting pipe as defined in Section 3.6.

The Acceptance Criteria for the LOCA are described in 10 CFR 50.46 (10 CFR 50.46 and Appendix K of 10 CFR 50 1974)[1] as follows:

1. The calculated peak fuel element clad temperature is below the requirement of 2,200°F.

2. The amount of fuel element cladding that reacts chemically with water or steam does not exceed 1 percent of the total amount of Zircaloy in the reactor.

3. The clad temperature transient is terminated at a time when the core geometry is still amenable to cooling. The localized cladding oxidation limit of 17 percent is not exceeded during or after quenching.

4. The core remains amenable to cooling during and after the break.

5. The core temperature is reduced and decay heat is removed for an extended period of time, as required by the long-lived radioactivity remaining in the core.

These criteria were established to provide significant margin in emergency core cooling system (ECCS) performance following a LOCA. WASH-1400 (USNRC 1975)[10] presents a recent study in regards to the probability of occurrence of RCS pipe ruptures.

Sequence of Events and Systems Operations

Should a major break occur, depressurization of the RCS results in a pressure decrease in the pressurizer. The reactor trip signal subsequently occurs when the pressurizer low pressure trip setpoint is reached. A safety injection signal is generated when the appropriate setpoint is reached. These countermeasures will limit the consequences of the accident in two ways:

1. Reactor trip and borated water injection supplement void formation in causing rapid reduction of power to a residual level corresponding to fission product decay heat. However, no credit is taken in the LOCA analysis for the boron content of the injection water. In addition, the insertion of control rods to shut down the reactor is neglected in the large break analysis.

2. Injection of borated water provides for heat transfer from the core and prevent excessive clad temperatures.

Description of Large Break Loss-of-Coolant Accident Transient

The sequence of events following a large break LOCA is presented in Table 15.4.1-1.

Before the break occurs, the unit is in an equilibrium condition; that is, the heat generated in the core is being removed via the secondary system. During blowdown, heat from fission product decay, hot internals and the vessel, continues to be transferred to the reactor coolant. At the beginning of the blowdown phase, the entire RCS contains subcooled liquid which transfers heat from the core by forced convection with some fully developed nucleate boiling. After the break develops, the time to departure from nucleate

boiling is calculated, consistent with Appendix K of 10 CFR 50.[1] Thereafter the core heat transfer is unstable, with both nucleate boiling and film boiling occurring. As the core becomes uncovered, both turbulent and laminar forced convection and radiation are considered as core heat transfer mechanisms.

The heat transfer between the RCS and the secondary system may be in either direction, depending on the relative temperatures. In the case of continued heat addition to the secondary system, the secondary system pressure increases and the main steam safety valves may actuate to limit the pressure. Makeup water to the secondary side is automatically provided by the emergency feedwater system. The safety injection signal actuates a feedwater isolation signal which isolates normal feedwater flow by closing the main feedwater isolation valves, and also initiates emergency feedwater flow by starting the emergency feedwater pumps. The secondary flow aids in the reduction of RCS pressure.

When the RCS depressurizes to 600 psia, the accumulators begin to inject borated water into the reactor coolant loops. The conservative assumption is made that accumulator water injected bypasses the core and goes out through the break until the termination of bypass. This conservatism is again consistent with Appendix K of 10CFR50. Since loss of offsite power (LOOP) is assumed, the RCPs are assumed to trip at the inception of the accident. The effects of pump coastdown are included in the blowdown analysis.

The blowdown phase of the transient ends when the RCS pressure (initially assumed at 2280 psia) falls to a value approaching that of the containment atmosphere. Prior to or at the end of the blowdown, the mechanisms that are responsible for the emergency core cooling water injected into the RCS bypassing the core are calculated not to be effective. At this time (called end-of-bypass) refill of the reactor vessel lower plenum begins. Refill is completed when emergency core cooling water has filled the lower plenum of the reactor vessel, which is bounded by the bottom of the fuel rods (called bottom of core recovery time).

The reflood phase of the transient is defined as the time period lasting from the end-of-refill until the reactor vessel has been filled with water to the extent that the core temperature rise has been terminated. From the latter stage of blowdown and then the beginning-of-reflood, the safety injection accumulator tanks rapidly discharge borated cooling water into the RCS, contributing to the filling of the reactor vessel downcomer. The downcomer water elevation head provides the driving force required for the reflooding of the reactor core. The low head and high head safety injection pumps aid in the filling of the downcomer and subsequently supply water to maintain a full downcomer and complete the reflooding process.

Continued operation of the ECCS pumps supplies water during longterm cooling. Core temperatures have been reduced to longterm steady state levels associated with dissipation of residual heat generation. After the water level of the refueling water storage tank (RWST) reaches a minimum allowable value, coolant for long-term cooling of the core is obtained by switching to the cold recirculation phase of operation, in which spilled borated water is drawn from the engineered safety features (ESF) containment sumps by the low head safety injection (residual heat removal) pumps and returned to the RCS cold legs. The containment spray system continues to operate to further reduce containment pressure.

Approximately 24 hours after initiation of the LOCA, the ECCS is realigned to supply water to the RCS hot legs in order to control the boric acid concentration in the reactor vessel.

Core and System Performance

Mathematical Model:

The requirements of an acceptable ECCS evaluation model are presented in Appendix K of 10 CFR 50 (Federal Register 1974).[1]

Large Break LOCA Evaluation Model

The analysis of a large break LOCA transient is divided into three phases: (1) blowdown, (2) refill, and (3) reflood. There are three distinct transients analyzed in each phase, including the thermal-hydraulic transient in the RCS, the pressure and temperature transient within the containment, and the fuel and clad temperature transient of the hottest fuel rod in the core. Based on these considerations, a system of interrelated computer codes has been developed for the analysis of the LOCA.

A description of the various aspects of the LOCA analysis methodology is given by Bordelon, Massie, and Zordon (1974).[6] This document describes the major phenomena modeled, the interfaces among the computer codes, and the features of the codes which ensure compliance with the Acceptance Criteria. The SATAN-VI, WREFLOOD, BART, LOCTA-IV, and COCO codes, which are used in the LOCA analysis, are described in detail by Bordelon et at. (1974)[5]; Kelly et al. (1974)[9]; Young et al. (1980)[8]; Bordelon and Murphy (1974)[4]; Bordelon and Murphy (1974)[3]. Code modifications are specified in References 2, 7 and 14. These codes assess the core heat transfer geometry and determine if the core remains amenable to cooling throughout and subsequent to the blowdown, refill, and reflood phases of the LOCA. The SATAN-VI computer code analyses the thermal-hydraulic transient in the RCS during blowdown and the WREFLOOD computer code calculates this transient during the refill and reflood phases to the accident. The COCO code is used for the complete containment pressure history for dry containments. The LOCTA-IV computer code calculates the thermal transient of the hottest fuel rod during the three phases. The Revised Pad Fuel Thermal Safety Model, described in Reference 14, generates the initial fuel rod conditions input to LOCTA-IC.

SATAN-VI calculates the RCS pressure, enthalpy, density, and the mass and energy flow rates in the RCS, as well as steam generator energy transfer between the primary and secondary systems as a function of time during the blowdown phase of the LOCA. SATAN-VI also calculates the accumulator water mass and internal pressure and the pipe break mass and energy flow rates that

are assumed to be vented to the containment during blowdown. At the end of the blowdown phase, these data are transferred to the WREFLOOD code. Also, at the end-of-blowdown, the mass and energy release rates during blowdown are input to the COCO code for use in the determination of the containment pressure response during blowdown. Additional SATAN-VI output data from the end-of-blowdown, including the core inlet flow rate and enthalpy, the core pressure, and the core power decay transient, are input to the LOCTA-IV code.

With input from the SATAN-VI code, WREFLOOD uses a system thermal-hydraulic model to determine the core flooding rate (that is, the rate at which coolant enters the bottom of the core), the coolant pressure and temperature, and the quench front height during the reflood phase of the LOCA. WREFLOOD also calculates the mass and energy flow addition to the containment through the break. WREFLOOD is also linked to the BART and LOCTA-IV codes. The heat transfer calculation for average fuel channel in the hot assembly during the reflood phase of the LOCA is performed by the BART[8] computer code using a mechanistic core heat transfer model. This information is used by LOCTA-IV throughout the analysis of the LOCA transient to calculate the fuel clad temperature and metal-water reaction of the hottest rod in the core.

The large break analysis was performed with the December 1981 version of the Evaluation Model modified to incorporate the BART[8] computer code.

Input Parameters and Initial Conditions:

The analysis presented in this section was performed with a reactor vessel upper head temperature equal to the RCS cold leg temperature.

The bases used to select the numerical values that are input parameters to the analysis have been conservatively determined from extensive sensitivity studies (Westinghouse 1974[12]; Salvatori 1974[11]). In addition, the requirements of Appendix K regarding specific model features were met by selecting models which provide a significant overall conservatism in the analysis. The assumptions which were made pertain to the conditions of the reactor and associated safety system equipment at the time that the LOCA

occurs, and include such items as the core peaking factors, the containment pressure, and the performance of the ECCS. Decay heat generated throughout the transient is also conservatively calculated.

Results:

Based on the results of the LOCA sensitivity studies (Westinghouse 1974[12]; Salvatori 1974[11]) the limiting large break was found to be the double ended cold leg guillotine (DECLG). Therefore, only the DECLG break is considered in the large break ECCS performance analysis. Calculations were performed for a range of Moody break discharge coefficients. The results of these calculations are summarized in Tables 15.4.1-1 and 15.4.1-2. The hot spot is defined to be the location of the maximum peak clad temperature. This location is given in Table 15.4.1-2 for each break size analyzed.

Containment data used to calculated ECCS back pressure is presented in Table 15.4.1-3.

Figures 15.4.1-1a through 15.4.1-16 present the transients for the principal parameters for the break sizes analyzed. The following items are noted:

Figures 15.4.1-1a through 15.4.1-3c

The following quantities are presented at the clad burst location and at the hot spot (location of maximum clad temperature), both on the hottest fuel rod (hot rod):

1. fluid quality;
2. mass velocity;
3. heat transfer coefficient.

The heat transfer coefficient shown is calculated by the LOCTA-IV code.

Figures 15.4.1-4a through 15.4.1-6c

The system pressure shown is the calculated pressure in the core. The flow rate from the break is plotted as the sum of both ends for the guillotine break cases. The core pressure drop shown is from the lower plenum, near the core, to the upper plenum at the core outlet.

Figure 15.4.1-7a through 15.4.1-9c — These figures show the hot spot clad temperature transient and the clad temperature transient at the burst location. The fluid temperature shown is also for the hot spot and burst location. The core flow (top and bottom) is also shown.

Figures 15.4.1-10a through 15 4.1-10f — These figures show the core reflood transient.

Figures 15.4.1-11a through 15.4.1-12c — These figures show the Emergency Core Cooling System flow for all of the cases analyzed. As described earlier, the accumulator delivery during blowdown is discarded until the end of bypass is calculated. Accumulator flow, however, is established in the refill and the reflood calculations. The accumulator flow assumed is the sum of that injected in the intact cold legs.

Figures 15.4.1-13a through 15.4.1-13c — The containment pressure transient is also provided.

Figures 15.4.1-14 a, b, c — These figures show the core power transient.

Figure 15.4.1-16 — This figure provides the containment wall condensing heat transfer coefficient for the limiting case break.

In addition to the above, Tables 15.4.1-4 and 15.4.1-5 present the reflood mass and energy release to the containment and the broken loop accumulator mass and energy flowrate to the containment, respectively.

The maximum clad temperature calculated for a large break is 2132.0°F which is less than the Acceptance Criteria limit of 2200°F. The maximum local metal-water reaction is 4.85 percent, which is well below the embrittlement limit of 17 percent as required by 10 CFR 50.46. The total core metal-water reaction is less than 0.3 percent for all breaks, as compared with the 1 percent criterion of 10 CFR 50.46. The clad temperature transient is

terminated at a time when the core geometry is still amenable to cooling. As a result, the core temperature will continue to drop and the ability to remove decay heat generated in the fuel for an extended period of time will be provided.

REFERENCES FOR SECTION 15.4.1

1. "Acceptance Criteria for Emergency Core Cooling System for Light Water Cooled Nuclear Power Reactors," 10 CFR 50.46 and Appendix K of 10 CFR 50, Federal Register 1974, Volume 39, Number 3.

2. Rahe, E. P. (Westinghouse), letter to J. R. Miller (USNRC), Letter No. NS-EPRS-2679, November 1982.

3. Bordelon, F. M., and Murphy, E. T., "Containment Pressure Analysis Code (COCO)," WCAP-8327 (Proprietary), WCAP-8326 (Non-Proprietary), June, 1974.

4. Bordelon, F. M. et al., "LOCTA-IV Program: Loss-of-Coolant Transient Analysis," WCAP-8301 (Proprietary) and WCAP-8305 (Non-Proprietary), 1974.

5. Bordelon, F. M. et al., "SATAN-VI Program: Comprehensive Space, Time Dependent Analysis of Loss-of-Coolant," WCAP-8302 (Proprietary) and WCAP-8306 (Non-Proprietary), 1974.

6. Bordelon, F. M.; Massie, H. W.; and Zordon, T. A., "Westinghouse ECCS Evaluation Model - Summary," WCAP-8339, 1974.

7. Rahe, E. P., "Westinghouse ECCS Evaluation Model, 1981 Version," WCAP-9220-P-A (Proprietary Version), WCAP-9221-P-A (Non-Proprietary Version), Revision 1, 1981.

8. Young, M. Y. et al., "BART-A1: A Computer Code for the Best Estimate Analysis of Reflood Transients," WCAP-9561-P-A (Proprietary) and WCAP-9695-A (Non-Proprietary).

9. Kelly, R. D. et al., "Calculational Model for Core Reflooding After a Loss-of-Coolant Accident (WREFLOOD Code," WCAP-8170 (Proprietary) and WCAP-8171 (Non-Proprietary), 1974.

10. U. S. Nuclear Regulatory Commission 1975, "Reactor Safety Study - An Assessment of Accident Risks in U. S. Commercial Nuclear Power Plant," WASH-1400, NUREG-75/014.

11. Salvatori, R., "Westinghouse ECCS - Plant Sensitivity Studies," WCAP-8340 (Proprietary) and WCAP-8356 (Non-Proprietary), 1974.

12. "Westinghouse ECCS Evaluation Model Sensitivity Studies," WCAP-8341 (Proprietary) and WCAP-8342 (Non-Proprietary), 1974.

13. "Bordelon, F. M., et al., "Westinghouse ECCS Evaluation Model - Supplementary Information," WCAP-8471 (Proprietary) and WCAP-8472 (Non-Proprietary), 1975.

14. Letter from J. F. Stoltz (NRC) to T. M. Anderson (Westinghouse), Subject: Review of WCAP-8720, Improved Analytical Models used in Westinghouse Fuel Rod Design Computations.

TABLE 15.4.1-1

LARGE BREAK

TIME SEQUENCE OF EVENTS

	DECLG (C_D = 0.8) (Sec)	DECLG (C_D = 0.6) (Sec)	DECLG (C_D = 0.4) (Sec)
START	0.0	0.0	0.0
Reactor Trip Signal	0.404	0.409	0.418
S. I. Signal	0.63	0.71	0.87
Acc. Injection	9.24	11.5	15.5
End of Blowdown	22.22	25.14	30.996
Bottom of Core Recovery	34.45	37.11	43.45
Acc. Empty	41.309	44.197	49.576
Pump Injection	25.63	25.71	25.87
End of Bypass	22.22	25.06	30.923

TABLE 15.4.1-2

LARGE BREAK

	DECLG (C_D = 0.8)	DECLG (C_D = 0.6)	DECLG (C_D = 0.4)
Results			
Peak Clad Temp. °F	1866.0	2009.0	2132.0
Peak Clad Location Ft.	7.25	7.0	7.0
Local Zr/H_2O Reaction (max) %	2.338	3.55	4.85
Local Zr/H_2O Location Ft.	7.25	7.0	7.0
Total Zr/H_2O Reaction %	<0.3	<0.3	<0.3
Hot Rod Burst Time sec	63.8	46.0	47.0
Hot Rod Burst Location Ft.	6.75	6.0	6.0
Calculation			
NSSS Power Mwt 102% of		2775	
Peak Linear Power kw/ft 102% of		12.632	
Peaking Factor (At License Rating)		2.32	
Accumulator Water Volume (ft^3)		1000	

Fuel region + cycle analyzed	Cycle	Region
UNIT 1	ALL	ALL

6% Steam Generator Tube Plugging in each steam generator is assumed.

TABLE 15.4.1-3

LARGE BREAK
CONTAINMENT DATA
(DRY CONTAINMENT)

NET FREE VOLUME	1.9×10^6 ft^3
INITIAL CONDITIONS	
Pressure	14.7 psia
Temperature	90°F
RWST Temperature	40°F
Service Water Temperature	NA
Outside Temperature	19°F
SPRAY SYSTEM	
Total Flow Rate	6000 gpm
Actuation Time	52 secs
SAFEGUARDS FAN COOLERS	
Number of Fan Coolers Operating	2
Fastests Post Accicent Initiation of Fan Coolers	43 secs

TABLE 15.4.1-3 (Continued)

LARGE BREAK
CONTAINMENT DATA
(DRY CONTAINMENT)

STRUCTURAL HEAT SINKS

Thickness (In)		Area (Ft^2)
0.348 Carbon Steel	48.0 Concrete	57,397
0.264 Carbon Steel	36.0 Concrete	20,241
0.125 Carbon Steel	24.0 Concrete	11,694
18.0 Concrete		315
22.56 Concrete		43,537
12.0 Concrete		10,811
48.0 Concrete		19,020
1.52 Stainless Steel		409
1.13 Stainless Steel		551
0.6 Stainless Steel		1939
0.336 Stainless Steel		2194
0.06 Stainless Steel		88481
6.672 Carbon Steel		3300
3.504 Carbon Steel		130
2.376 Carbon Steel		2324
1.7568 Carbon Steel		4323
0.87 Carbon Steel		8787
0.744 Carbon Steel		17734
0.324 Carbon Steel		16929
0.06 Carbon Steel		654508

TABLE 15.4.1-4

REFLOOD MASS/ENERGY RELEASES* (C_D = 0.4)

TIME (SEC)	TOTAL MASS FLOWRATE (LBM/SEC)	TOTAL ENERGY FLOWRATE 10^5 BTU/SEC
44.023	0.0	0.0
50.045	48.177	0.617
64.970	66.77	0.841
84.170	127.19	1.121
104.170	292.42	1.515
125.770	300.31	1.469
164.420	340.72	1.483

*Accumulator nitrogen was released between 53.0 and 93.0 seconds at a mass flow rate of 96.135 lbm/sec.

TABLE 15.4.1-5

BROKEN LOOP ACCUMULATOR FLOWRATE TO CONTAINMENT FOR LIMITING CASE - DECLG (C_D = 0.4)

TIME (SEC)	MASS FLOWRATE* (LBM/SEC)
0.0	4598.0
3.01	3499.1
4.01	3281.7
5.01	3100.7
8.01	2690.5
11.01	2397.8
16.01	2052.5
21.01	1811.8
24.01	1700.5
24.87	0.0

*Enthalpy of accumulator water is 58 BTU/LBM

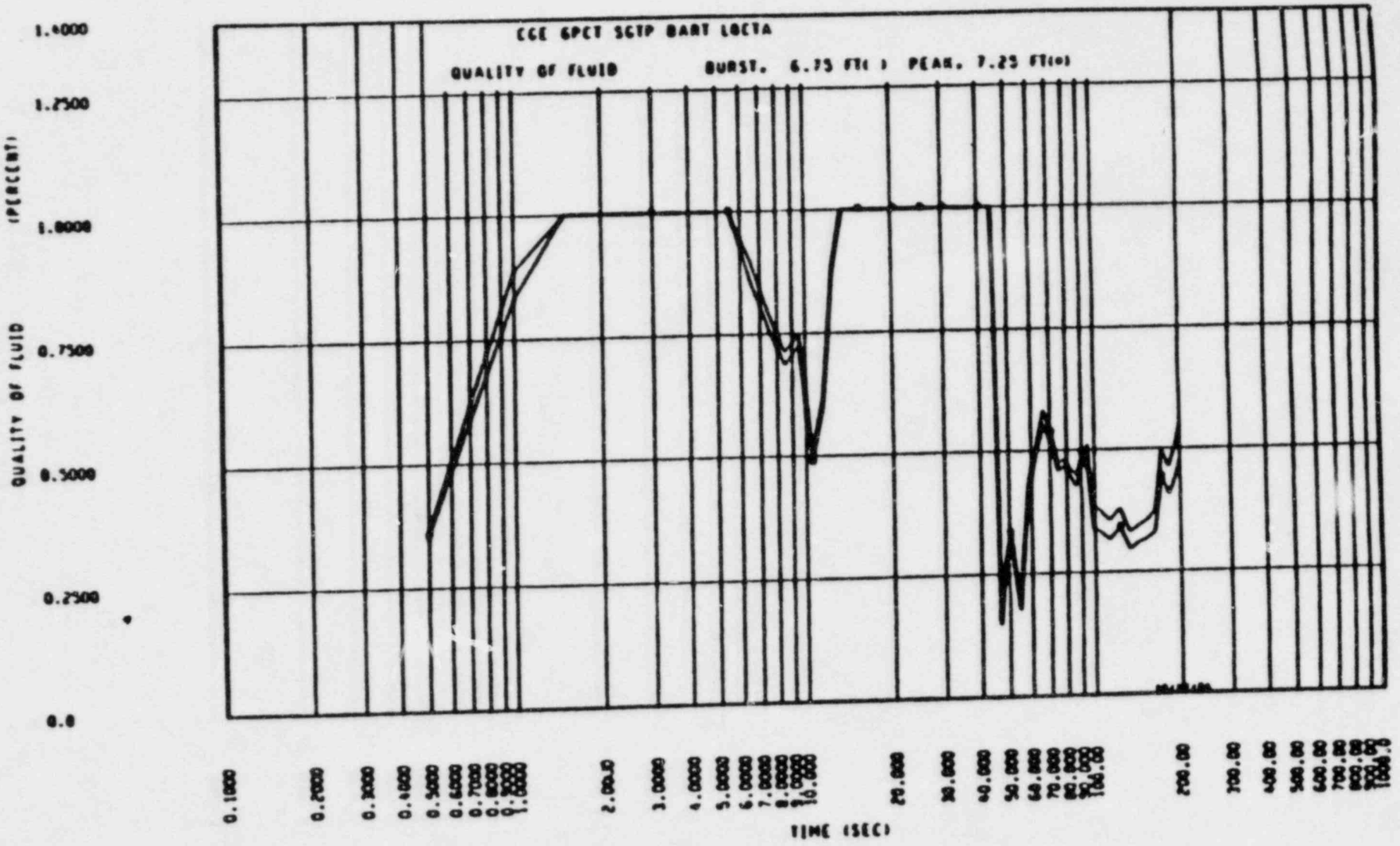

Figure 15.4.1-1a. Fluid Quality (C_D = 0.8)

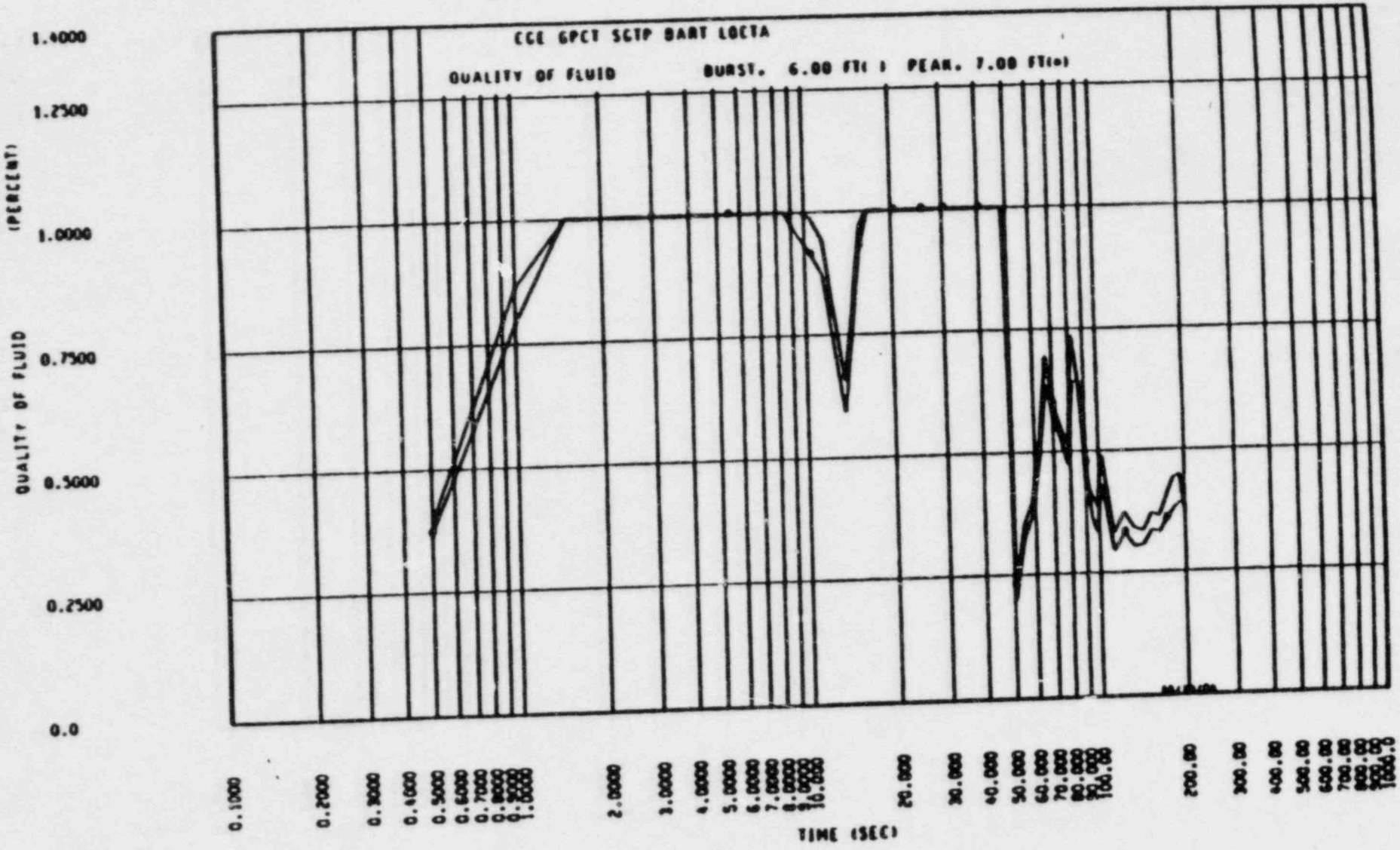

Figure 15.4.1-1b. Fluid Quality (C_D = 0.6)

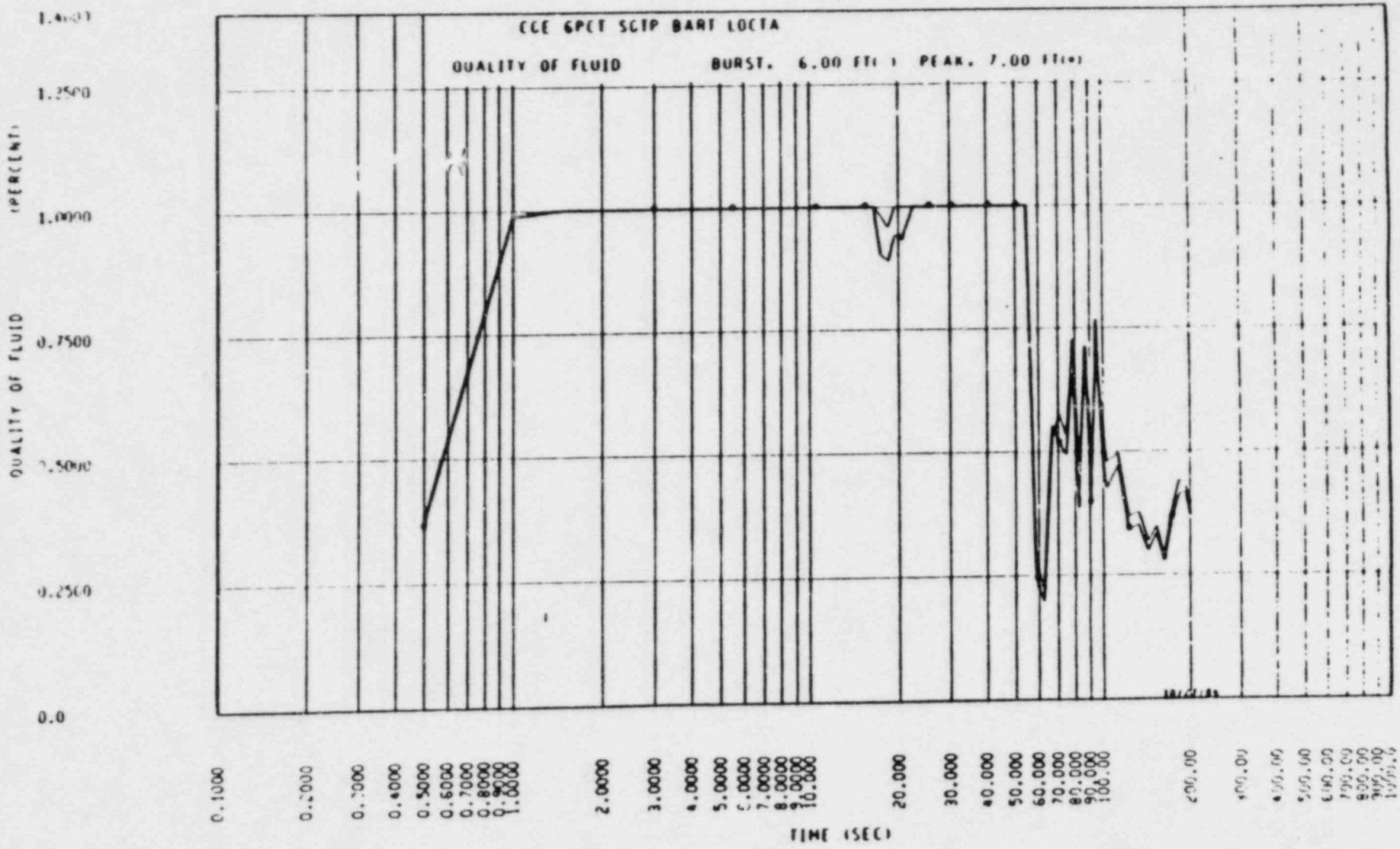

Figure 15.4.1-1c. Fluid Quality (C_D = 0.4)

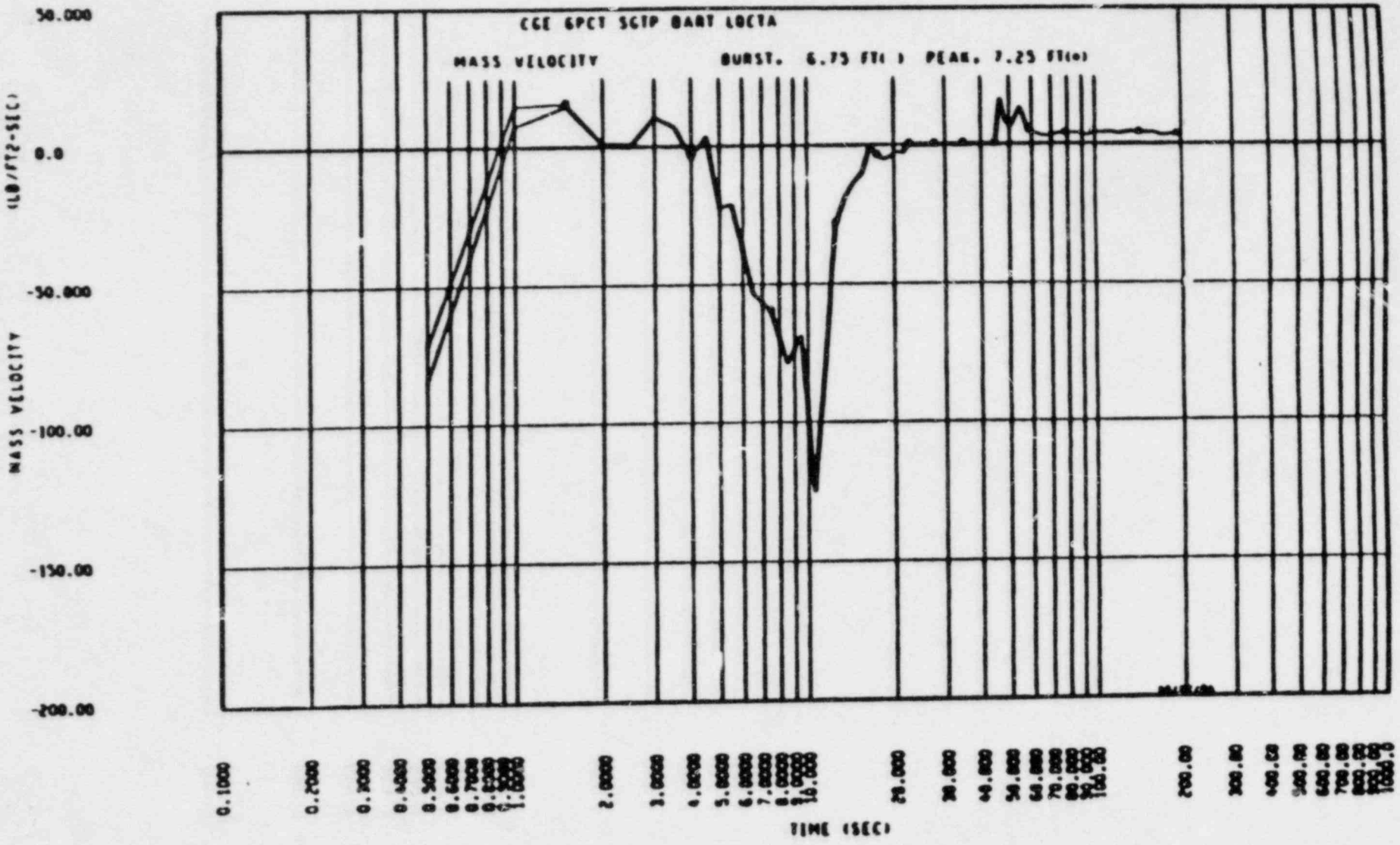

Figure 15.4.1-2a. Mass Velocity (C_D = 0.8)

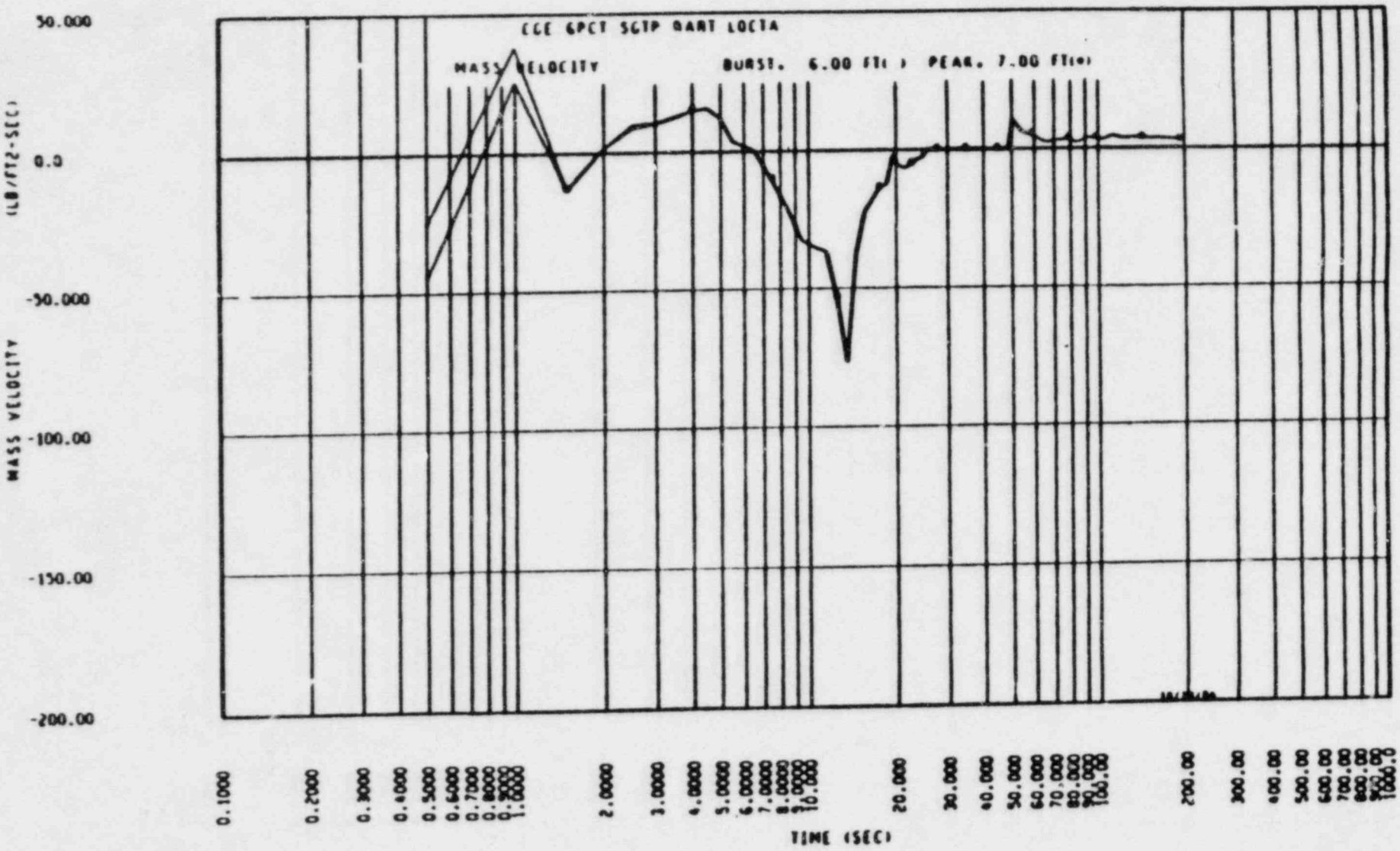

Figure 15.4.1-2b. Mass Velocity (C_D = 0.6)

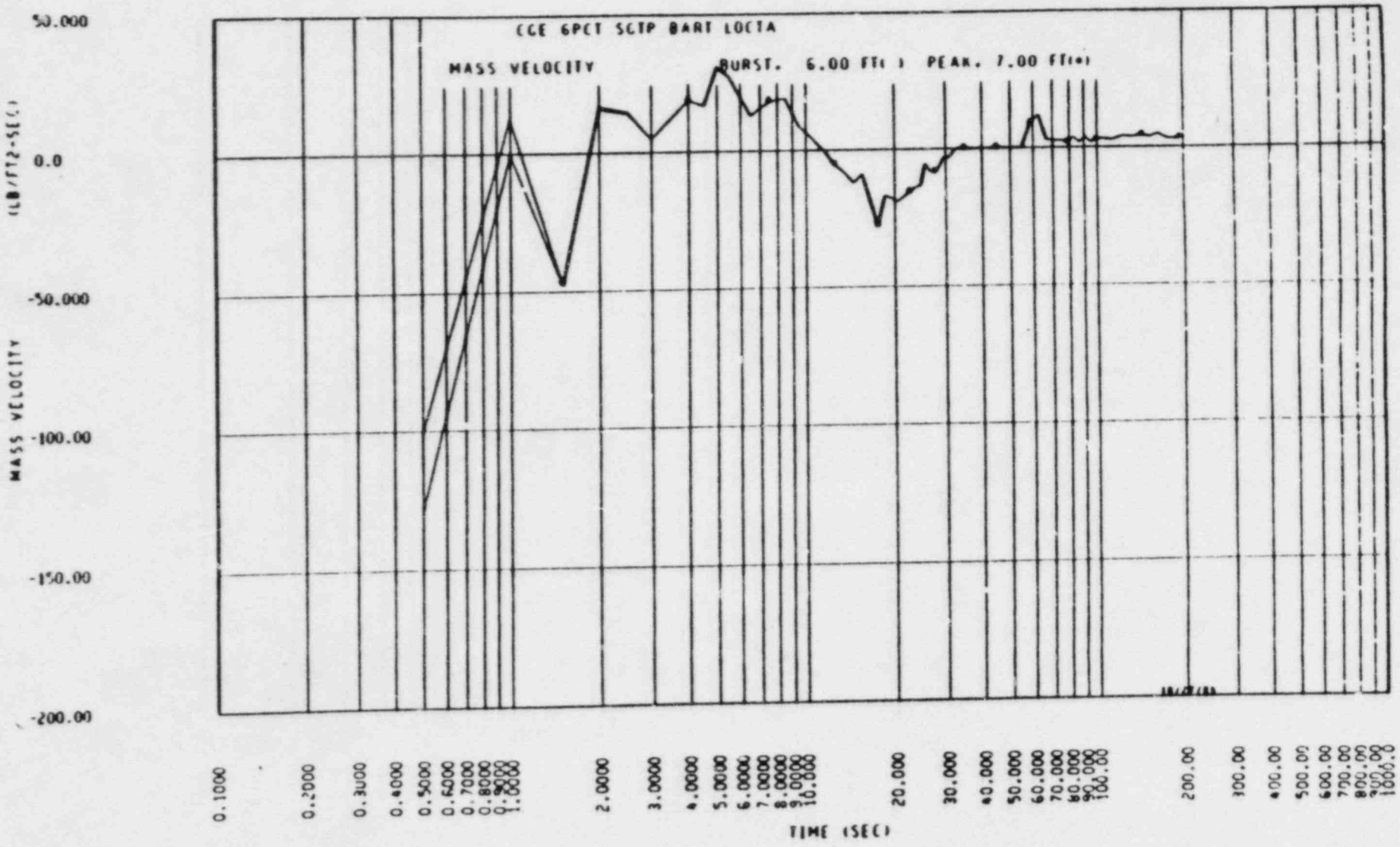

Figure 15.4.1-2c. Mass Velocity (C_D = 0.4)

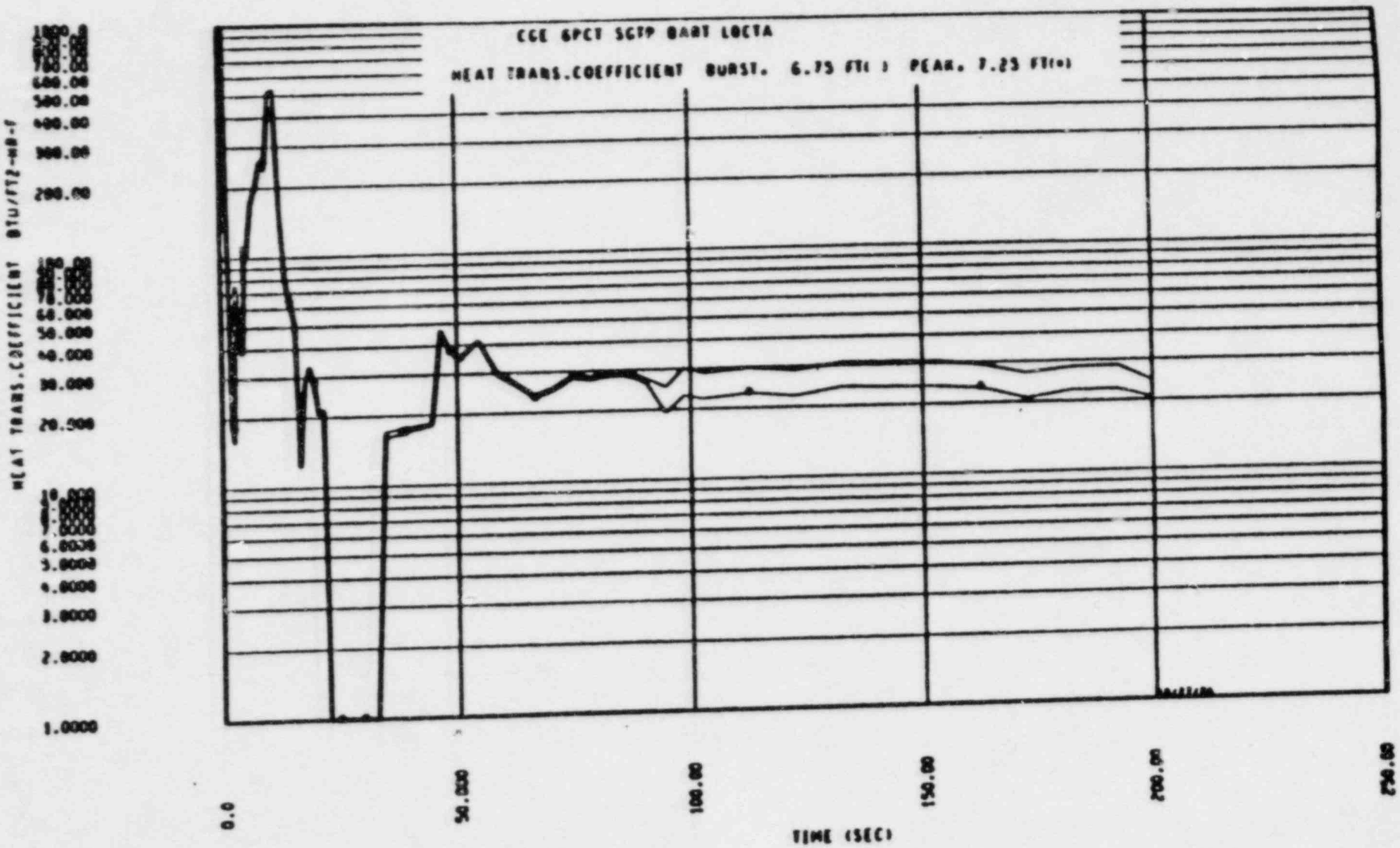

Figure 15.4.1-3a. Heat Transfer Coefficient (C_D = 0.8)

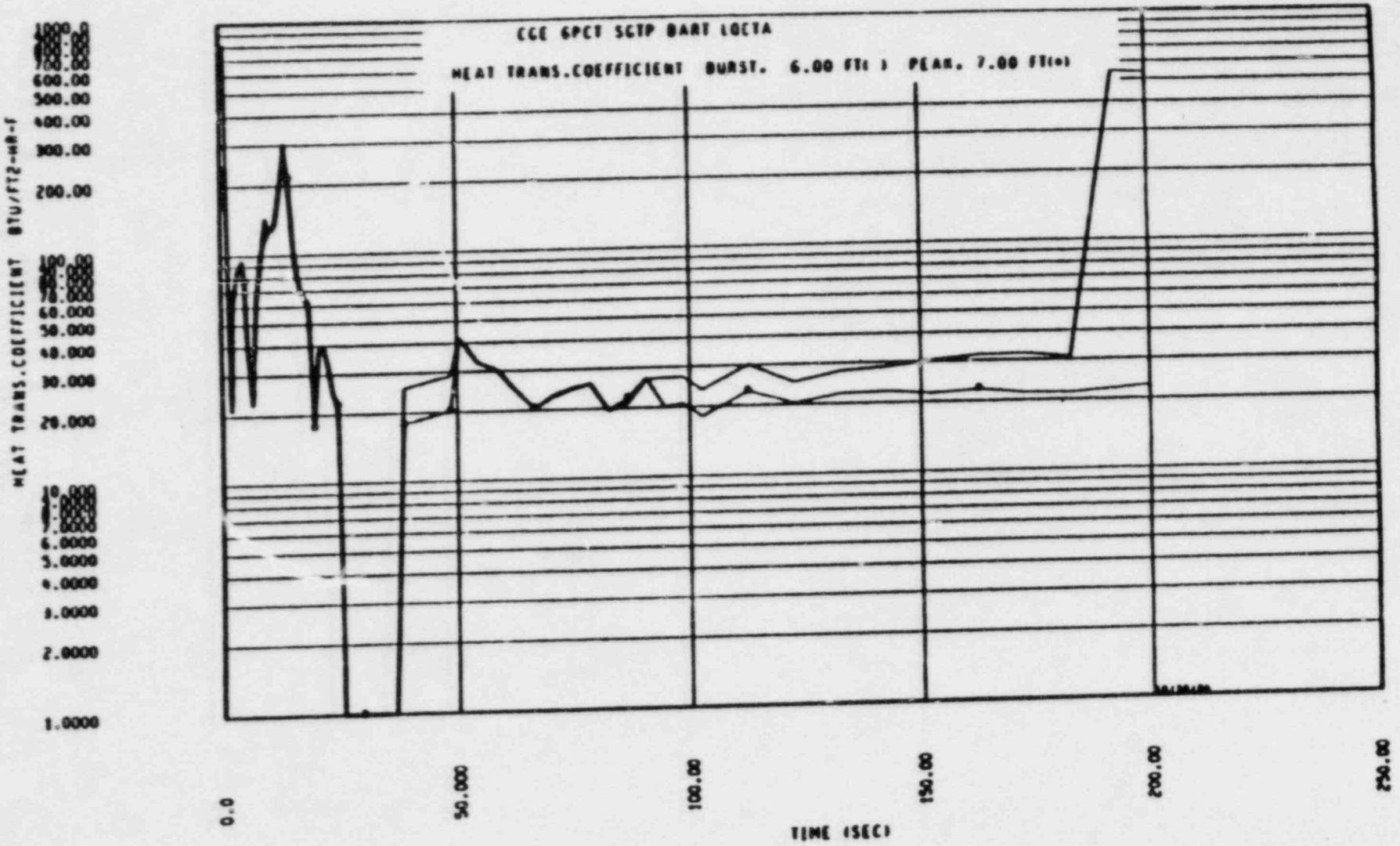

Figure 15.4.1-3b. Heat Transfer Coefficient (C_D = 0.6)

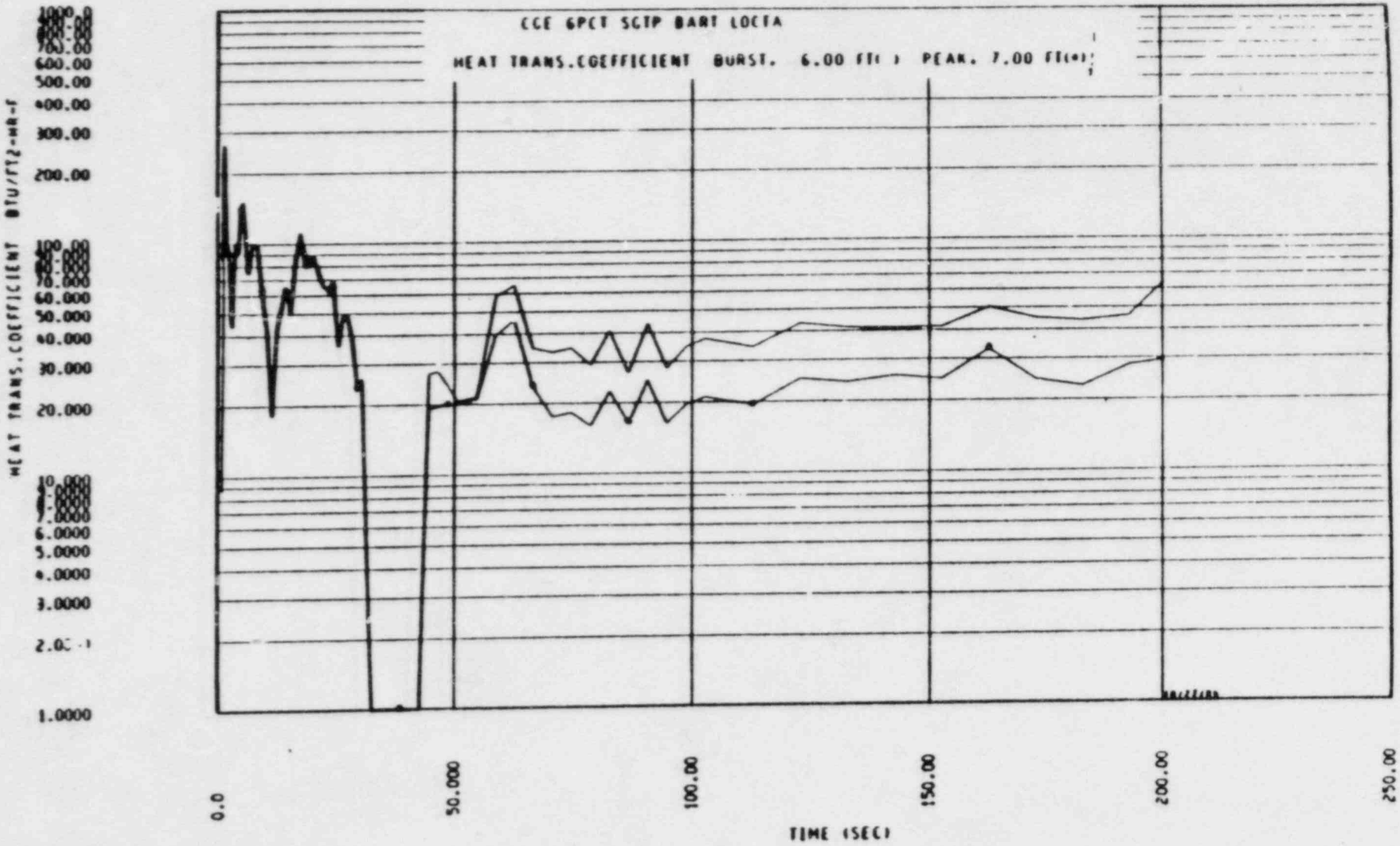

Figure 15.4.1-3c. Heat Transfer Coefficient (C_D = 0.4)

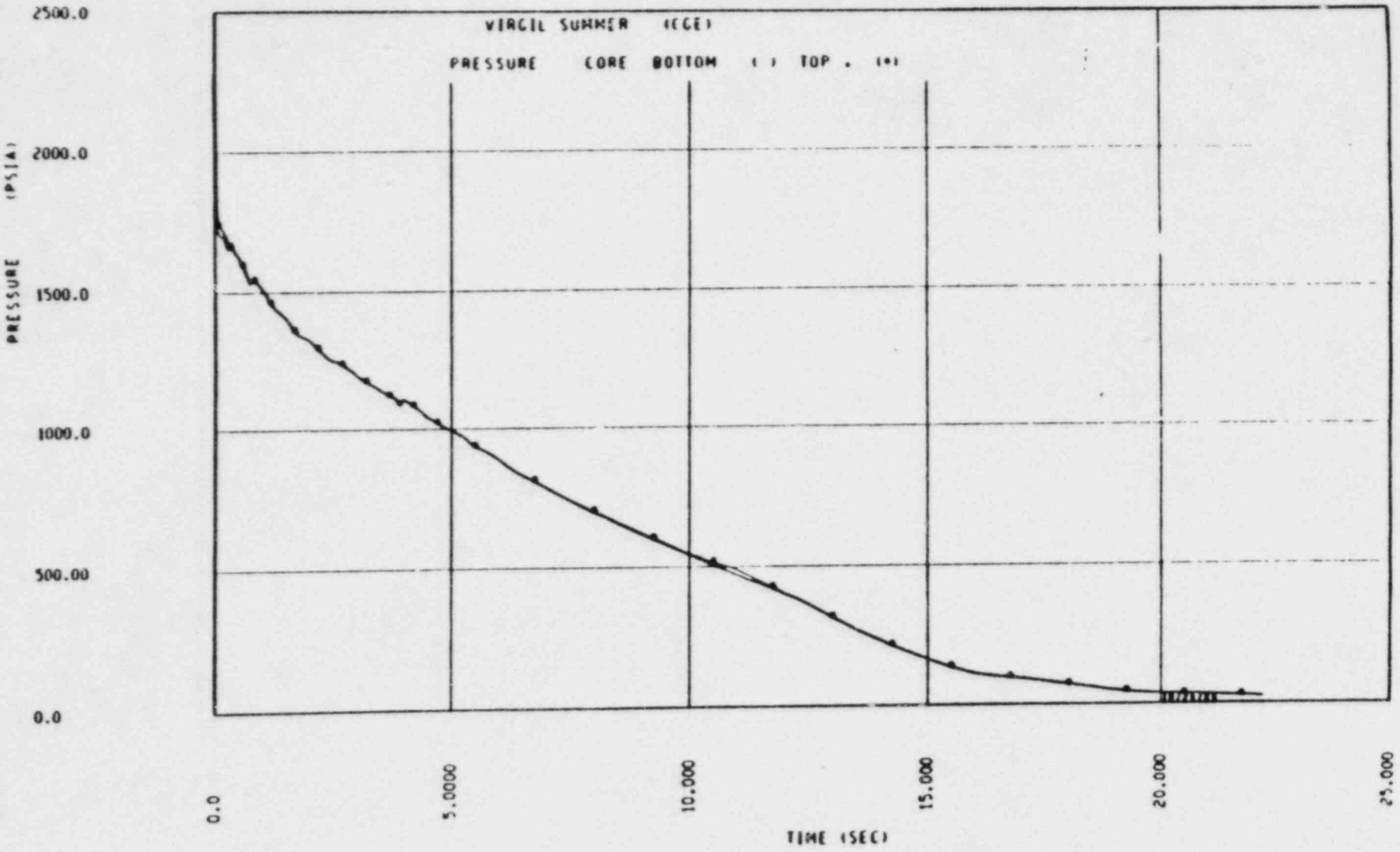

Figure 15.4.1-4a. Core Pressure (C_D = 0.8)

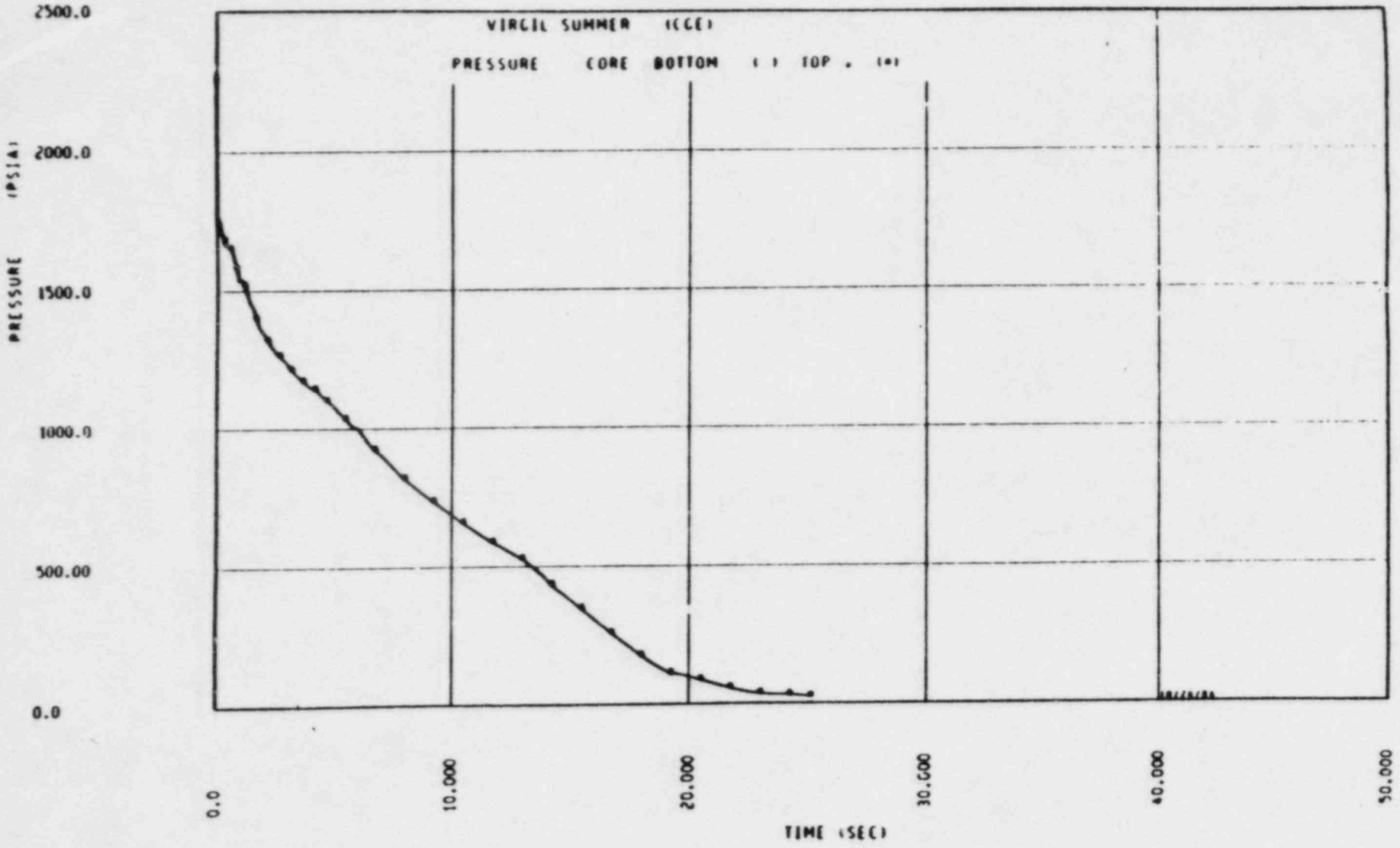

Figure 15.4.1-4b. Core Pressure (C_D = 0.6)

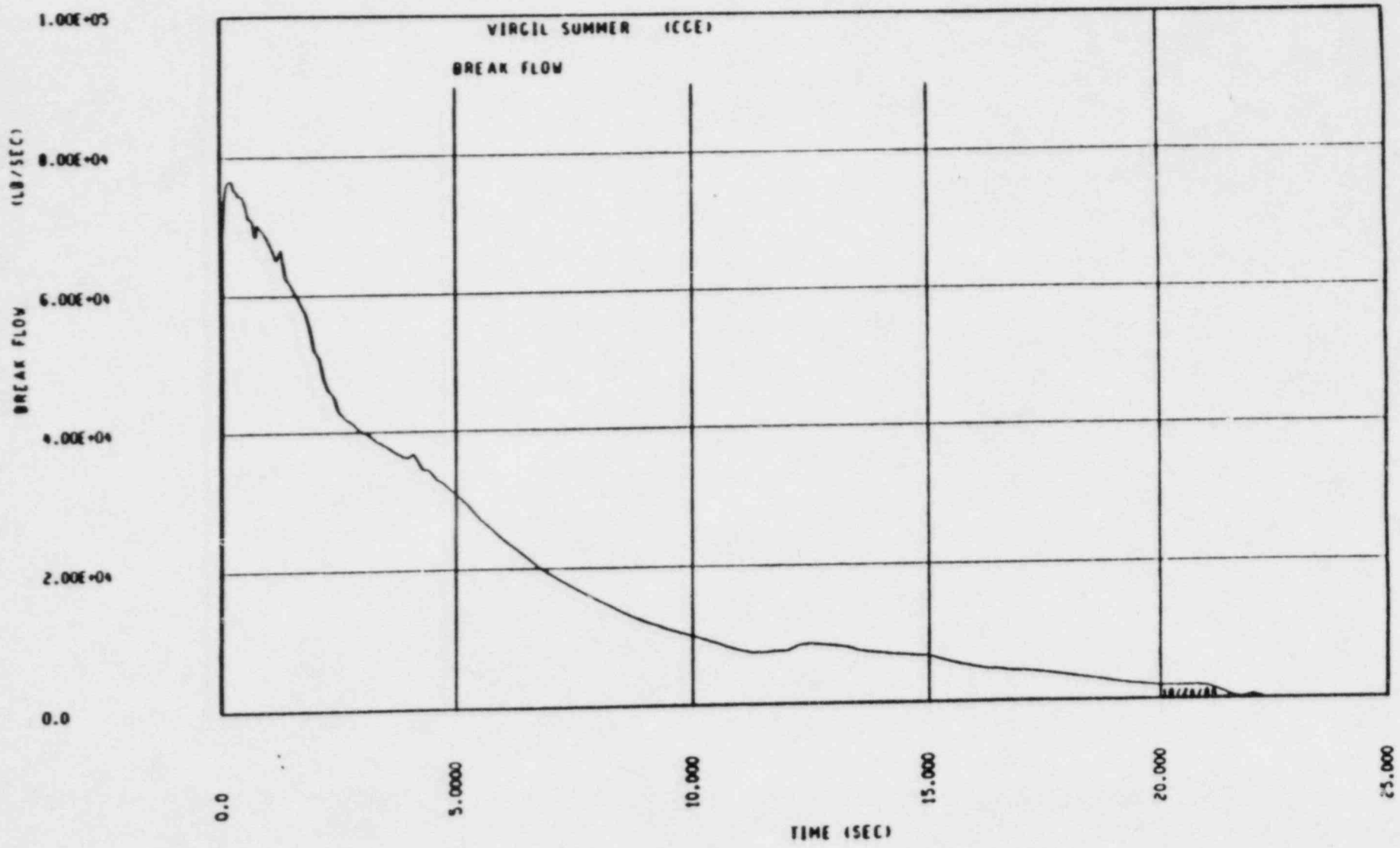

Figure 15.4.1-5a. Break Flow Rate (C_D = 0.8)

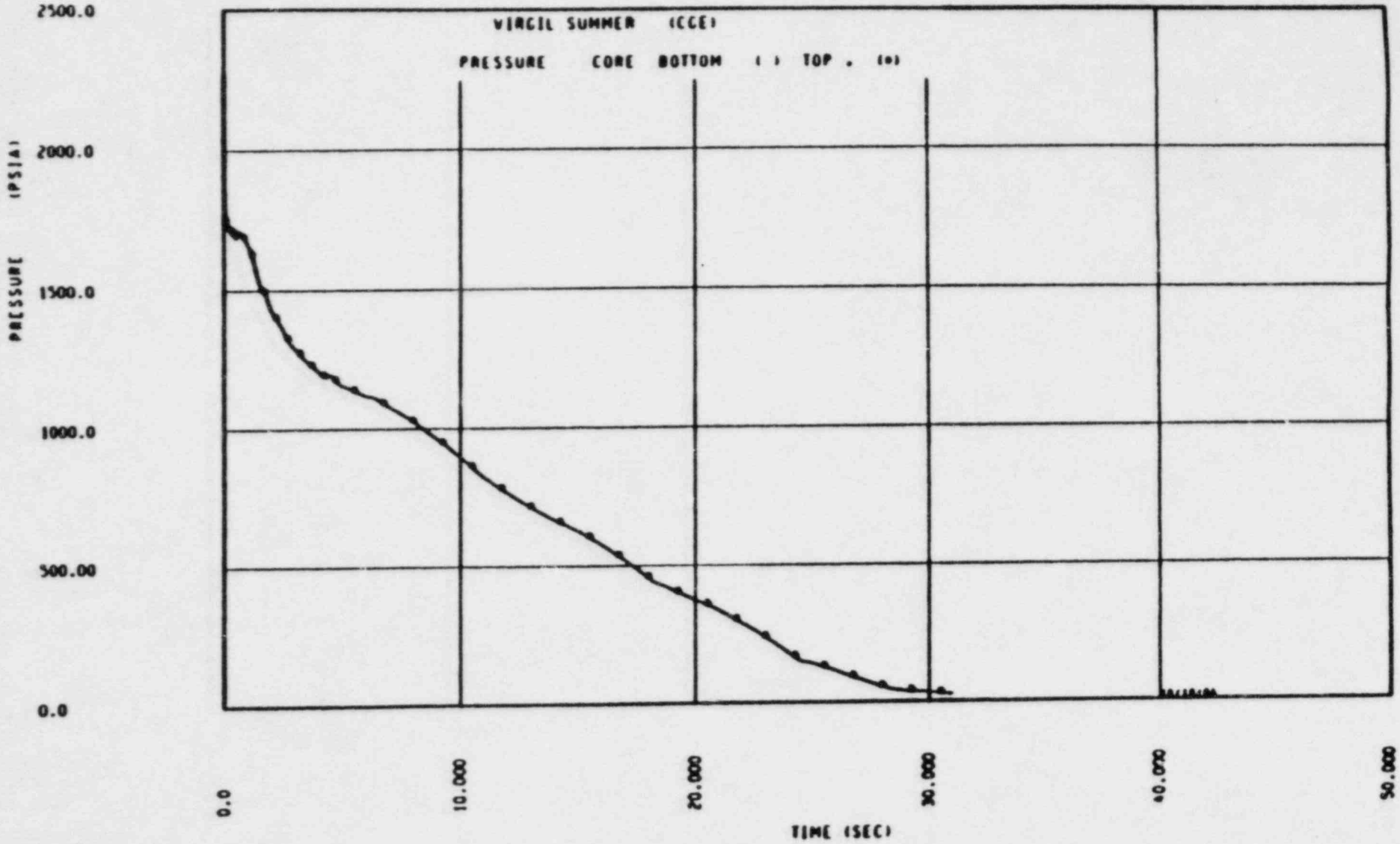

Figure 15.4.1-4c. Core Pressure (C_D = 0.4)

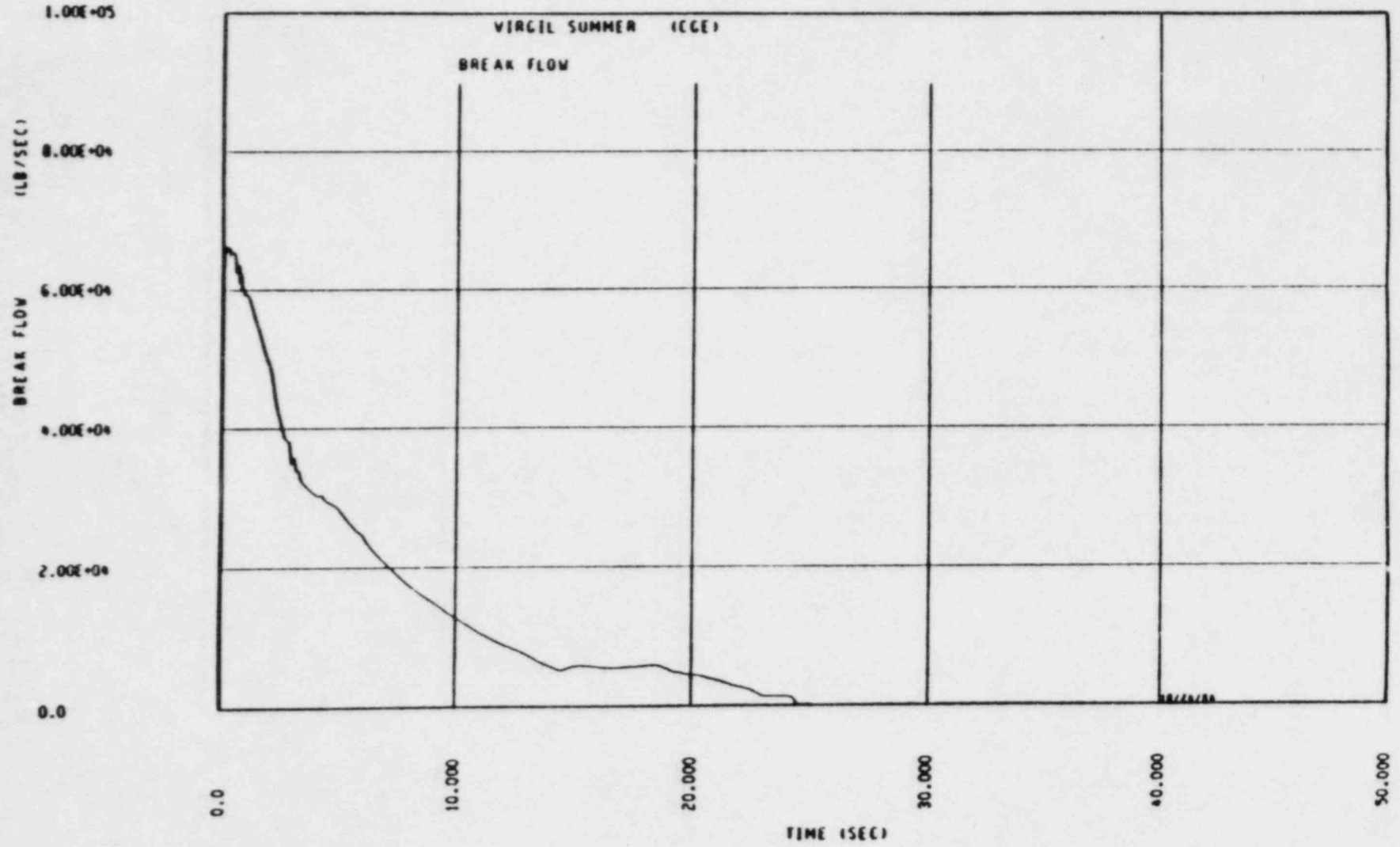

Figure 15.4.1-5b. Break Flow Rate (C_D = 0.6)

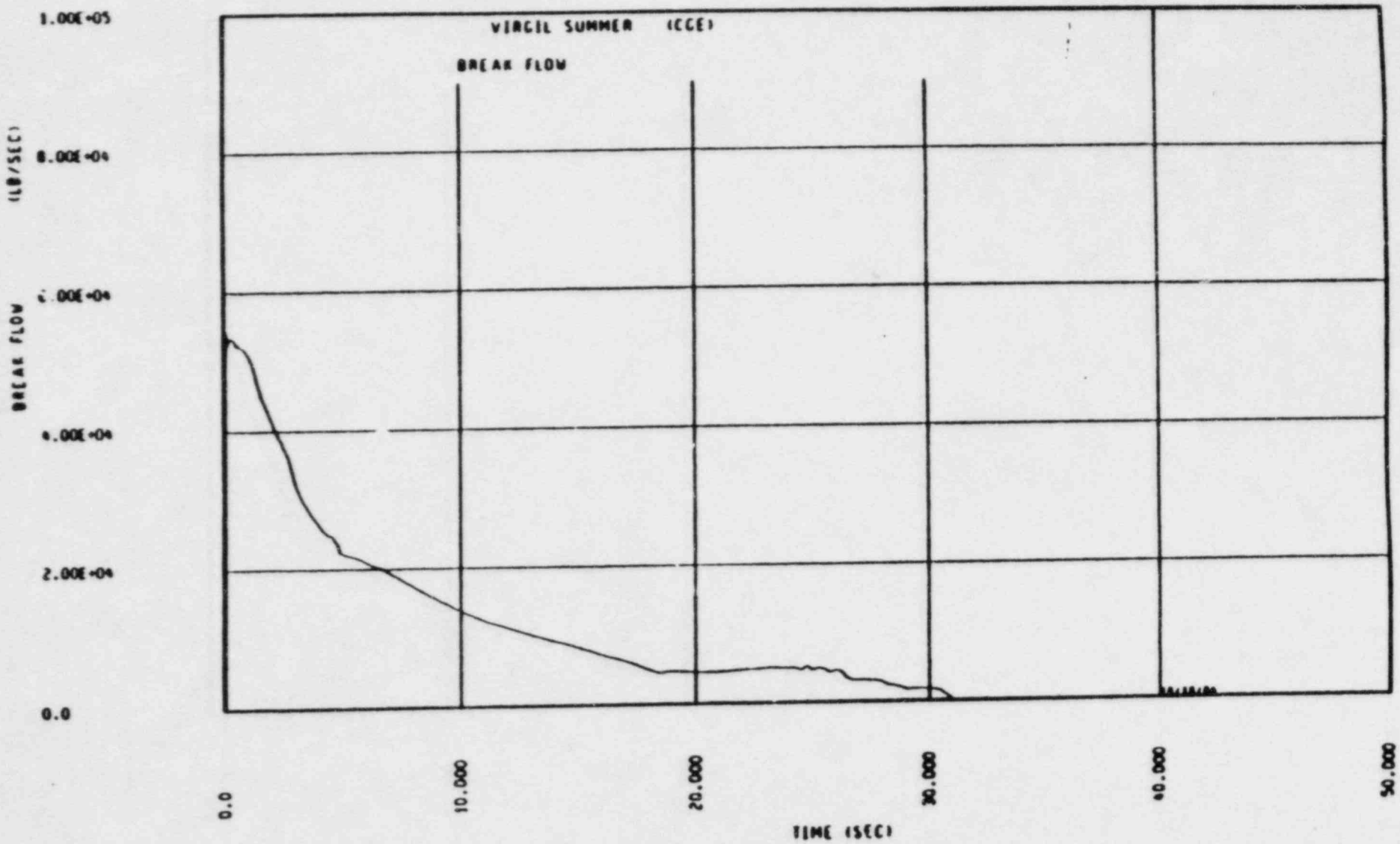

Figure 15.4.1-5c. Break Flow Rate (C_D = 0.4)

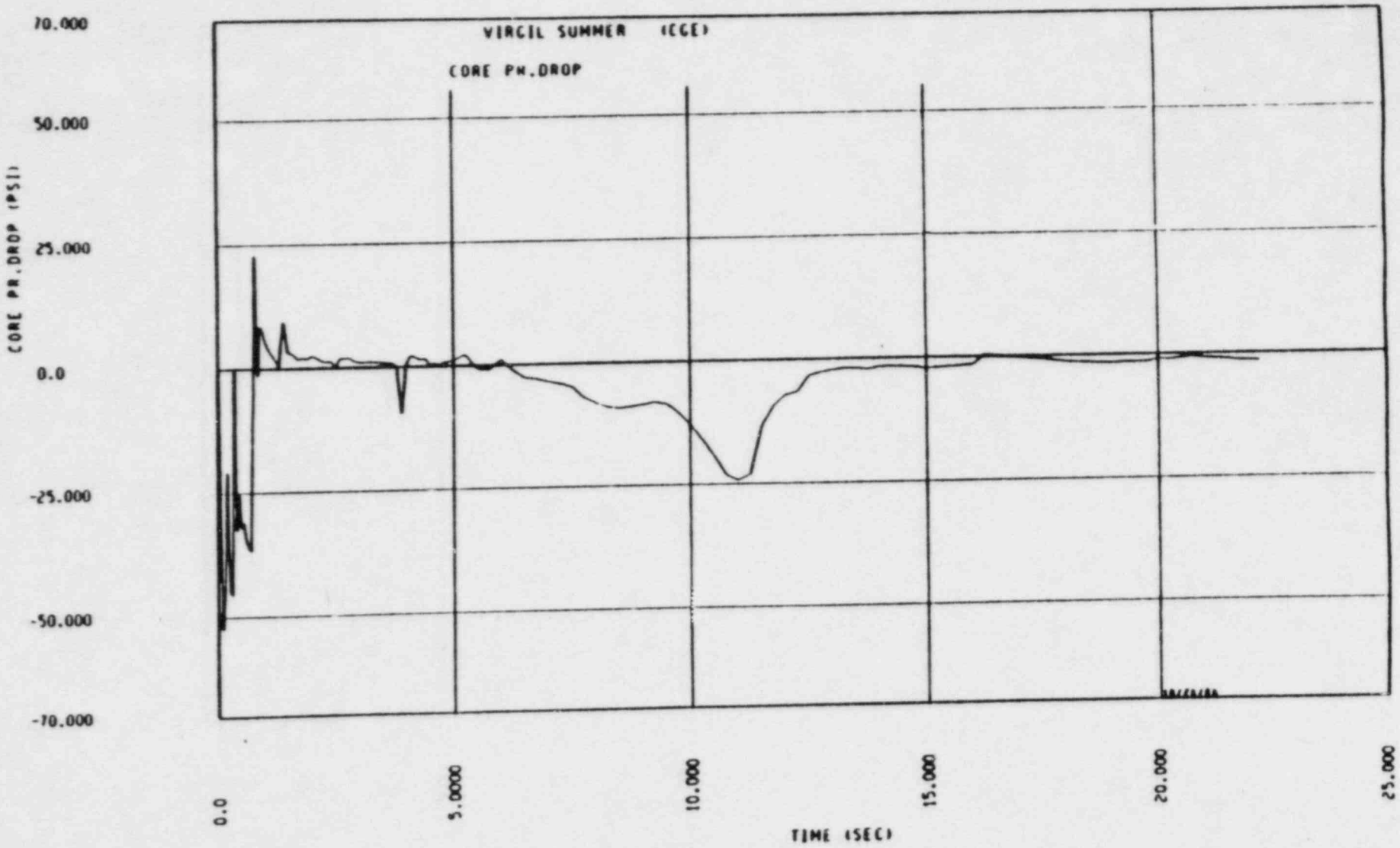

Figure 15.4.1-6a. Core Pressure Drop (C_D = 0.8)

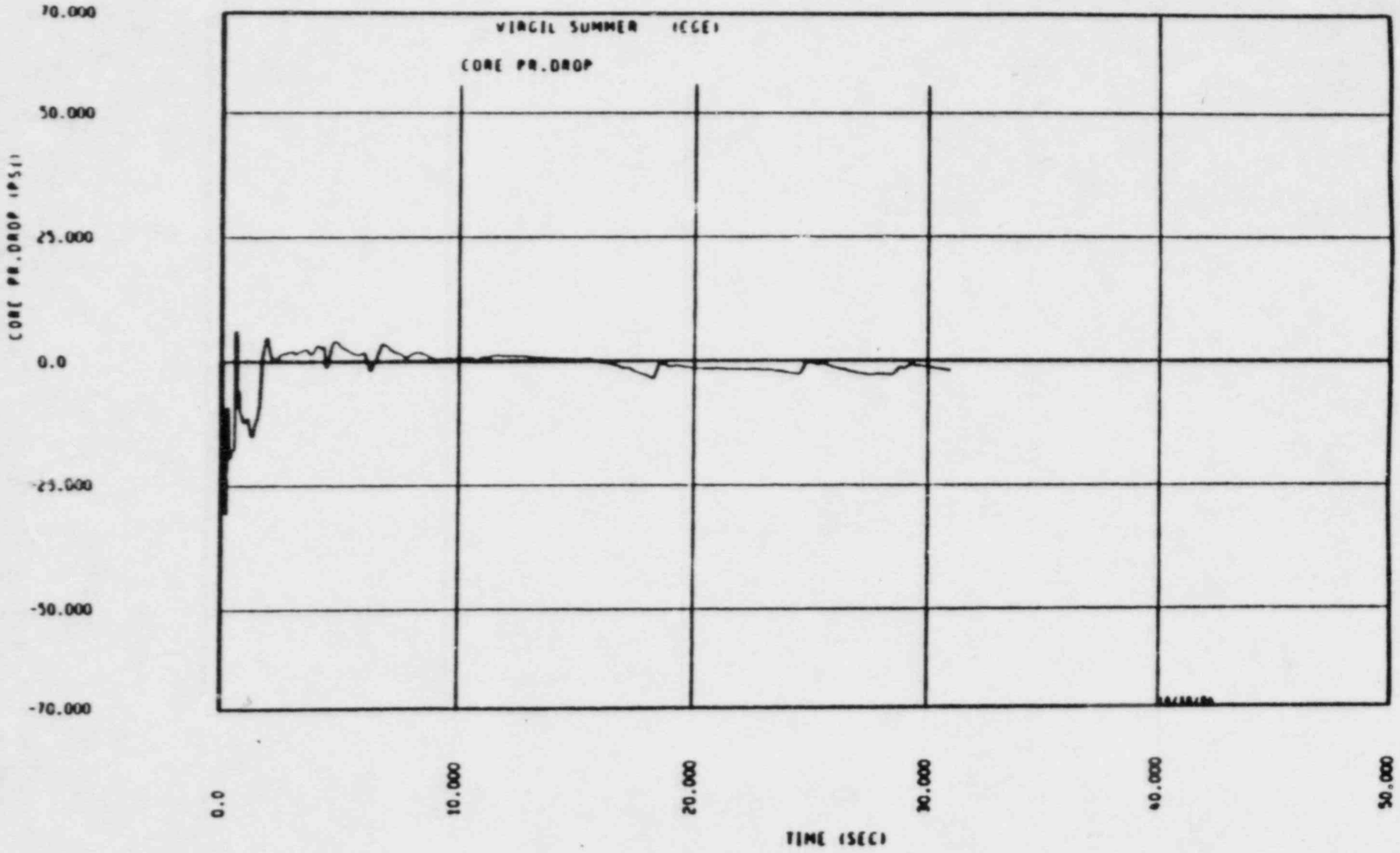

Figure 15.4.1-6c. Core Pressure Drop (C_D = 0.4)

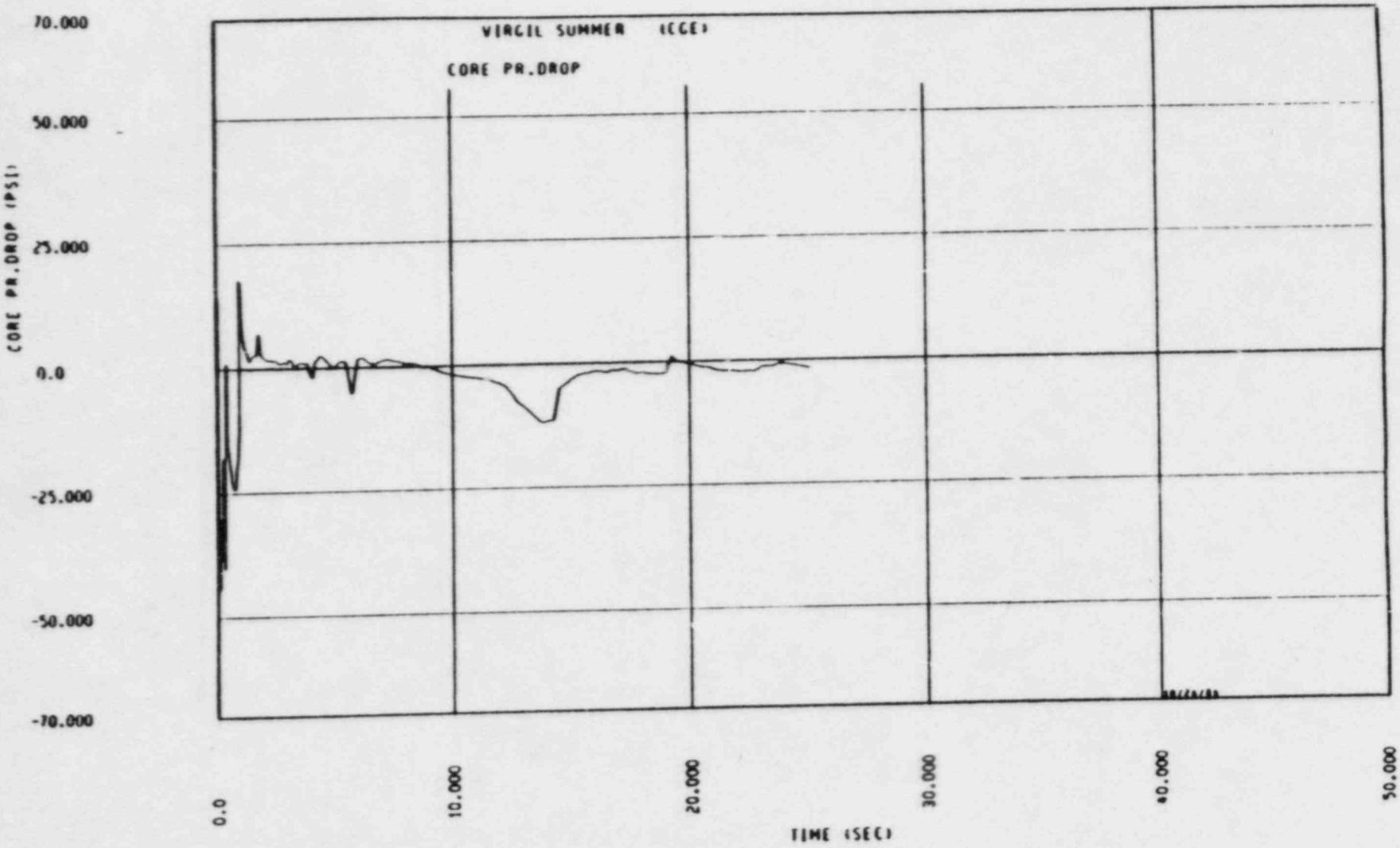

Figure 15.4.1-6b. Core Pressure Drop (C_D = 0.6)

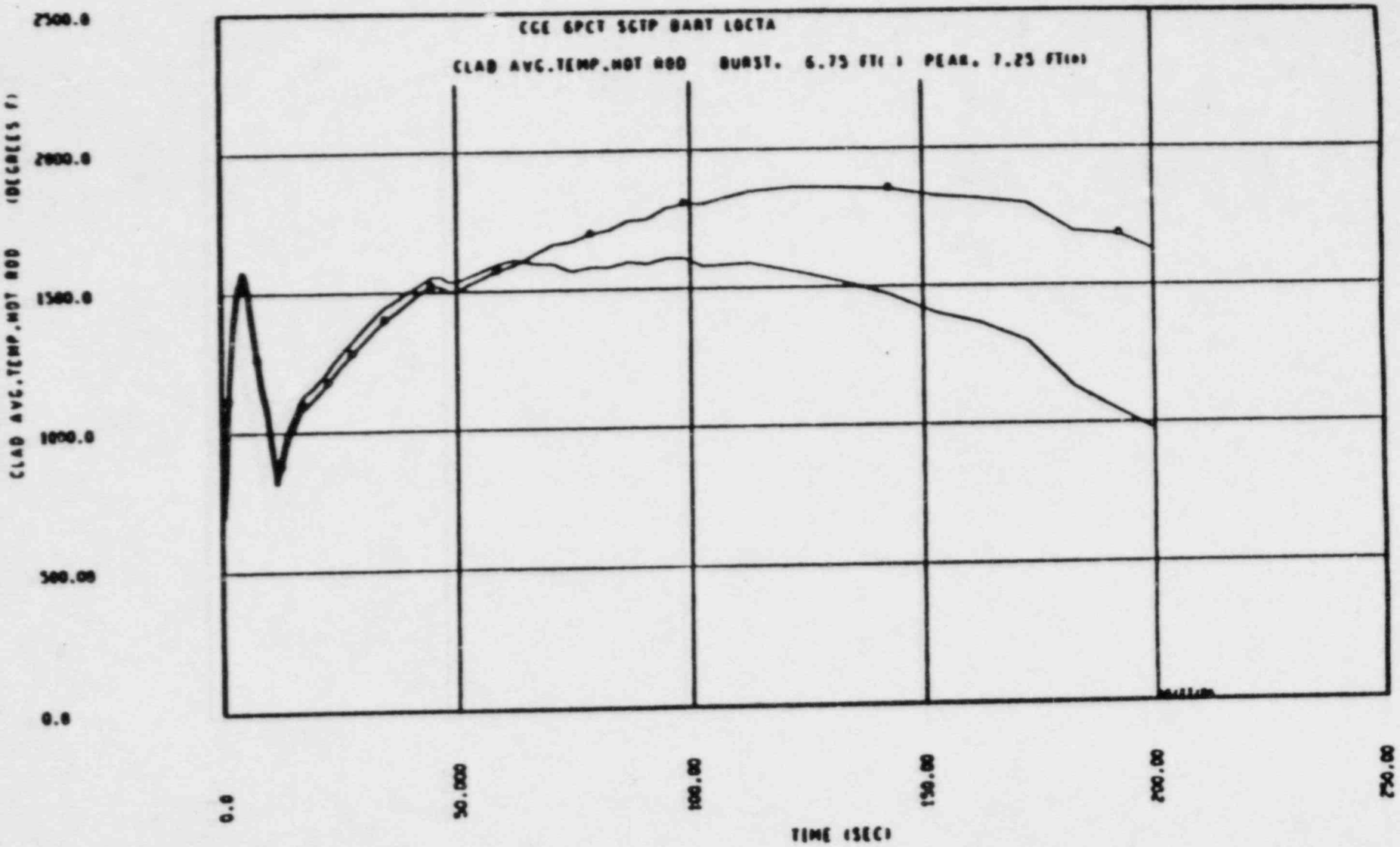

Figure 15.4.1-7a. Peak Clad Temperature (C_D = 0.8)

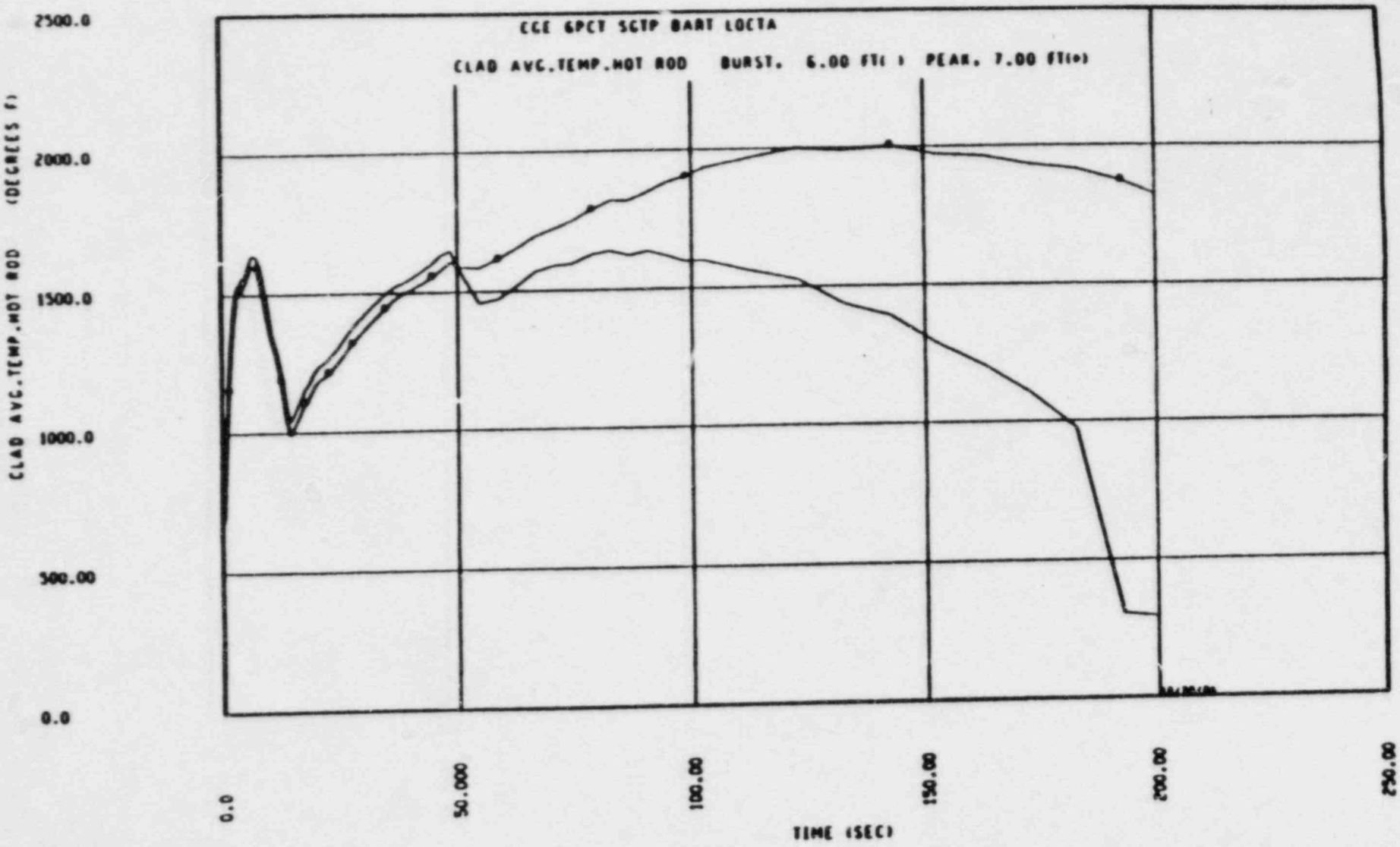

Figure 15.4.1-7b. Peak Clad Temperature (C_D = 0.6)

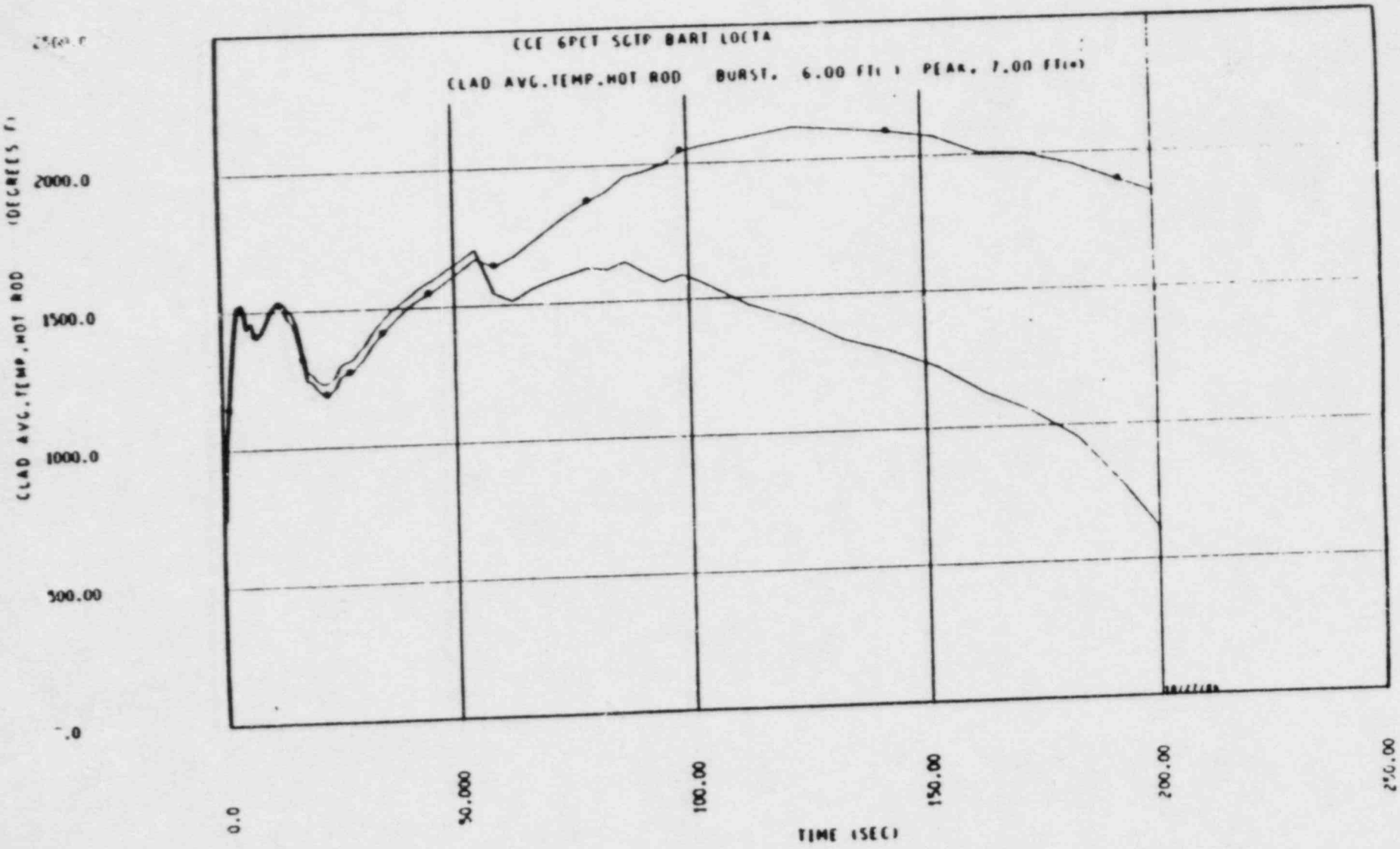

Figure 15.4.1-7c. Peak Clad Temperature (C_D = 0.4)

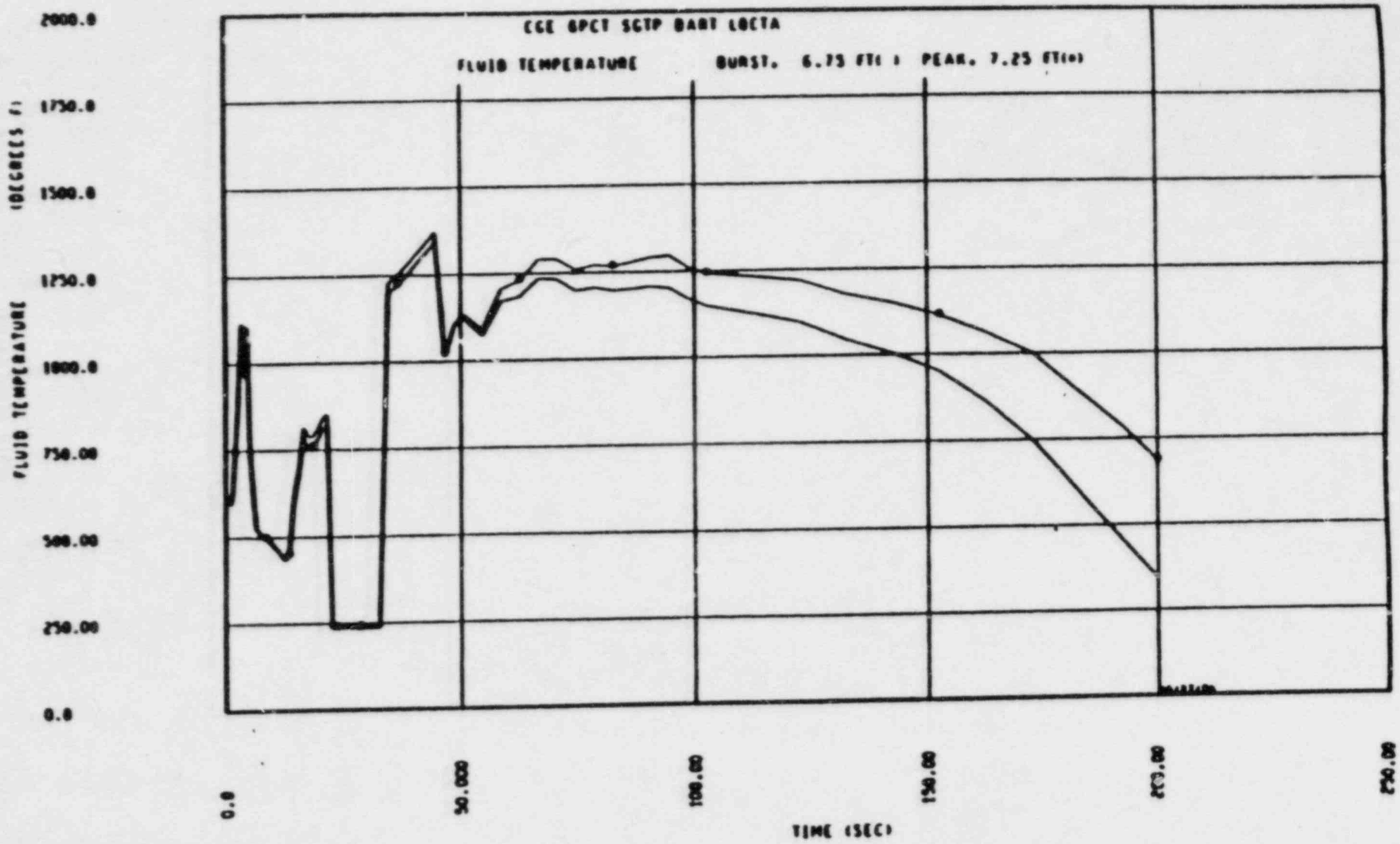

Figure 15.4.1-8a. Fluid Temperature (C_D = 0.8)

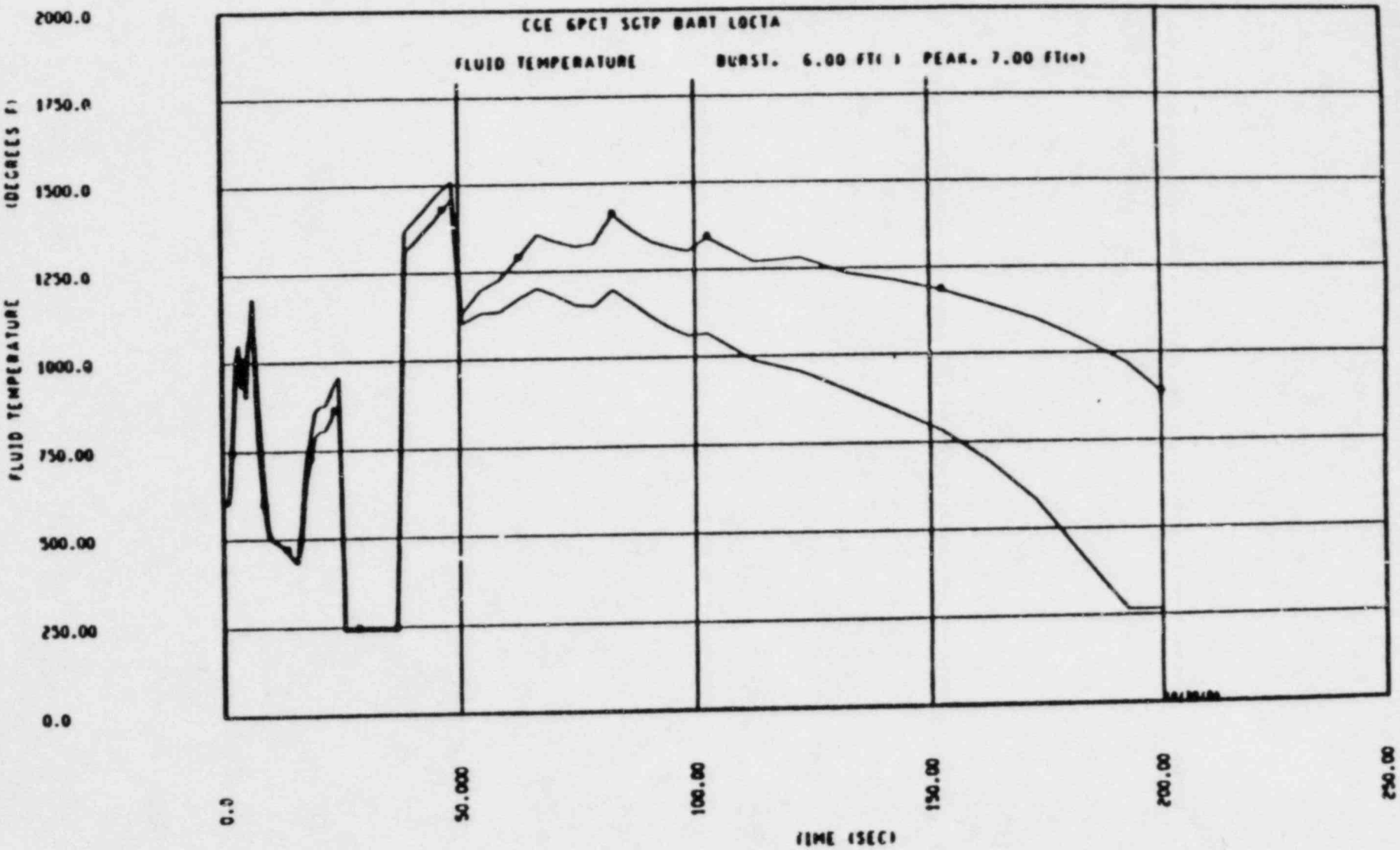

Figure 15.4.1-8b. Fluid Temperature (C_D = 0.6)

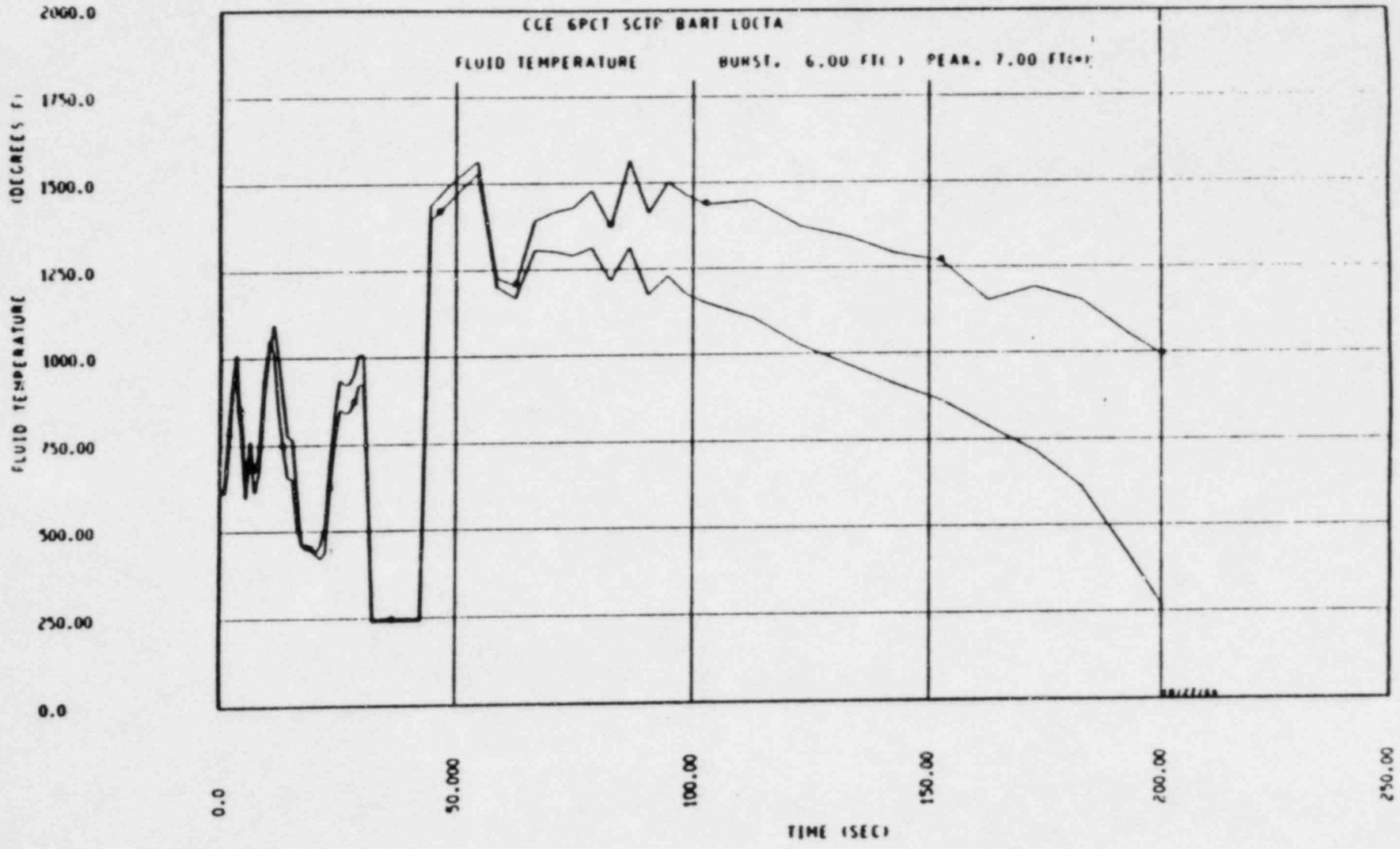

Figure 15.4.1-8c. Fluid Temperature (C_D = 0.4)

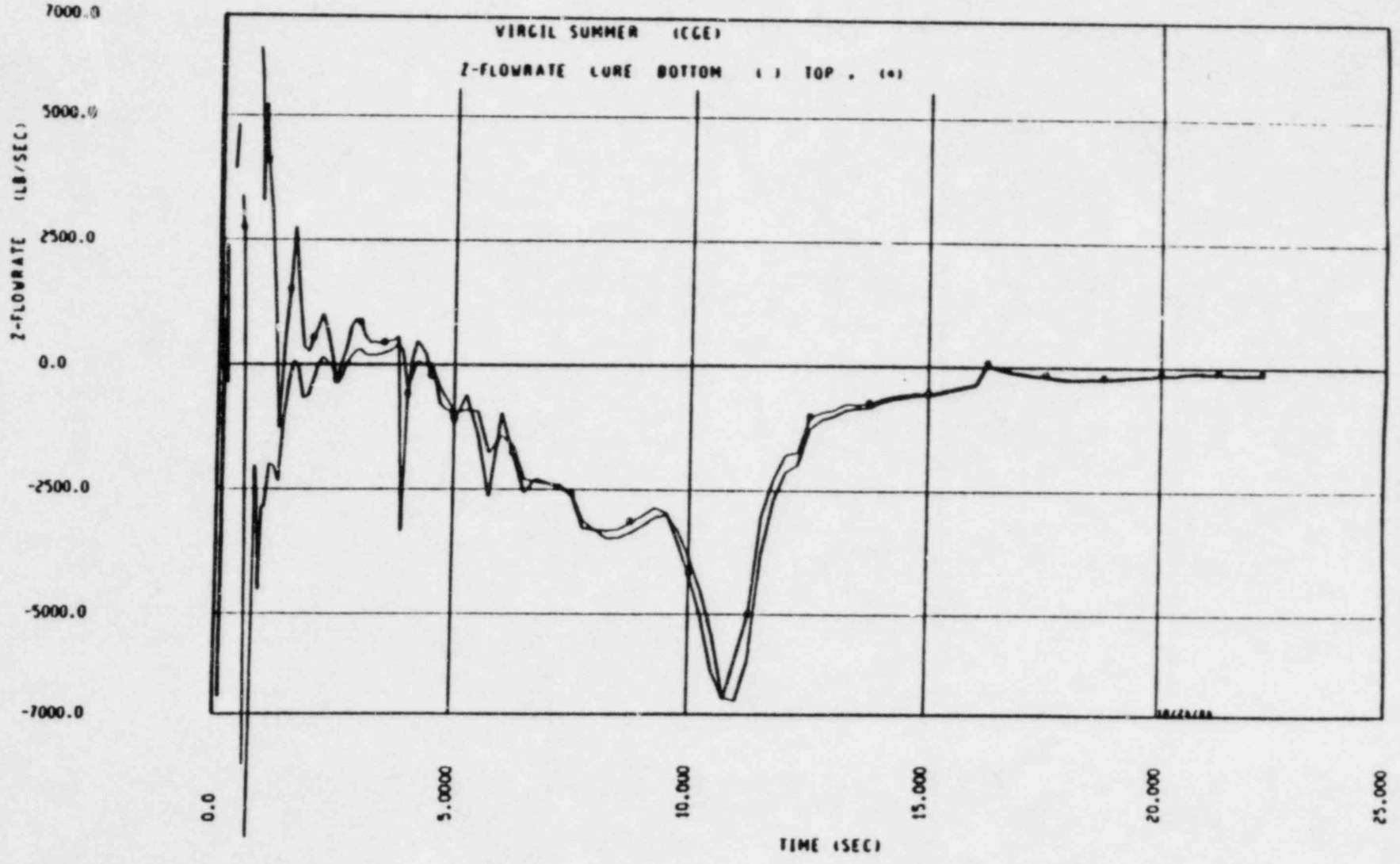

Figure 15.4.1-9a. Core Flow - Top and Bottom (C_D = 0.8)

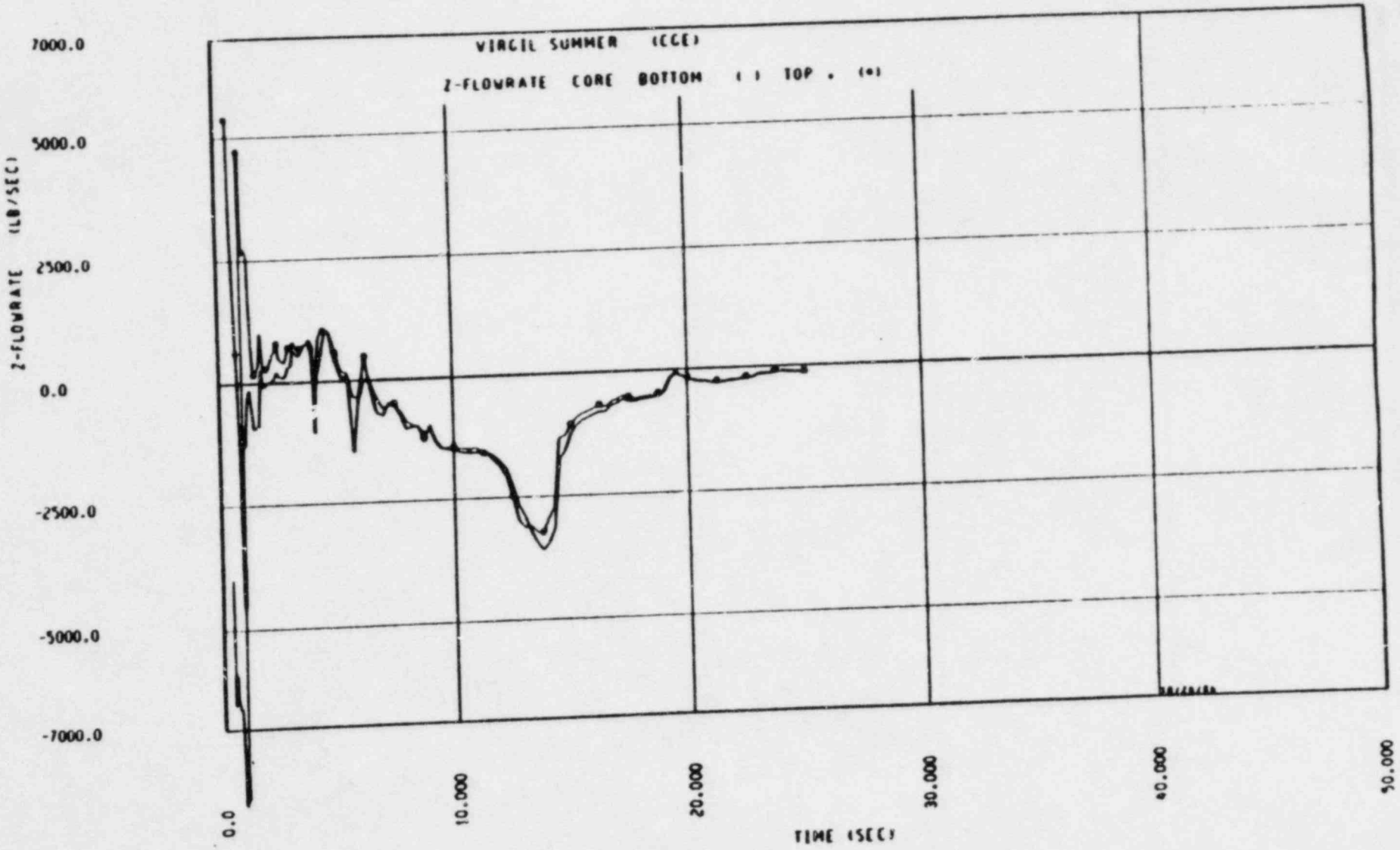

Figure 15.4.1-9b. Core Flow - Top and Bottom (C_D = 0.6)

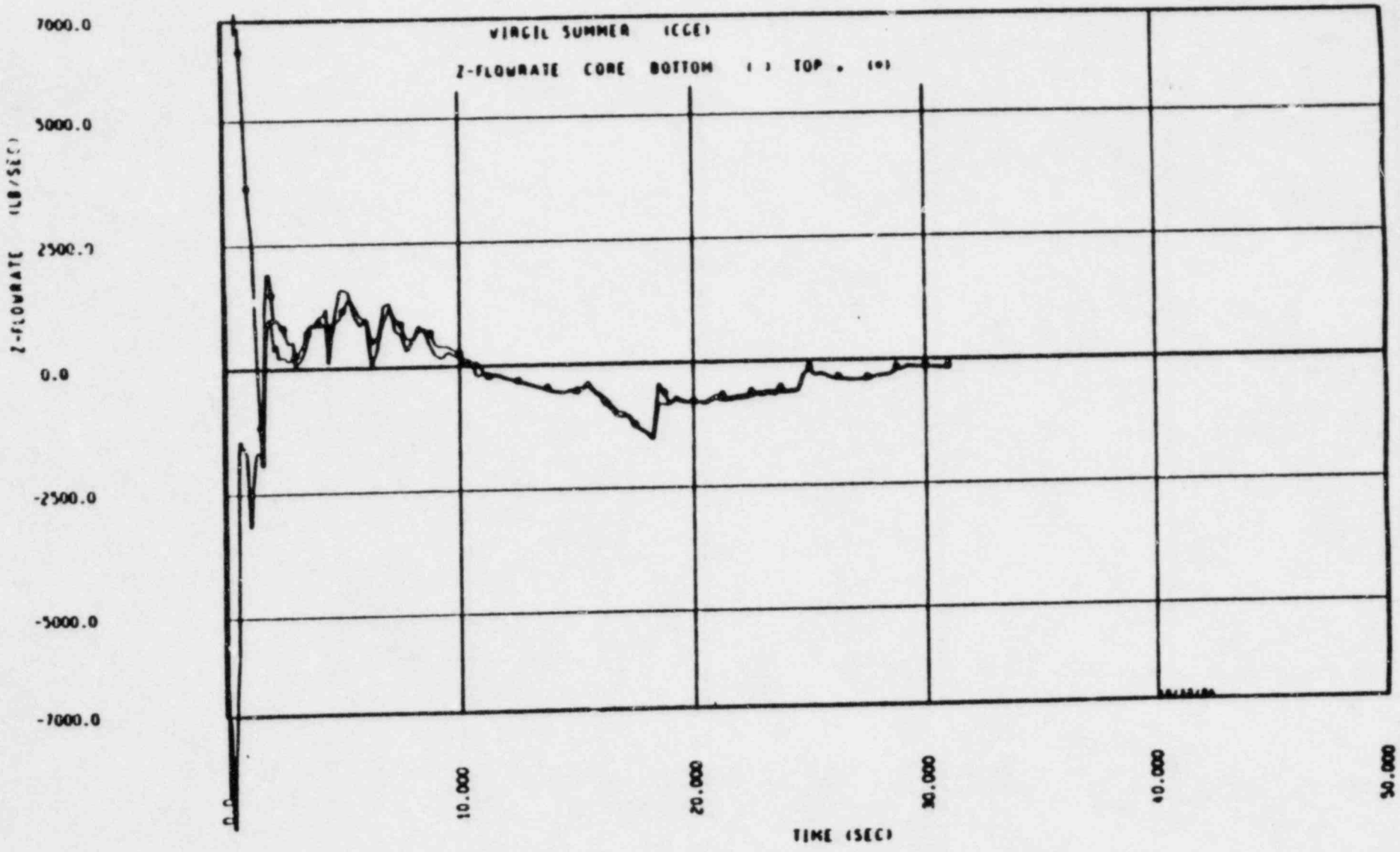

Figure 15.4.1-9c. Core Flow - Top and Bottom (C_D = 0.4)

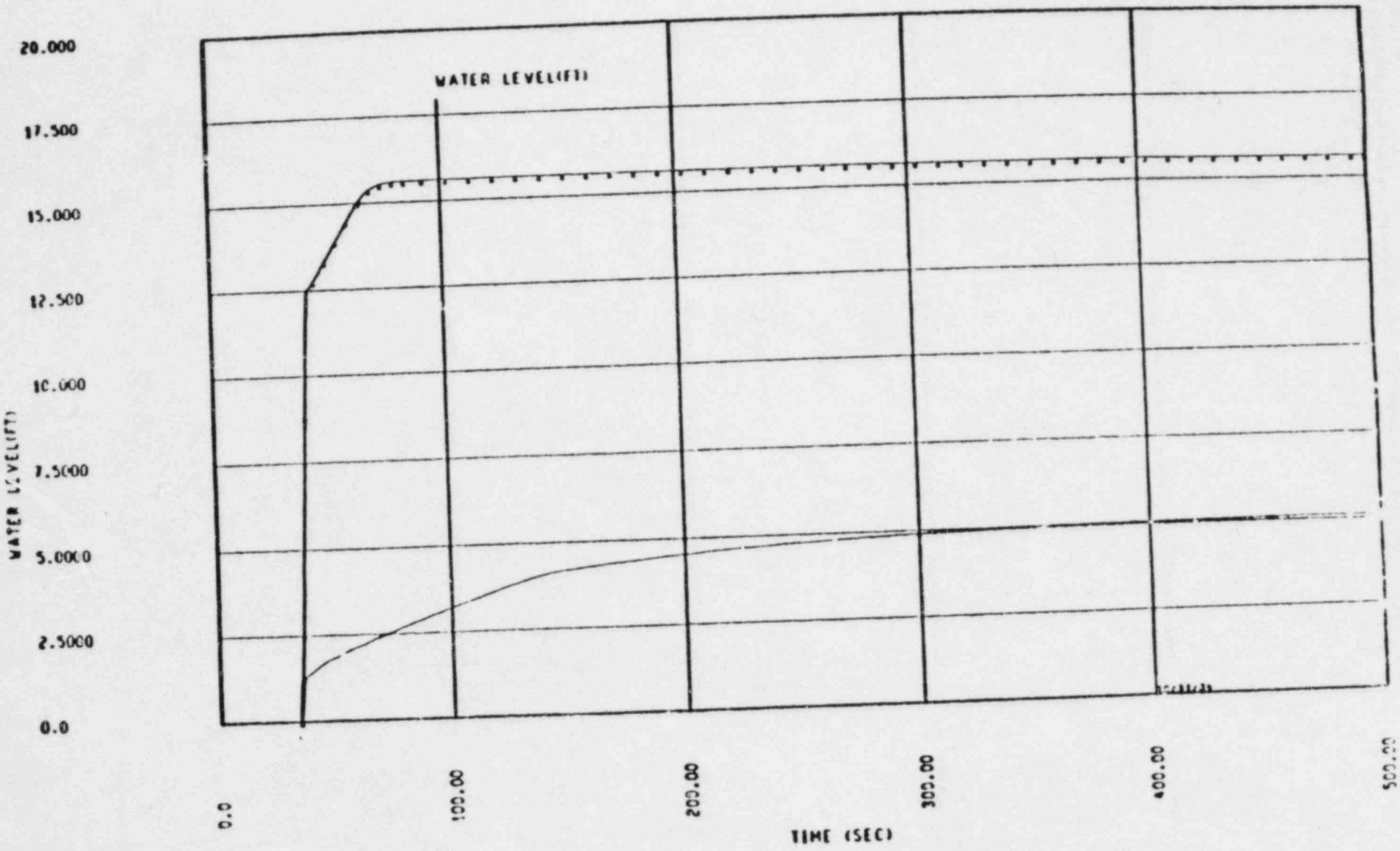

Figure 15.4.1-10a. Reflood Transient Downcomer and Core Water Levels (C_D = 0.8)

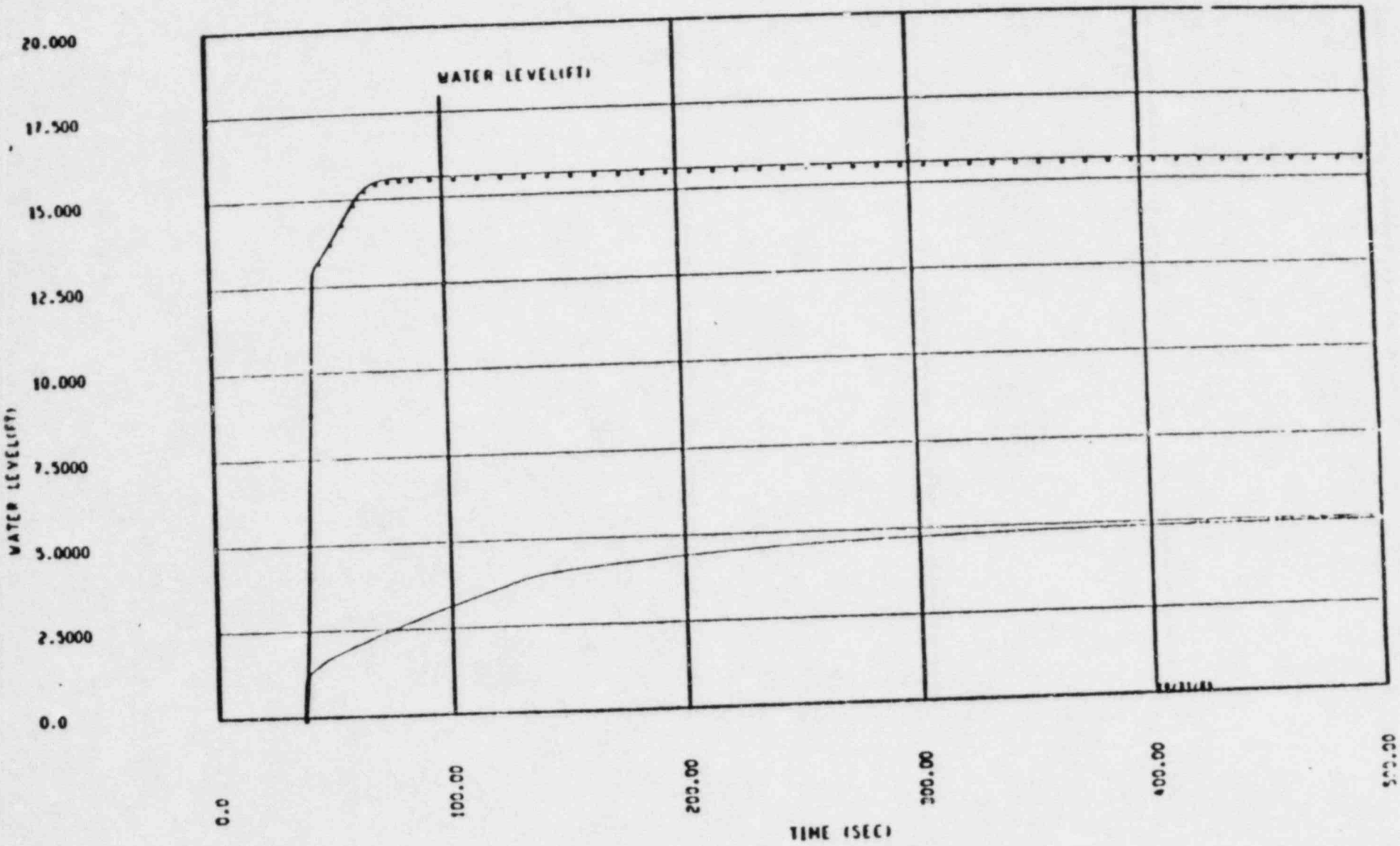

Figure 15.4.1-10b. Reflood Transient Downcomer and Core Water Levels (C_D = 0.6)

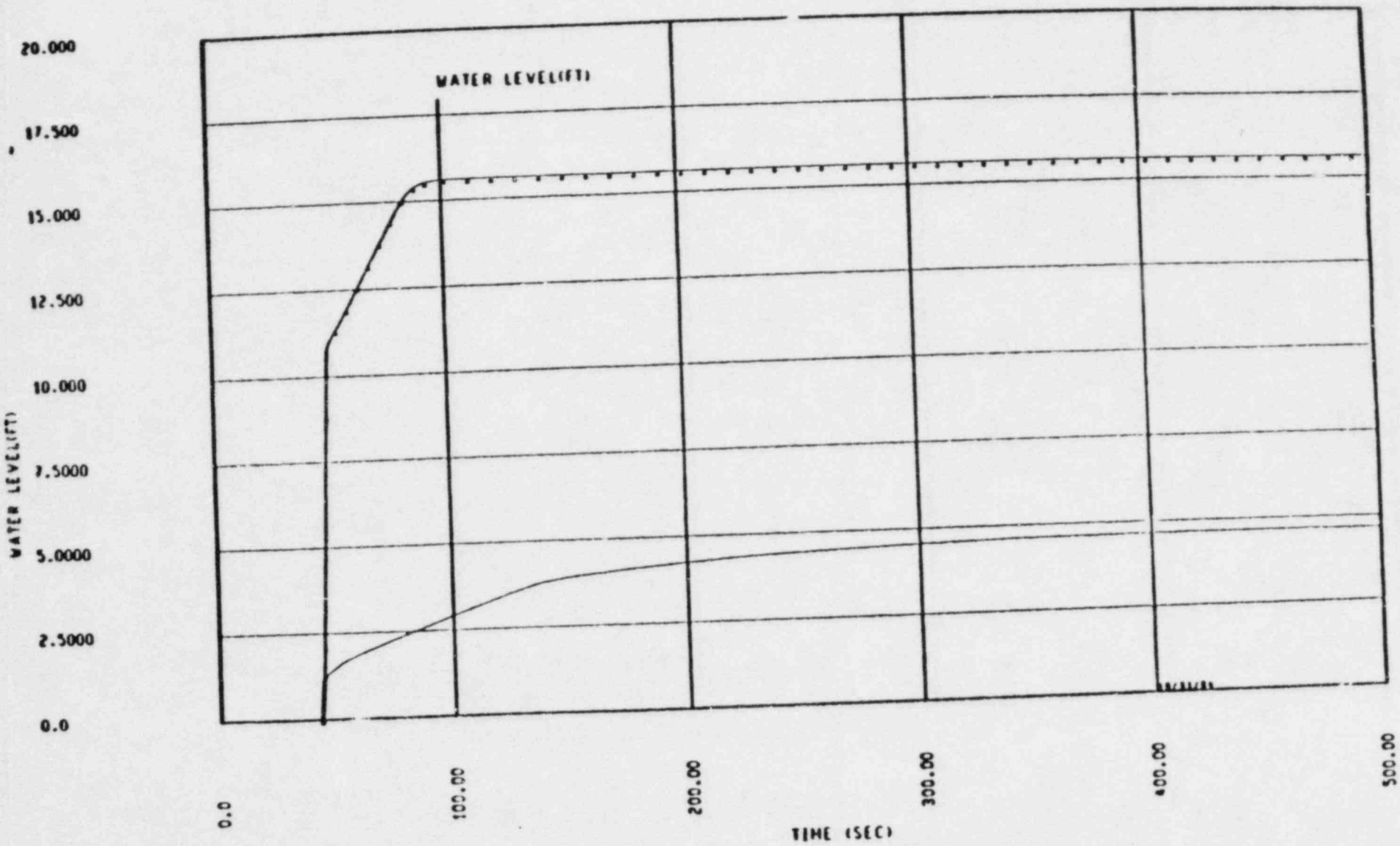

Figure 15.4.1-10c. Reflood Transient Downcomer and Core Water Levels (C_D = 0.4)

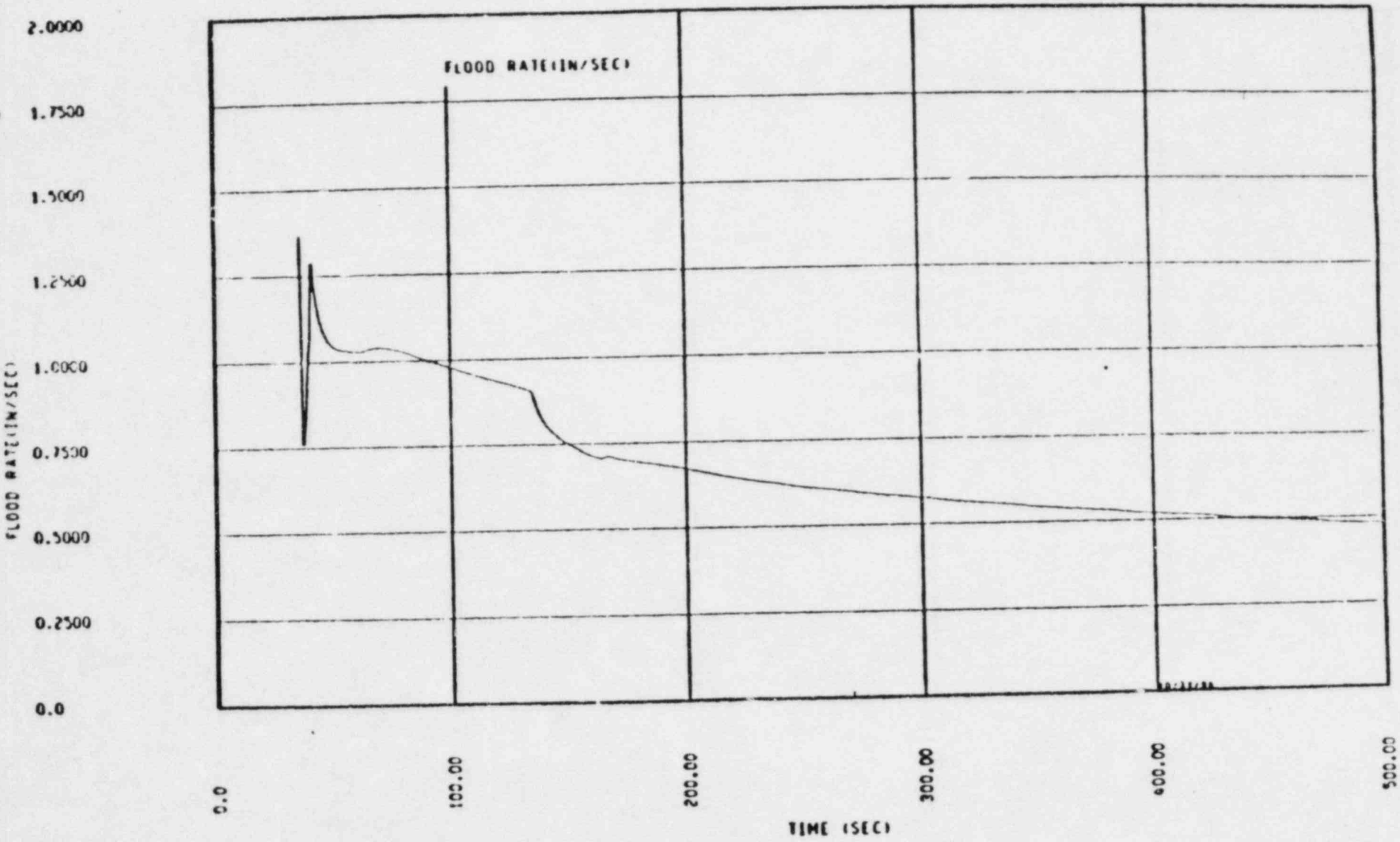

Figure 15.4.1-10d. Reflood Transient Core Inlet Velocity (C_D = 0.8)

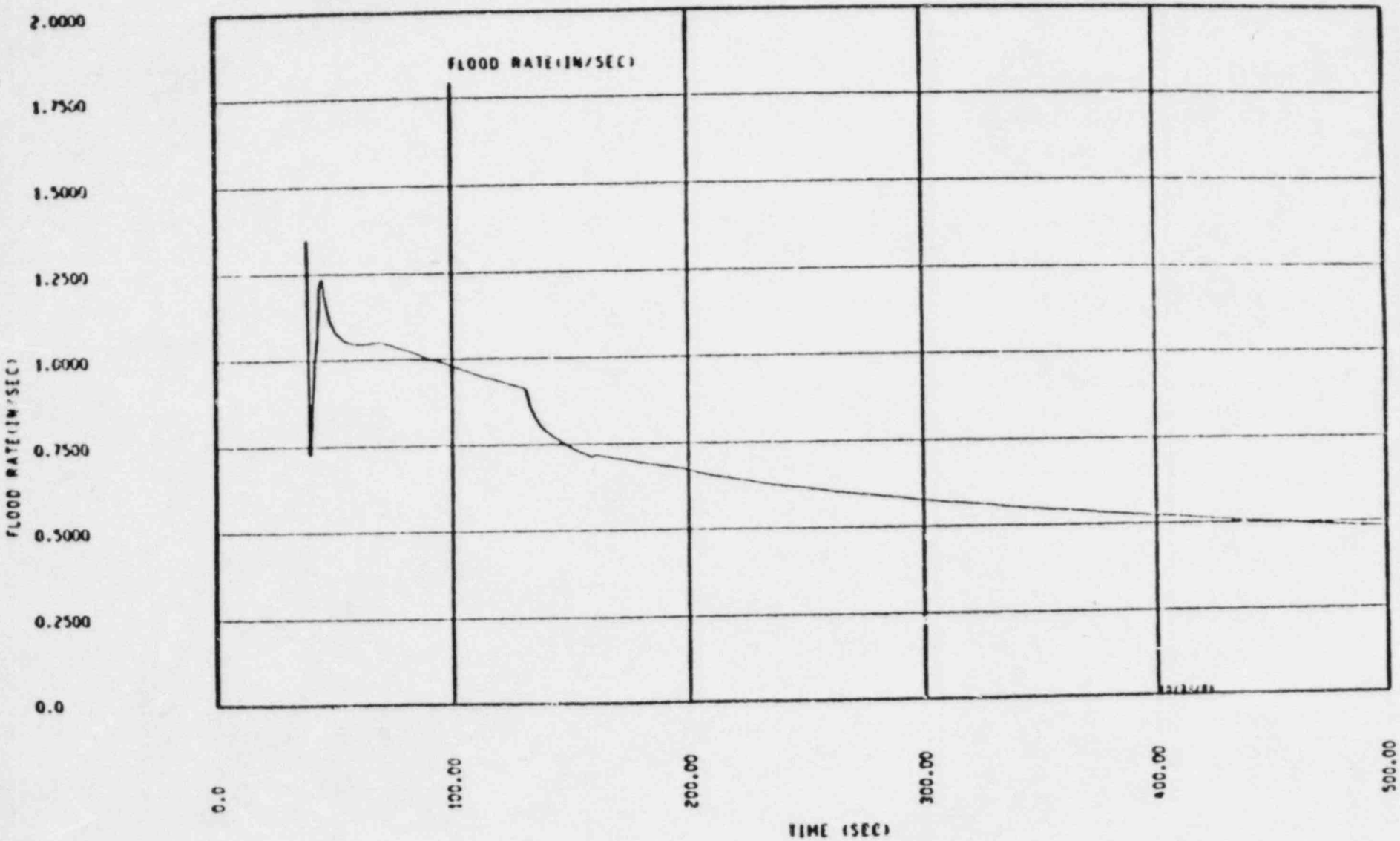

Figure 15.4.1-10e. Reflood Transient Core Inlet Velocity (C_D = 0.6)

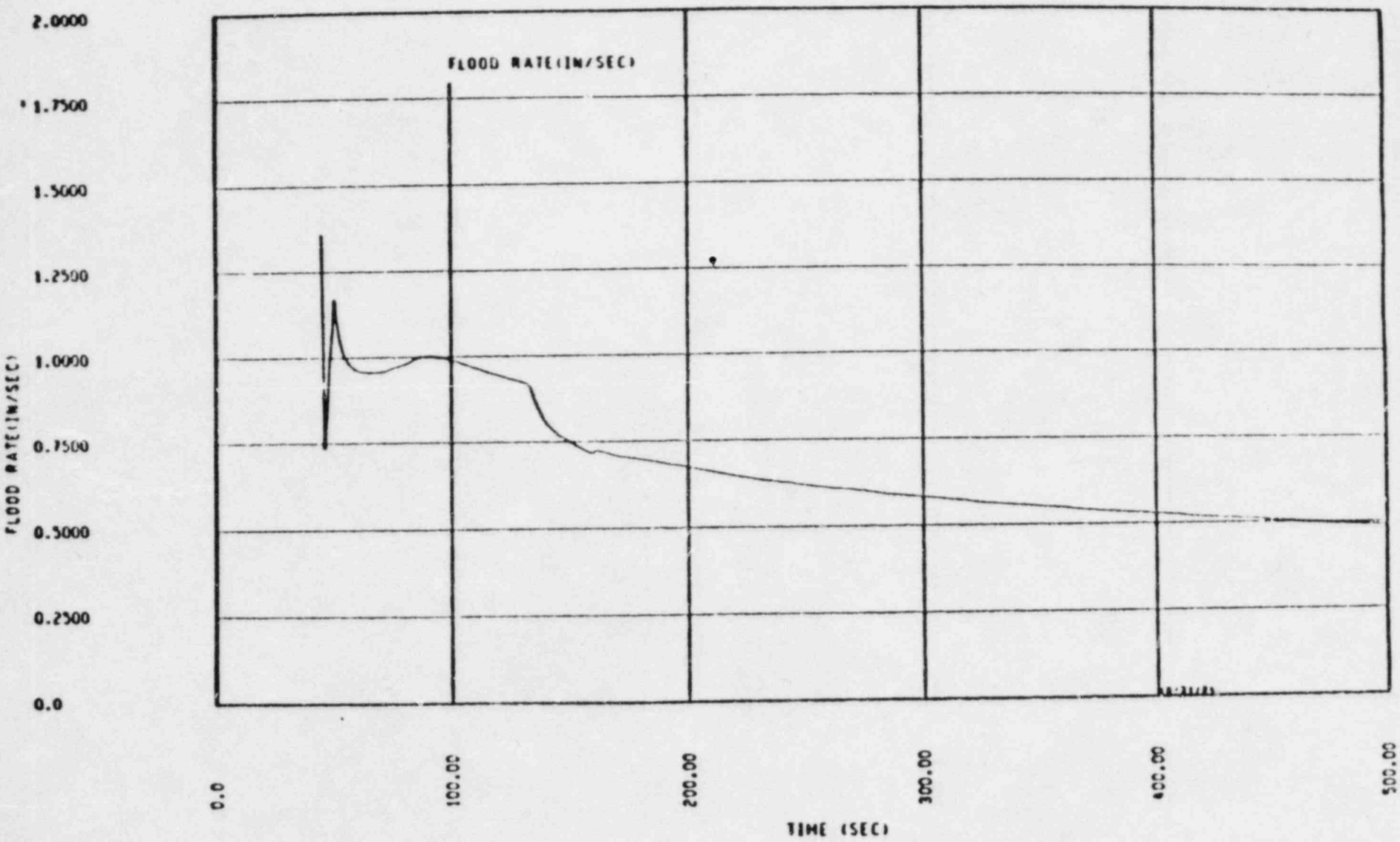

Figure 15.4.1-10f. Reflood Transient Core Inlet Velocity (C_D = 0.4)

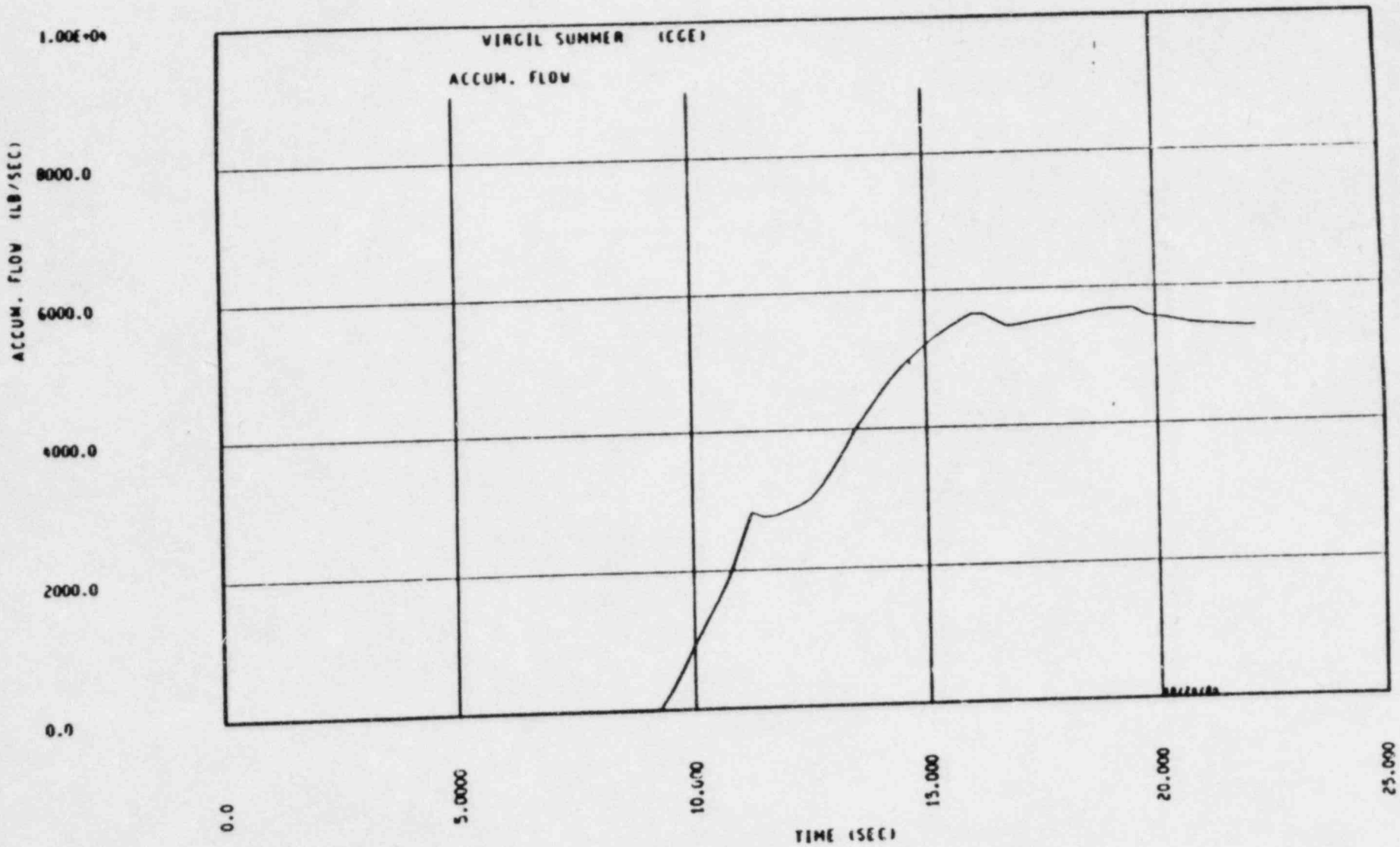

Figure 15.4.1-11a. Accumulator Flow-Blowdown (C_D = 0.8)

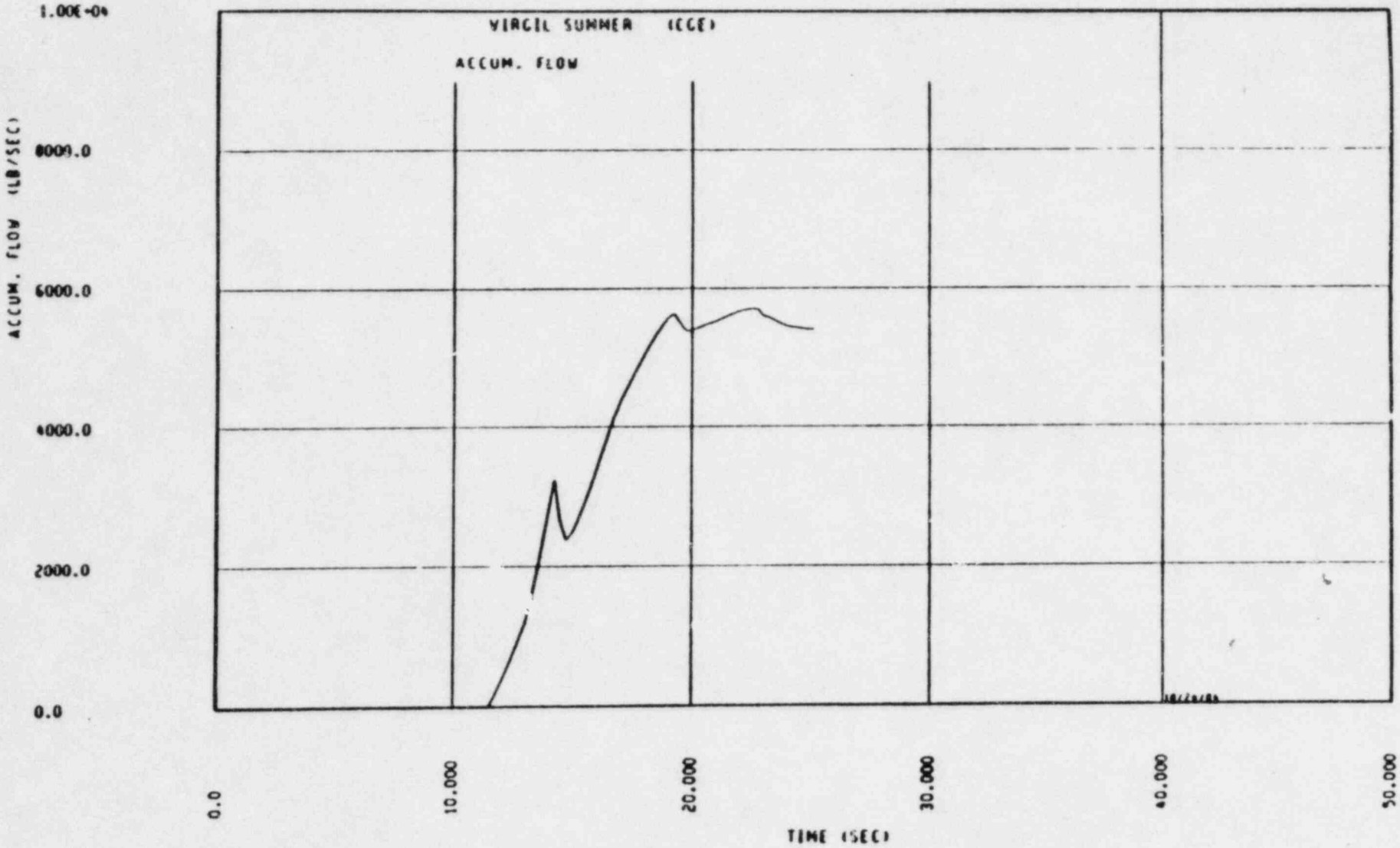

Figure 15.4.1-11b. Accumulator Flow-Blowdown (C_D = 0.6)

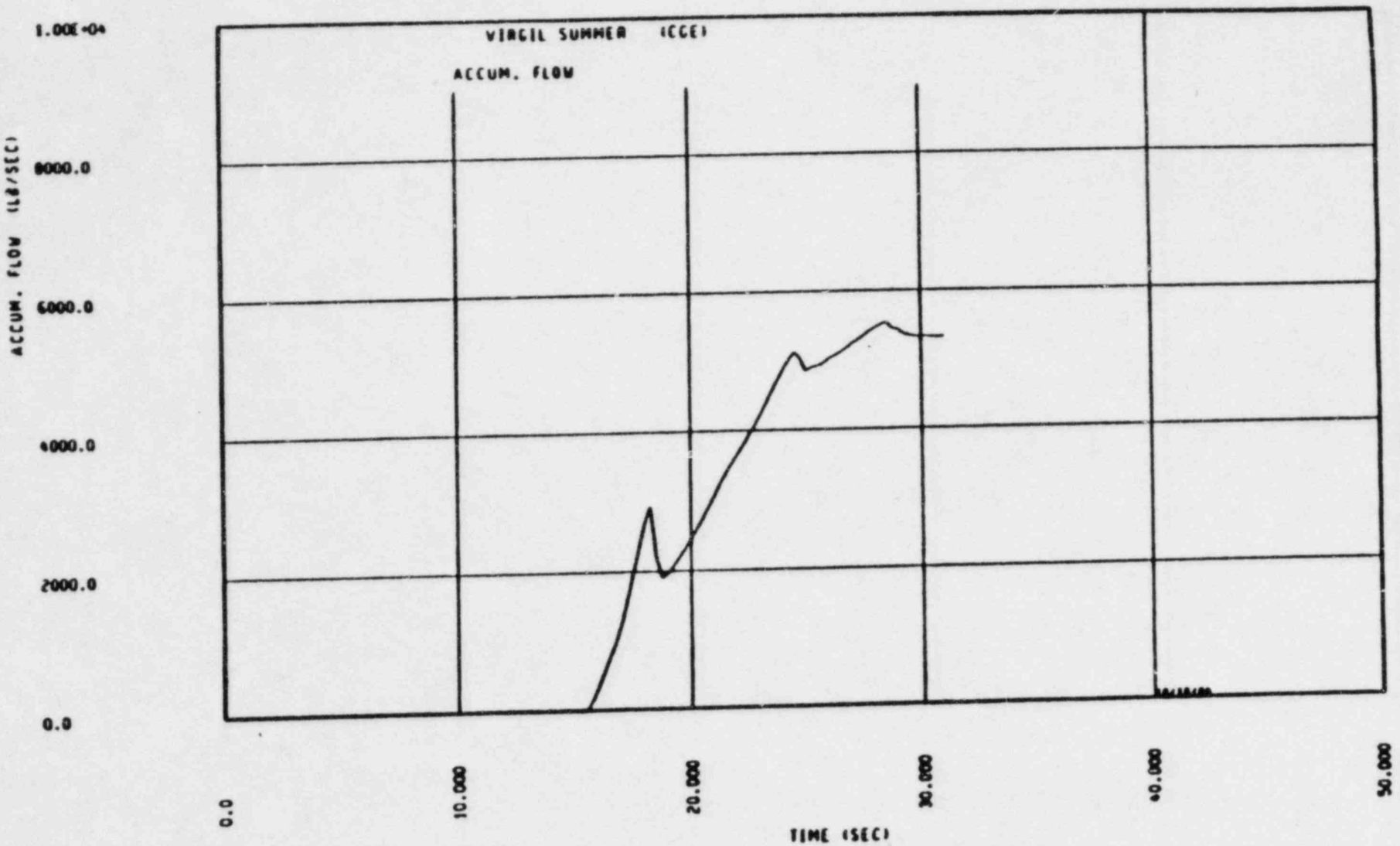

Figure 15.4.1-11c. Accumulator Flow-Blowdown (C_D = 0.4)

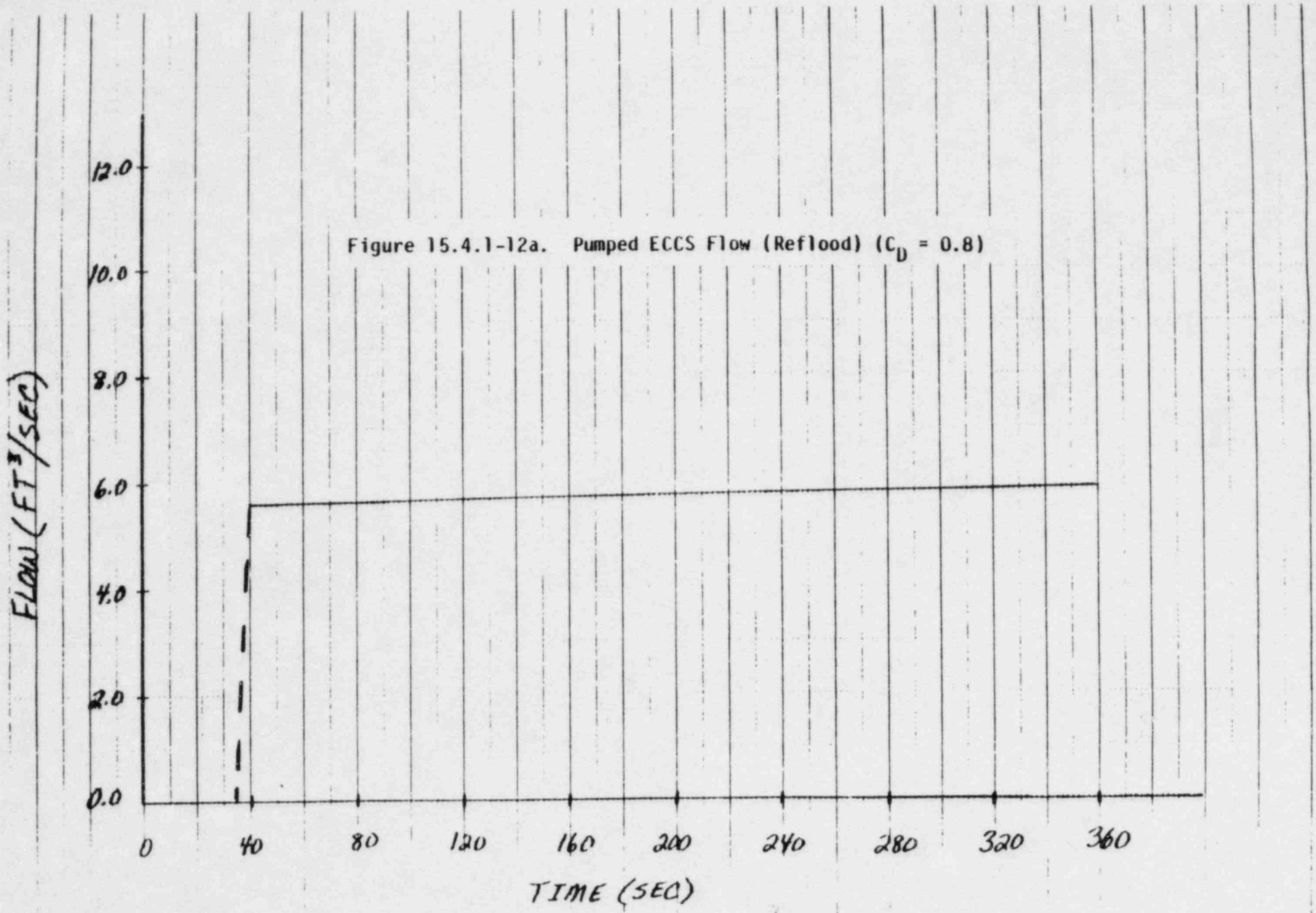

Figure 15.4.1-12a. Pumped ECCS Flow (Reflood) (C_D = 0.8)

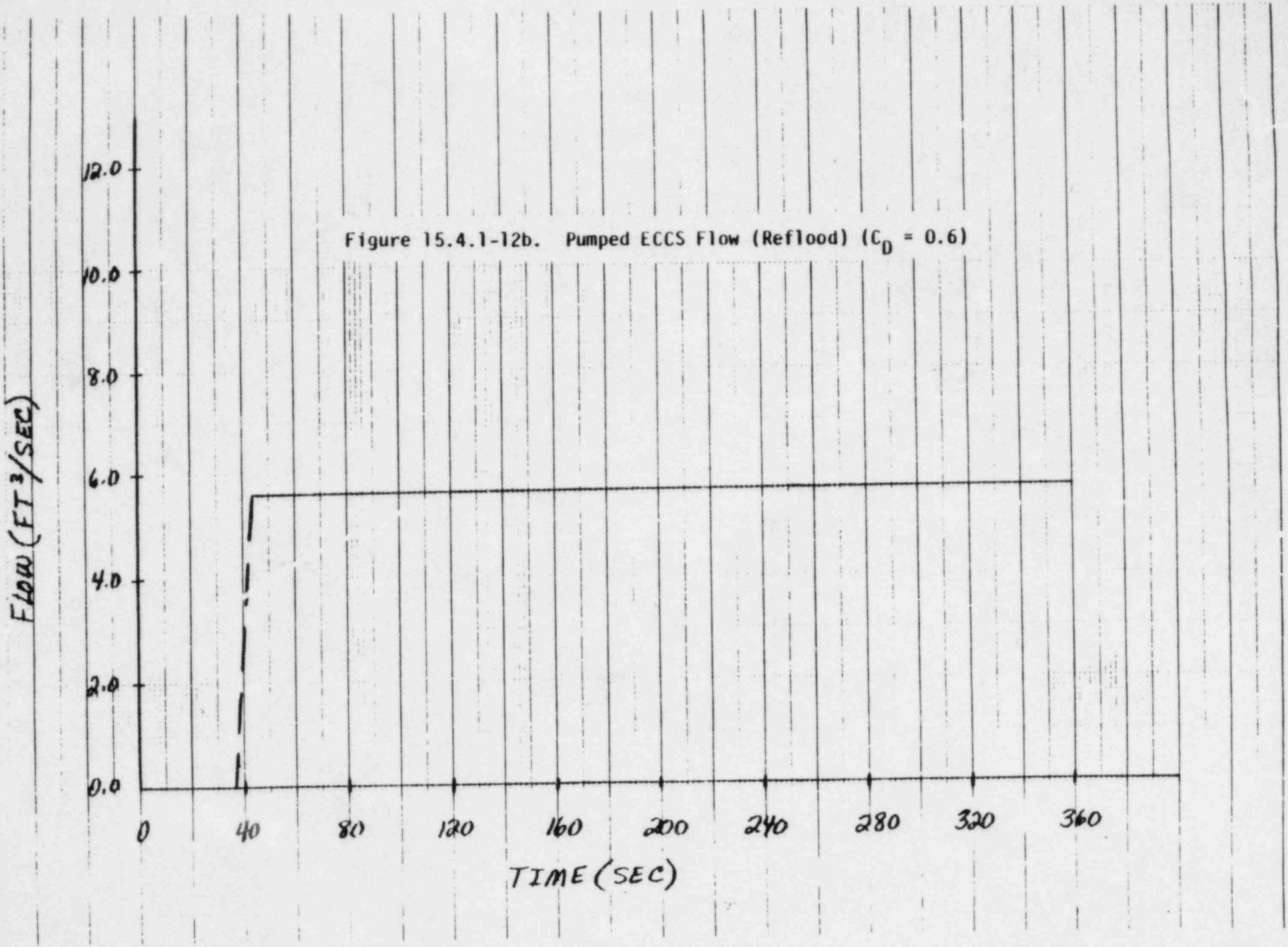

Figure 15.4.1-12b. Pumped ECCS Flow (Reflood) (C_D = 0.6)

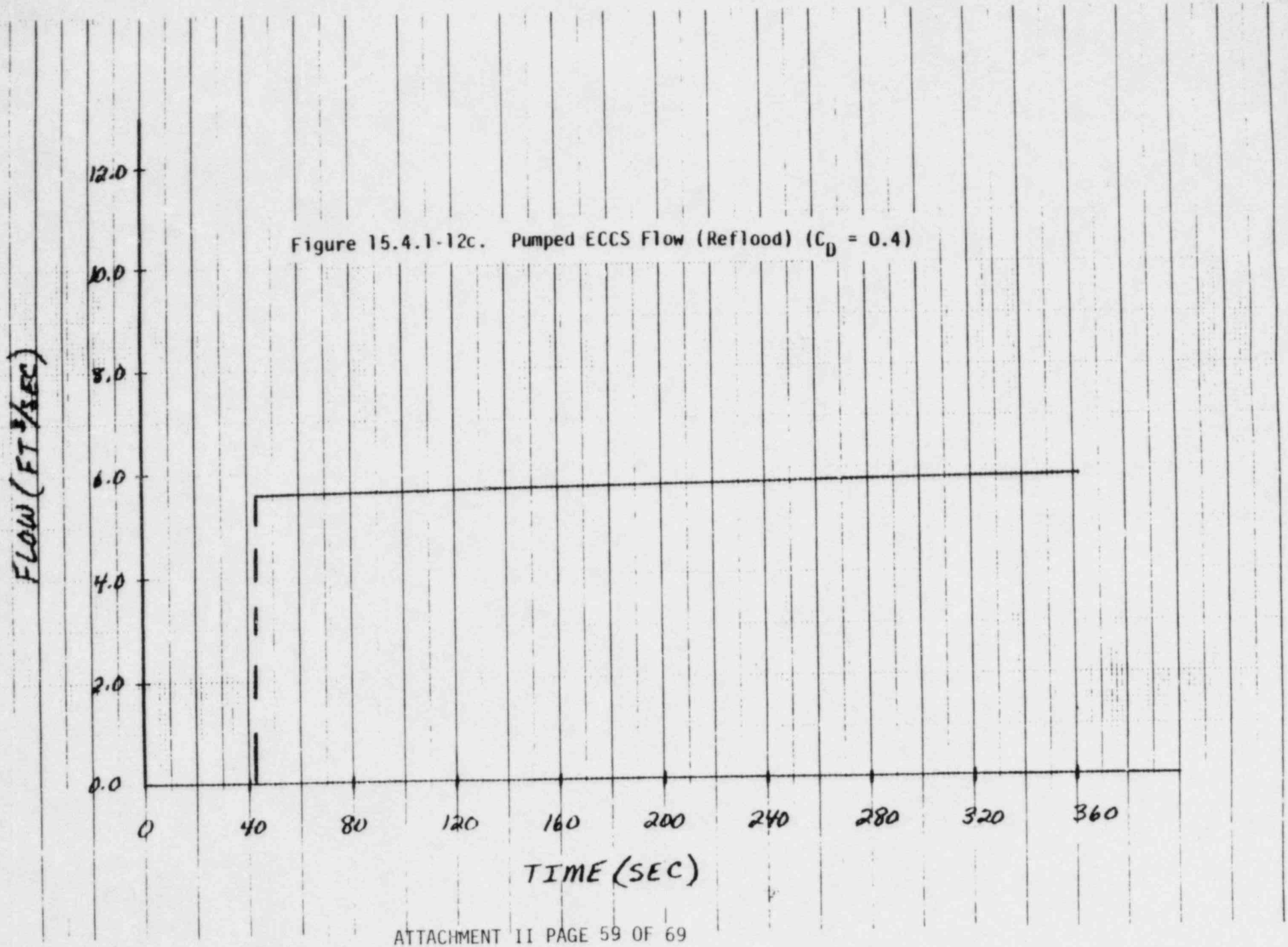

Figure 15.4.1-12c. Pumped ECCS Flow (Reflood) (C_D = 0.4)

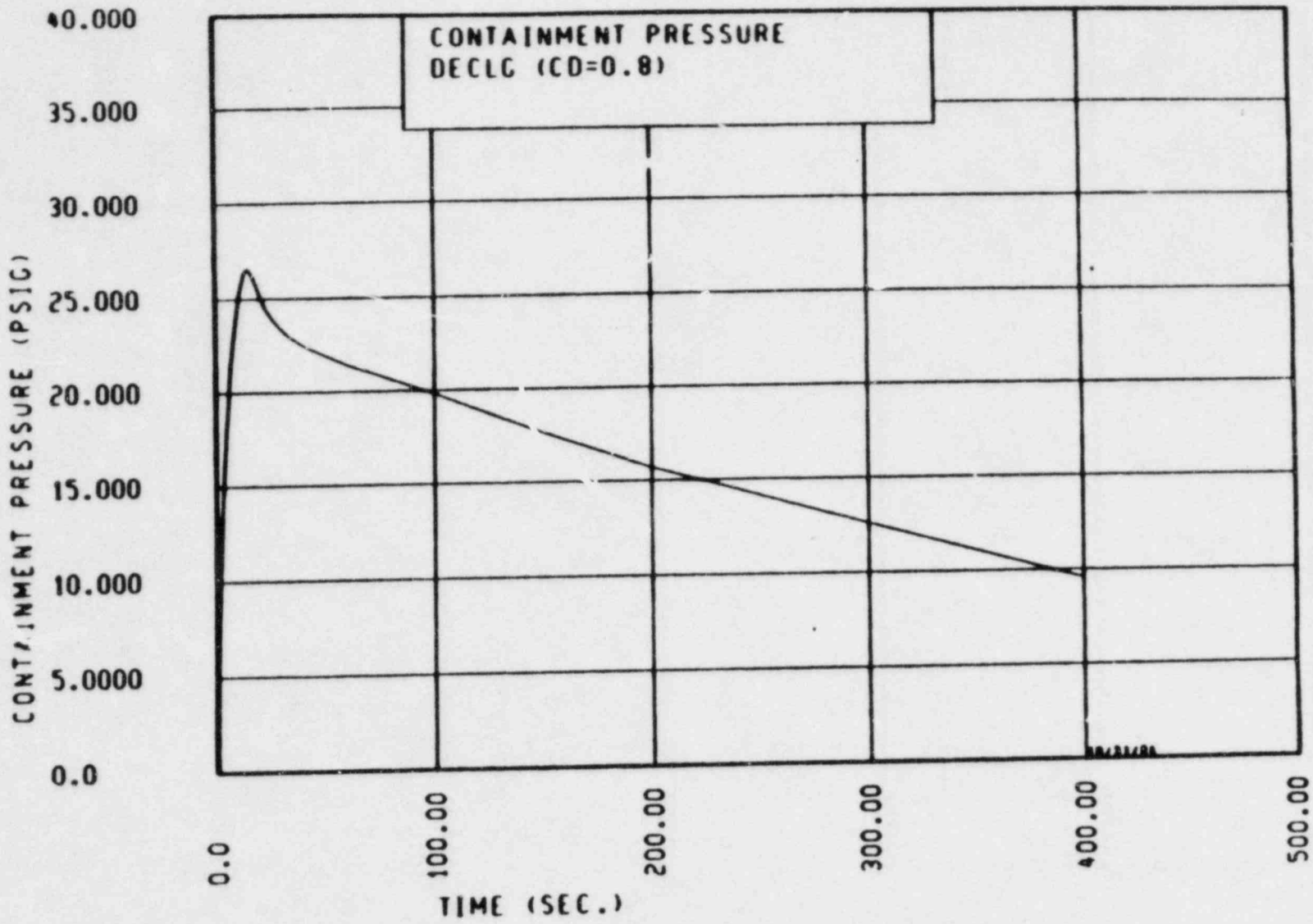

Figure 15.4.1-13a. Containment Pressure (C_D = 0.8)

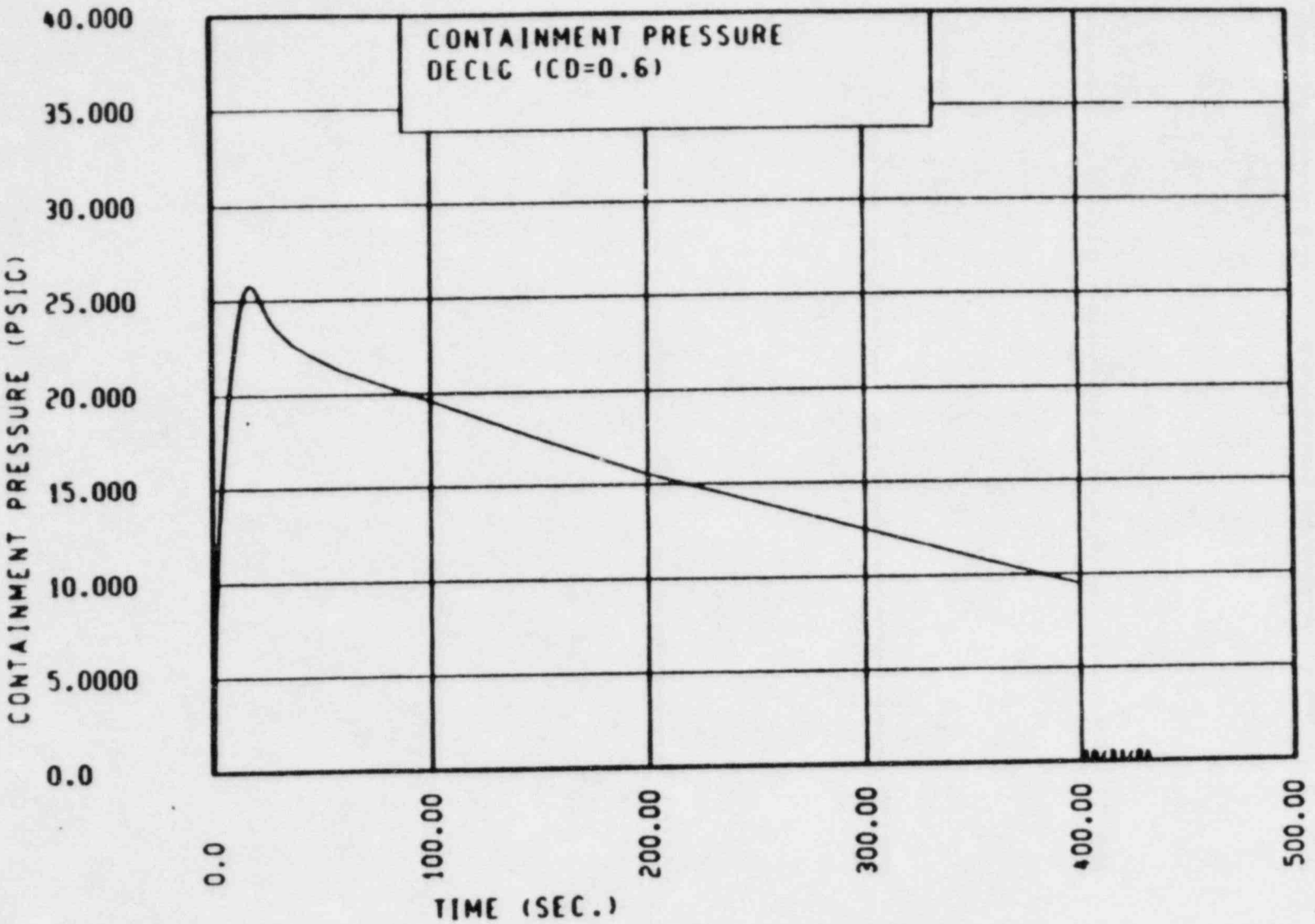

Figure 15.4.1-13b. Containment Pressure (C_D = 0.6)

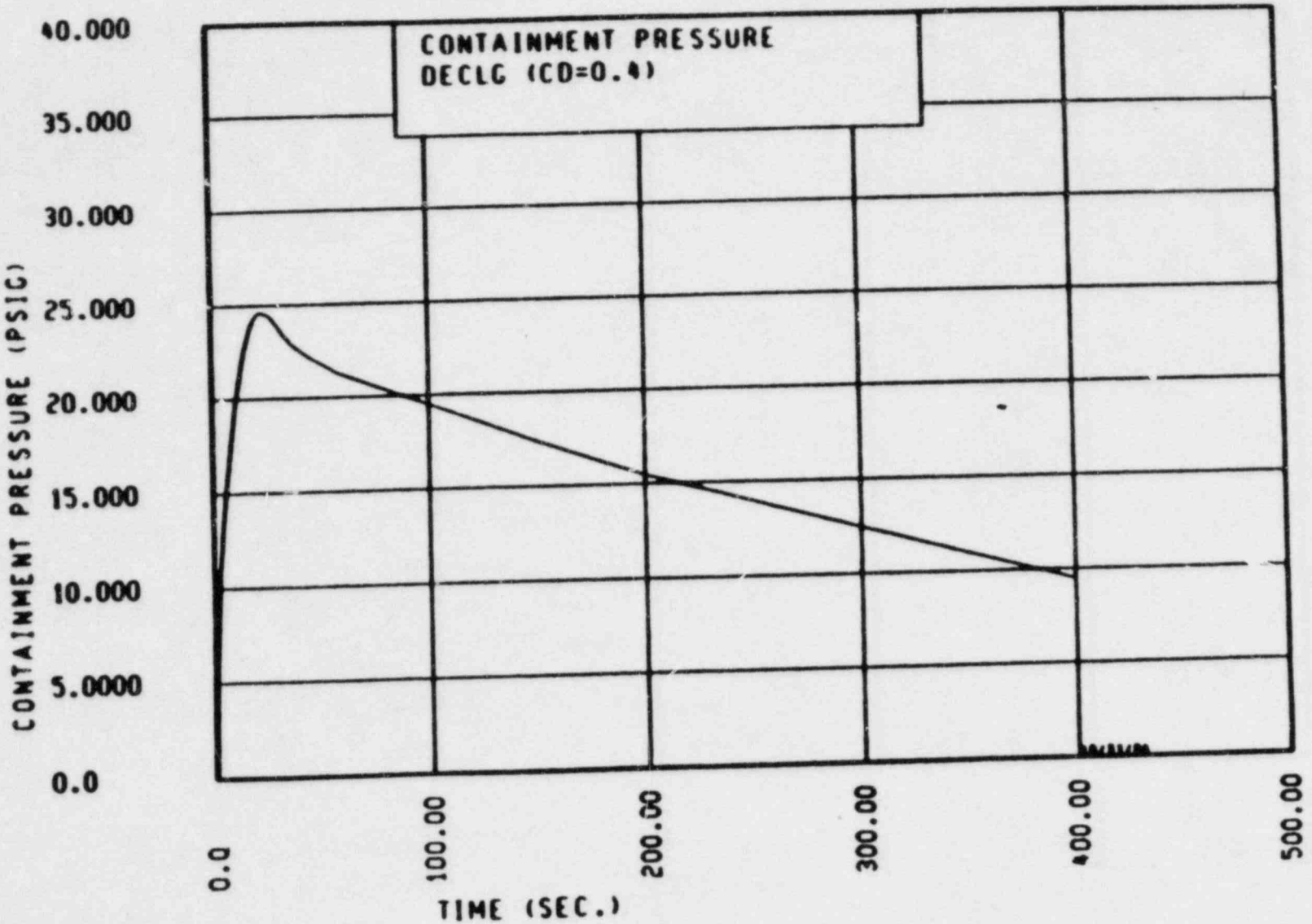

Figure 15.4.1-13c. Containment Pressure (C_D = 0.4)

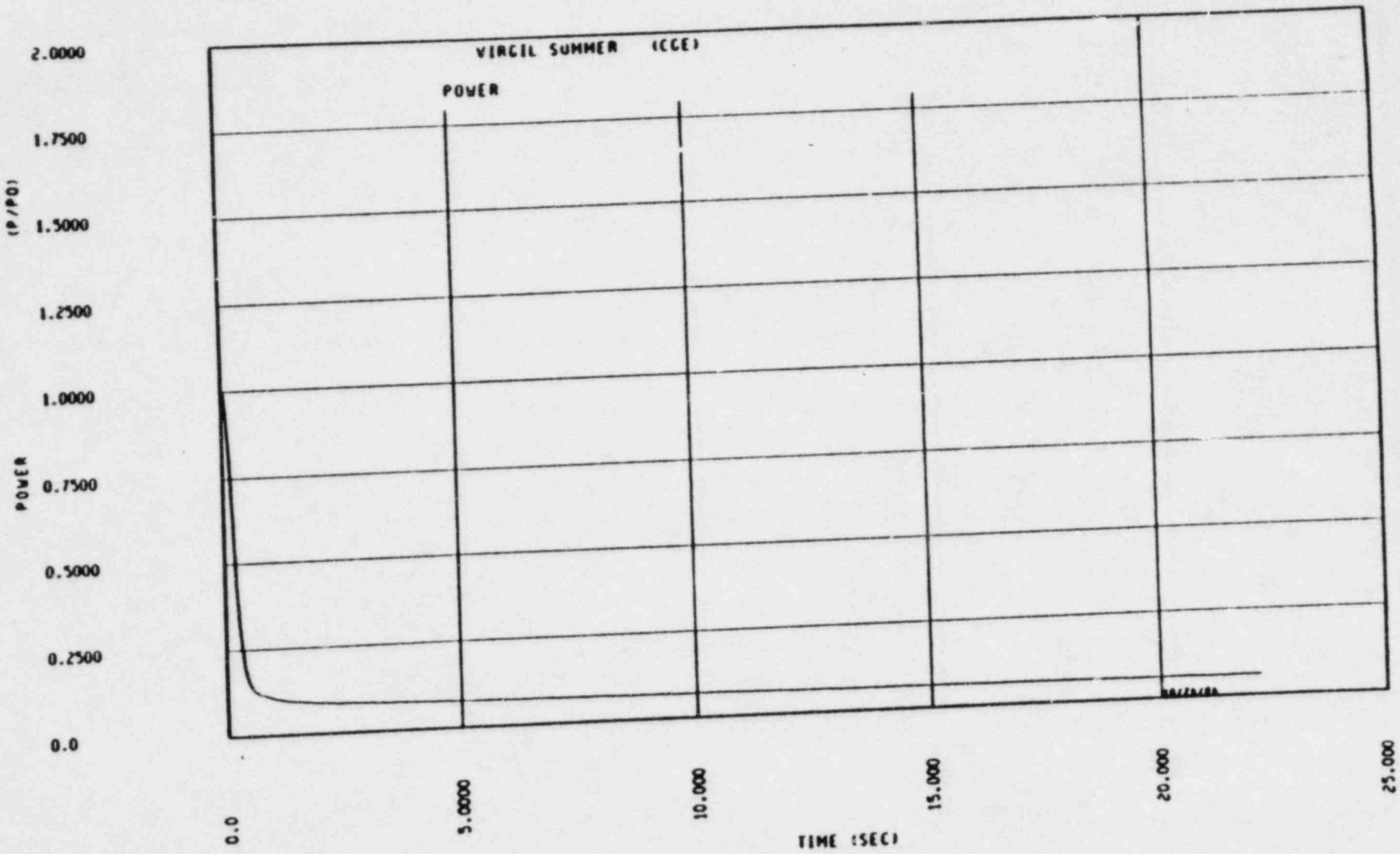

Figure 15.4.1-14a. Core Power Transient (C_D = 0.8)

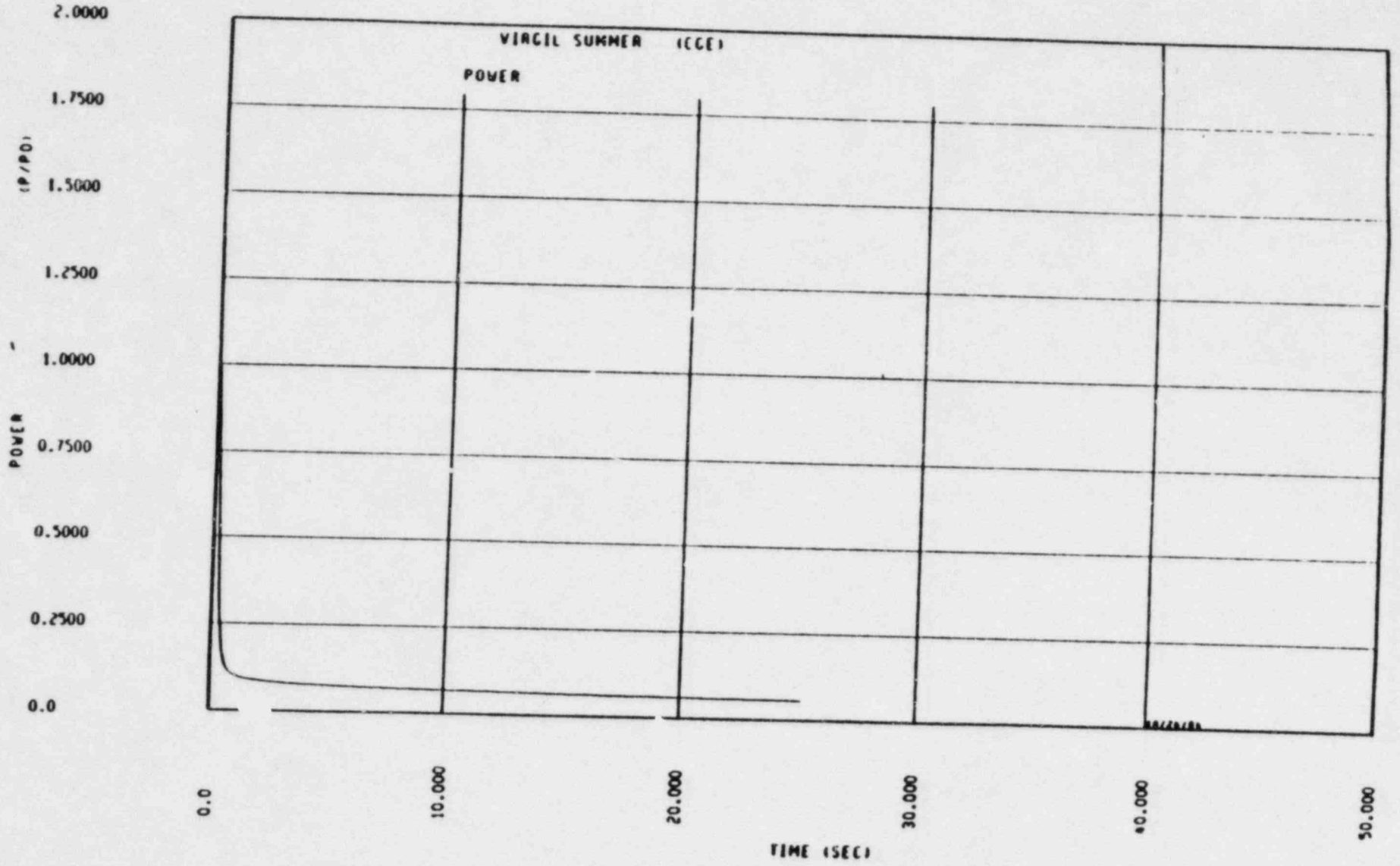

Figure 15.4.1-14b. Core Power Transient (C_D = 0.6)

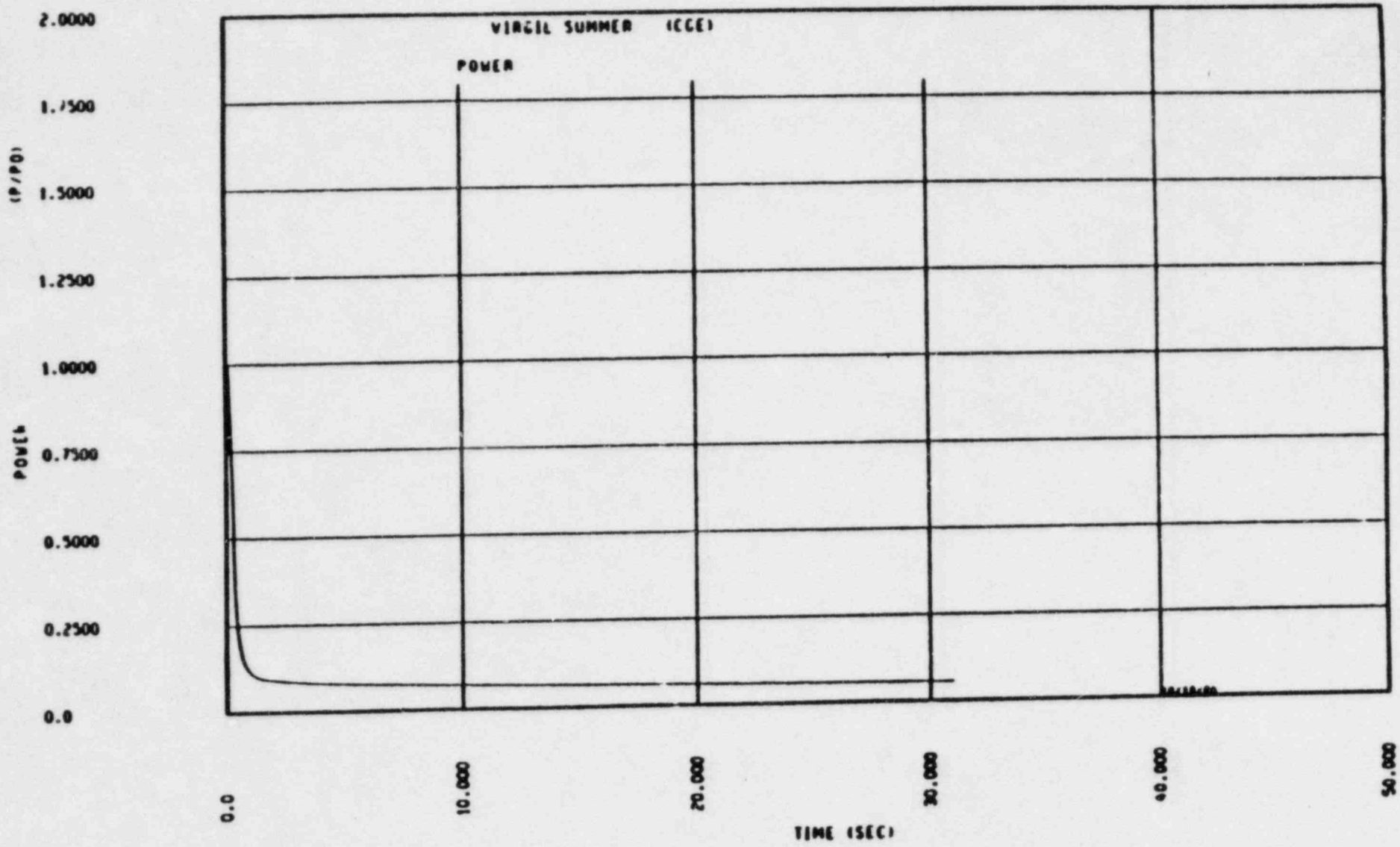

Figure 15.4.1-14c. Core Power Transient (C_D = 0.4)

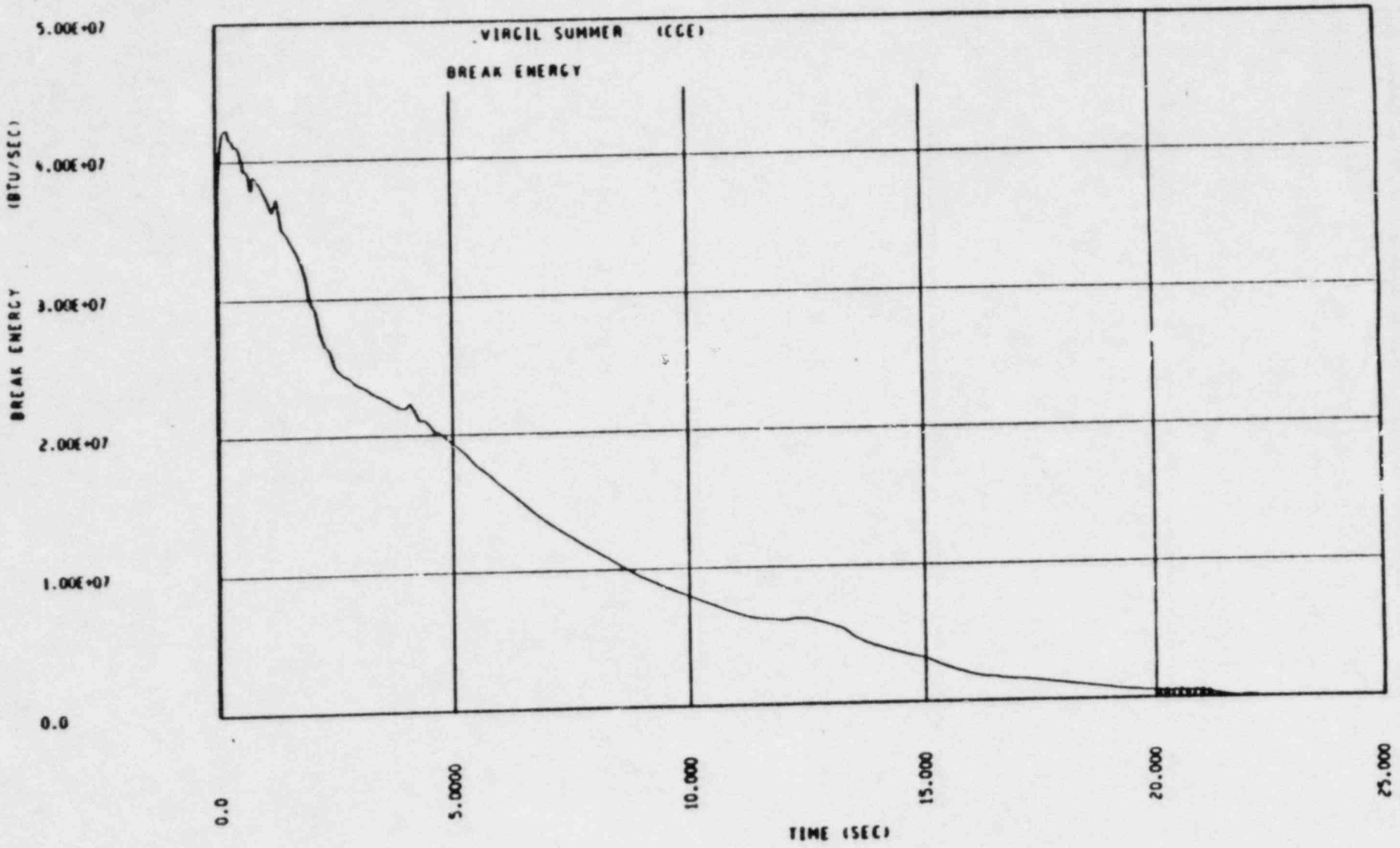

Figure 15.4.1-15a. Break Energy Released to Containment (C_D = 0.8)

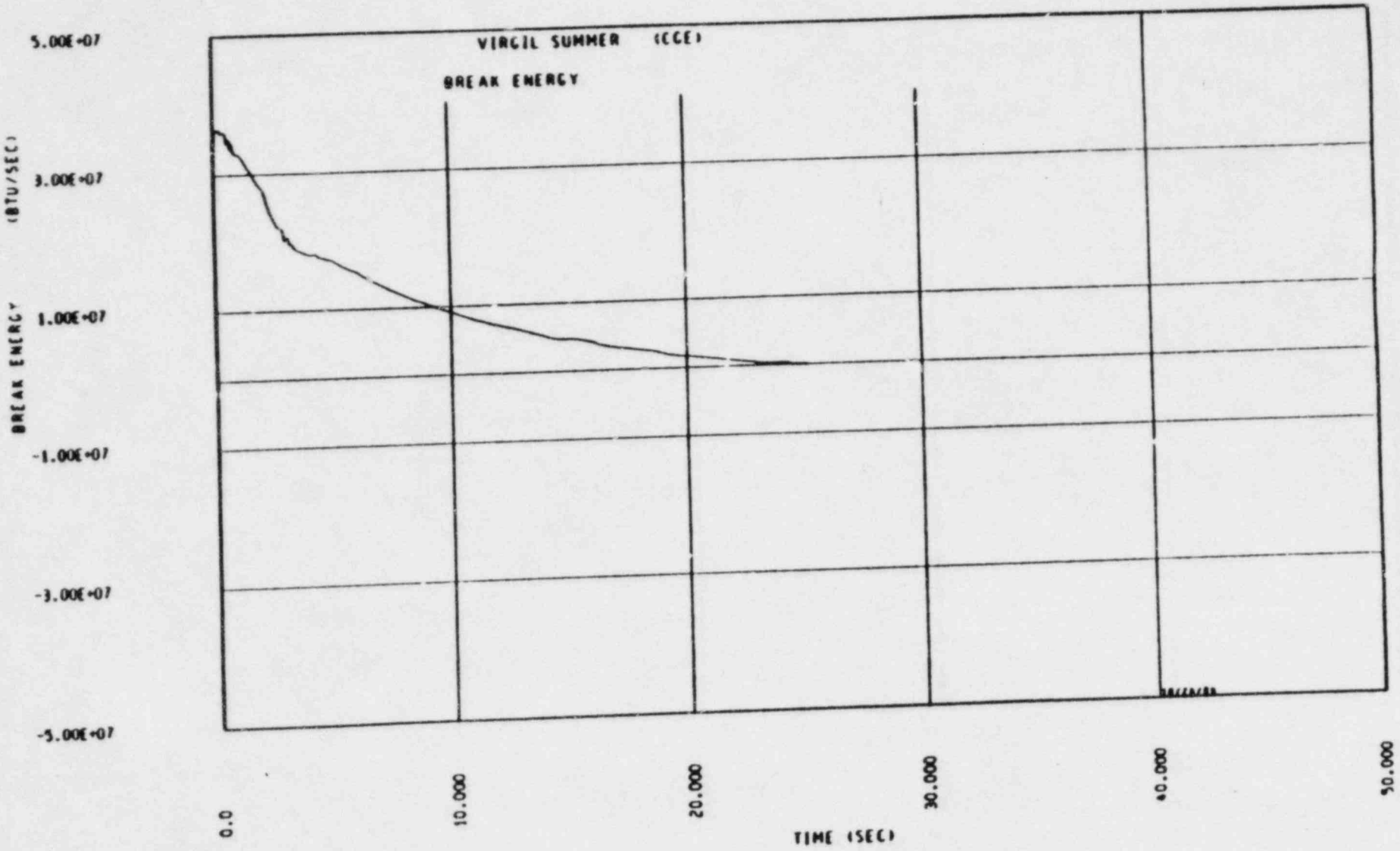

Figure 15.4.1-15b. Break Energy Released to Containment (C_D = 0.6)

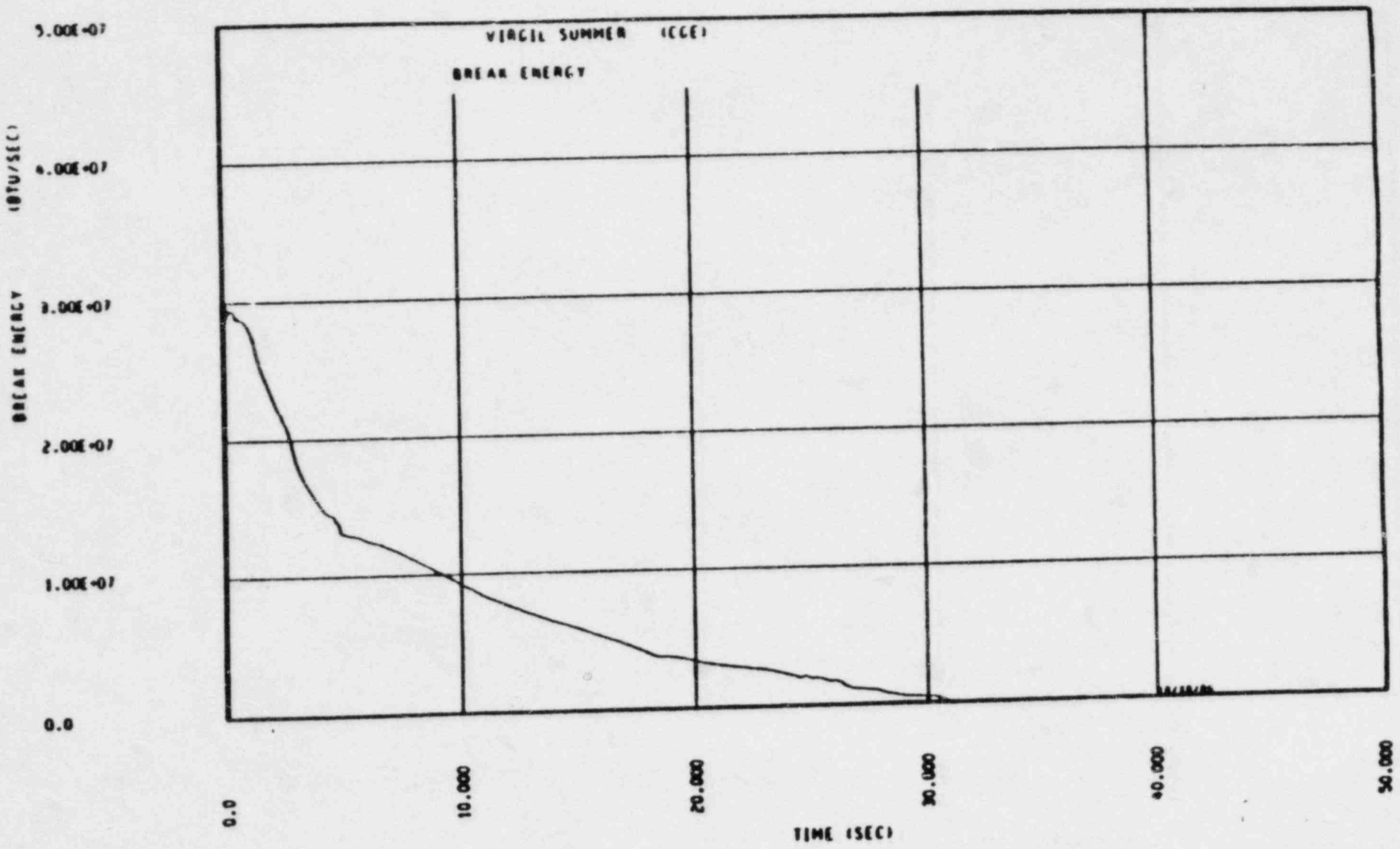

Figure 15.4.1-15c. Break Energy Released to Containment (C_D = 0.4)

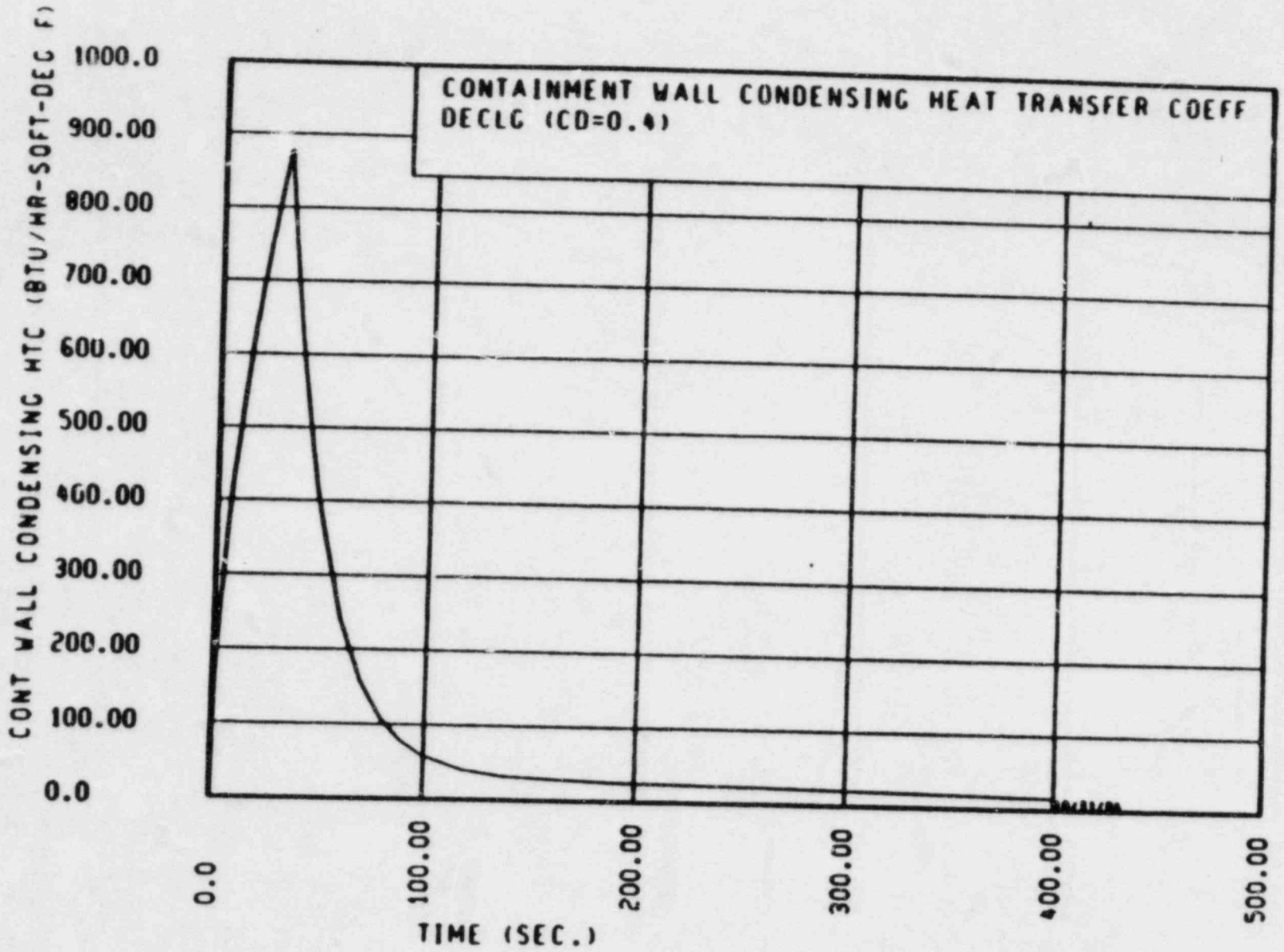

Figure 15.4.1-16. Containment Wall Heat Transfer Coefficient (C_D = 0.4)